Fate and Removal of Emerging Contaminants in Water and Wastewater Treatment Plants

Faculty of Industrial Engineering
Department of Civil, Constructional and Environmental Engineering

Ph.D. School of Civil Engineering and Architecture
Ph.D. Course in Environmental and Hydraulic Engineering - XXXII Cycle

Ph.D. student
Ing. Camilla Di Marcantonio

Supervisor
Prof. Agostina Chiavola

Co-Supervisor
Prof. Maria Rosaria Boni

SAPIENZA
UNIVERSITÀ DI ROMA

Abstract

Organic MicroPollutants (OMPs) – also called Emerging Contaminants or Contaminants of Emerging Concern – include a wide number of chemicals belonging to different classes, e.g. pharmaceuticals and personal care products (PPCPs), drugs of abuse and their metabolites, steroids and hormones, endocrine-disrupting compounds, surfactants, perfluorinated compounds, phosphoric ester flame retardants, industrial additives and agents, siloxanes, artificial sweeteners, and gasoline additives (Barbosa et al., 2016; Bletsou et al., 2015; Chiavola et al., 2019). In the last two decades, increasing attention has been dedicated to OMPs, as a matter of high risk for public health and environment. (Naidu et al., 2016; Rodriguez-Narvaez et al., 2017; Thomaidi et al., 2016; Vilardi et al., 2017).

OMPs are characterized by low environmental concentrations (about ng/L or µg/L), high toxicity, very low biodegradability and resistance to degradation and to conventional treatments. Consequently, they tend to be bioaccumulated in aquatic environments, and to enter the food chain through agriculture products and drinking water (Clarke and Smith, 2011). Measurement of OMPs in the aquatic medium became possible only in the last 20 years, thanks to the improvement of sensitivity and accuracy of the analytical methods; among the different methods, liquid chromatography coupled with high-resolution tandem mass spectrometry (LC-HRMS/MS) is increasingly applied for the analysis of some known and unknown emerging contaminants in water. However, for a number of OMPs, the optimization of analysis conditions and procedures is still insufficient to allow routine monitoring (Boni et al., 2018).

The scientific community established that one of the main source of release in the environment is represented by the wastewater treatment plants (WWTPs), which are not specifically designed and operated to remove OMPs (Sousa et al., 2017). Therefore, improvements of the WWTPs performance are needed to reduce the load of OMPs released into the environment through either the final effluent and wasted sludge (Trapido et al., 2014). Extent of their removal/transformation in the different units of the WWTPs is still not completely known and depends on numerous parameters and conditions. Therefore, it would be very useful to assess the removal efficiency achievable in the main treatment units, and particularly in the biological process which often represents the core of the plants; it is also important to assess if efficiency can be enhanced by properly modifying the operating conditions (e.g. the sludge retention time). Among the treatment processes investigated so far for the removal of OMPs from wastewater, the biological treatments provided interesting and promising possibilities, in terms of costs and environmental impact with respect to physical-chemical processes, at least for a number of OMPs (Ahmed et al., 2017). Assessment of effective removal in the biological processes is made more complicated because various OMPs transformations can take place in the reactor, determining new compounds release (transformation by-products, TPs) which, to some extent, differ in the environmental behaviour and ecotoxicological profile from the original substance (parent compound, PCs) (Hollender et al., 2017). Furthermore, TPs may be more toxic, persistent and less biodegradable of their parents and

are usually unknown and unpredictable. These issues highlight the needs of further investigation which must be based also on non-target screening (NTS) approach (Schollée et al., 2018).

In an attempt to fill some of the gaps in the knowledge of OMPs behaviour in water treatment plants, various aspects of the subject were approached in the present Ph.D. thesis.

In order to contribute to fill some of the gaps in the knowledge about OMPs in water treatment plants, different aspects of this problem were addressed in the present Ph.D. thesis.

Among the wide class of OMPs, the first step of the present study focused on some drugs of abuse, specifically Benzoylecgonine (BE), 11-nor-9carboxy-Δ9-THC (THC-COOH) and Methamphetamine, and on the most abundant perfluorinated compounds present in the environment, which are Perfluorooctanoic acid (PFOA) and Perfluorooctanesulfonic acid (PFOS). The double purpose of this part of the thesis, carried out through laboratory scale investigations, was (1) to optimize the analytical method for the detection of these compounds in wastewater and sludge of a WWTP and (2) to determine the removal rate through abiotic and biotic processes in the biological reactor of the WWTP. The results obtained allowed to assess the optimal conditions of the analytical method: therefore, under these conditions, the method is suitable for rapid and reproducible measurements, minimizing the interferences due to the other compounds always found in wastewater and sludge. About goal (2), contribution of biodegradation and other processes (e.g. adsorption and volatilization) was quantified and the kinetic parameters determined. Furthermore, it was evaluated through a standard respirometric procedure (n. 209 OECD) if the presence of these contaminants at increasing concentrations can negatively affect the microbial activity in the biological reactor, and particularly the nitrification and COD oxidation processes.

Complementary to the assessment of the removal achieved by the activated sludge processes was the in-depth analysis of the enzyme biocatalytic activity with the aim to enhance the efficiency of the OMPs degradation in the biological reactor. This investigation was carried out at the Auckland University, New Zealand, during a 6-months period of research. Particularly, this innovative approach can induce the synthesis of OMPs degrading enzymes by exposing microbes to cycles of stressing and non-stressing environmental conditions. In the present study, stimulation of oxidoreductase production by microbial cells was favoured by varying the dissolved oxygen concentration within the reactor. This strategy showed to be successful, being capable of enhancing the removal rate of some OMPs; furthermore, its implementation at full-scale would contribute to reduce the energy cost of the aeration system and also allow simultaneous nitrification-denitrification within the same tank (Han et al., 2018; He et al., 2018).

As mentioned above, in parallel to the concern about OMPs removal processes, a new issue was highlighted in the past ten years: the formation of transformation products (TPs) from wastewater and water treatment. These substances are often unknown and can be more toxic than their precursors (Li et al., 2017). Several studies focused on TPs produced by wastewater treatment and on their environmental risk assessment (Bletsou et al., 2015; Schollée et al., 2018, 2016; Schymanski et al., 2015). However, the knowledge and scientific data concerning TP monitoring in drinking water are still limited.

Since TPs are often unknown and therefore unexpected, an analytical method of detection that can identify compounds for which no previous knowledge is available, is required; to this purpose, non-target screening (NTS) based on liquid chromatography (LC) coupled to high-resolution tandem mass spectrometry (HR MS/MS) represents the last innovation and challenge related to OMPs detection. The aim of this part of the thesis was to define a useful workflow for TPs monitoring. The workflow was validated through the application to real scale water treatment plants in The Netherlands and Belgium during a three-months period of research at the KWR, Water Research Institute (The Netherland). Particularly, validation was carried out in the Rapid Sand Filter (RSF), since it is one of the most commonly water treatment applied worldwide; furthermore, a number of studies reported the removal of OMPs occurred in rapid sand filters mainly due to biotic processes (Hedegaard et al., 2014; Hedegaard and Albrechtsen, 2014; Zearley and Summers, 2012).

Acknowledgments

The research activities were carried out in collaboration with The University of Auckalnd (New Zealand) and KWR Water research institute (The Netherlands) and with the support of Acea Elabori Spa (Rome). I would like to express my sincere gratitude to:

- Dr Alessandro Frugis, Dr Stefano Biagioli, Dr Valentina Gioia, Dr Simone Leoni, Dr Tommaso Calchetti and Dr Giancarlo Cecchini of Acea Elabori Spa;
- Prof. Naresh Singal and Dr Amrita Bains of The University of Auckland;
- Dr. Andrea Mizzi Brunner, Dr Nikki van Bel and Dr Cheryl Bertelkamp of KWR Water Research Institute.

My special thanks are extended to Professor Agostina Chiavola and Professor Maria Rosaria Boni, my scientific mentors.

List of contents

List of tables

List of figures

Introduction

Organic MicroPollutants – also called Emerging Contaminants or Contaminants of Emerging Concern – include a wide number of chemicals belonging to different classes, e.g. pharmaceuticals and personal care products (PPCPs), drugs of abuse and their metabolites, steroids and hormones, endocrine-disrupting compounds, surfactants, perfluorinated compounds, phosphoric ester flame retardants, industrial additives and agents, siloxanes, artificial sweeteners, and gasoline additives (Barbosa et al., 2016; Bletsou et al., 2015; Chiavola et al., 2019). In the last two decades, increasing attention has been dedicated to OMPs, as a potential source of high risk for public health and environment. (Naidu et al., 2016; Rodriguez-Narvaez et al., 2017; Thomaidi et al., 2016; Vilardi et al., 2017).

OMPs are characterized by low environmental concentrations (about ng/L or µg/L), high toxicity, very low biodegradability and resistance to degradation and to conventional treatments. Consequently, they tend to bioaccumulate in aquatic environments, and enter the food chain through agriculture products and drinking water (Clarke and Smith, 2011). Measurement of OMPs in the aquatic medium became possible only in the last 20 years, thanks to the improvement of sensitivity and accuracy of the analytical methods. Among the various analytical methods, liquid chromatography coupled with high-resolution tandem mass spectrometry (LC-HRMS/MS) is increasingly applied for the analysis of known and unknown emerging contaminants in water. However, for a number of OMPs, the optimization of analysis conditions and procedures is still insufficient to allow routine monitoring (Boni et al., 2018).

The scientific community established that Wastewater Treatment Plants (WWTPs), which are not specifically designed and operated to remove OMPs, are one of the main sources of release in the environment (Sousa et al., 2017). Therefore, an improvement of the WWTPs performance is essential to reduce the load of OMPs released into the environment through both the final effluent and the wasted sludge (Trapido et al., 2014). At the moment, the extent of OMP removal/transformation in WWTPs is still not completely known and depends on various parameters and conditions. Therefore, it would be very useful to assess the removal efficiency achievable in the main treatment units and particularly in the biological process which is often the core of the plants, and also the prospects of its enhancement by proper modifications in the operating conditions (e.g. the sludge retention time). Among the investigated treatment processes for the removal of OMPs from wastewater, biological treatments showed interesting and promising possibilities in terms of costs and environmental impact, at least for a certain number of OMPs (Ahmed et al., 2017). The biological and physicochemical processes of water treatment cause various transformations in OMPs: they can end in OMPs removal but also in the production of new compounds (transformation products, TPs) that, to some extent, differ in environmental behaviour and ecotoxicological profile from the original substance (parent compounds, PCs) (Hollender et al., 2017). For instance, TPs are usually unknown as well as unexpected compounds; they sometimes turn out to be more toxic, persistent and less biodegradable than their parents. Therefore, further investigation is

strongly requires to obtain a better knowledge an understanding; to this purpose, the non-target screening (NTS) approach can represent a useful tool (Schollée et al., 2018).

In an attempt to fill some of the gaps in the knowledge of OMPs behaviour in water treatment plants, various aspects were approached in the present Ph.D. thesis.

The main goal is the study of the presence and fate of emerging contaminants in water treatment plants, with the aim to find out how they can be removed efficiently and by which processes.

The research approach was structured in order to increase, step by step, the complexity of hypothesis and experimental conditions for each stage of the research (Figure 1). The specific aims/steps of the study can be synthesized as following:

1) development and optimization of analytical methods for the detection of target OMPs in wastewater;
2) study of the removal processes of some OMPs during activated sludge treatment, at a laboratory scale and under controlled conditions, in order to assess the contribution of the processes involved (e.g. biodegradation or adsorption);
3) study, at a laboratory scale, of how enzyme biocatalytic processes contribute to the removal of target OMPs during activated sludge treatment, and how to improve the overall efficiency of the treatment;
4) study of the actual performance of WWTPs at full-scale, considering several plants layouts and a list of target OMPs;
5) study of the transformation products formed by biological treatments through a non-target screening approach.

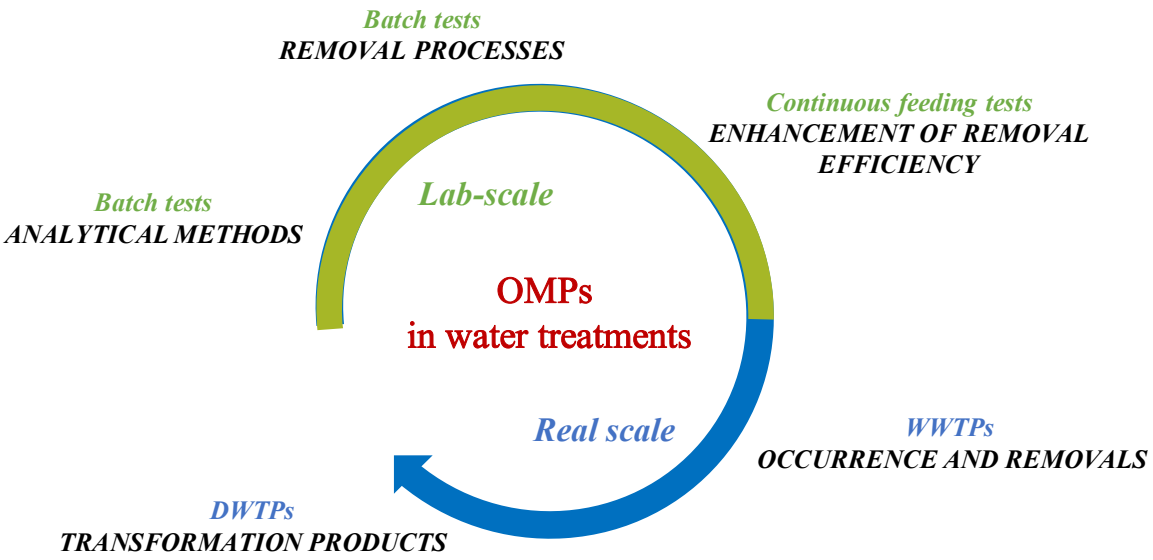

Figure 1 Graphical abstract

Policy

It must be pointed out that at the moment not for all OMPs regulation poses limits on wastewater discharge. However, in the *Proposal for regulation of the European Parliament and of the Council on minimum requirements for water reuse* is included a clause that considers the possibility to add further requirements for water quality about substances of emerging concern, such as pharmaceuticals and pesticides, according to technical and scientific progress (COM(2018) 337 final). This is one of the results of a long legislative process about water policy started in 2000 by the European Community (Directive 2000/60/EC), which, among the other actions, has the aim to protect the environment from any adverse effect caused by the effluent discharge into waters.

The Directive 2000/60/EC was the first mark in the European water policy, which set up a strategy to define high risk substances to be prioritized (Directive 2000/60/EC). A set of 33 priority substances and the respective environmental quality standards (EQS) were ratified by the Directive 2008/105/EC (The European Parliament, 2008). In 2013, the European Union Directive 2013/39/EU recommended to pay attention to the monitoring and treatment options for a group of 45 priority substances, with the aim of meeting the protection of aquatic compartments and human health. In that Directive, two pharmaceuticals (the non-steroid anti-inflammatory diclofenac and the synthetic hormone 17-alpha-ethinylestradiol) and a natural hormone (17-beta-estradiol) were recommended to be included in a first watch list of 10 substances for European Union monitoring. In the first quarter of 2015, the watch list of substances for European Union-wide monitoring (as set out in Article 8b of Directive 2008/ 105/EC) was amended in the Decision 2015/495/EU of 20 March 2015 and finally updated in Decision 2018/840/EU. Besides the abovementioned substances (diclofenac, 17-beta-estradiol and 17-beta-estradiol), three macrolide antibiotics (azithromycin, clarithromycin and erythromycin) were included in the list, together with another natural hormone (estrone), some pesticides, a UV filter and an antioxidant. The frequent occurrence of OMPs in the environment and the low efficiency/ineffectiveness of conventional WWTPs to remove such compounds, has made necessary the amendment of the framework to cover a larger set of hazardous compounds; furthermore, more recommendations for wastewater treatment steps or even new treatment scenarios were considered, as proved by the latest updates of the European water policy (COM(2018) 337 final). Moreover, stricter limits on OMPs concentrations in drinking water were also proposed by the European Community (COM(2017) 753 final), including some perfluoroalkyl substances, steroids and pesticides (Figure 2). However, since priority substances are currently not included in routine monitoring programmes at EU level, but may pose a significant ecotoxicological risk, a recent study (Brack et al., 2017) proposed some specific solutions for the forthcoming water frame directive review in 2019, based on the developments of EU collaborative projects and Norman Networks contributions. Thus, ten recommendations were developed to improve monitoring and strengthen comprehensive prioritization of pollutants, to foster consistent assessment and support solution- oriented management of surface waters. Also the Global Water Research Coalition (GWRC) developed an International Priority List of pharmaceuticals relevant for

the water cycle, based on the compounds that present a potential risk in water supply (Global Water Research Coalition, 2008). According to GWRC, 44 compounds are classified in three main groups: Class I (10), Class II (18) and Class III (16), based on the following criteria: human toxicity, ecotoxicity, degradability, resistance to treatment and occurrence in the environment (Rizzo et al., 2019).

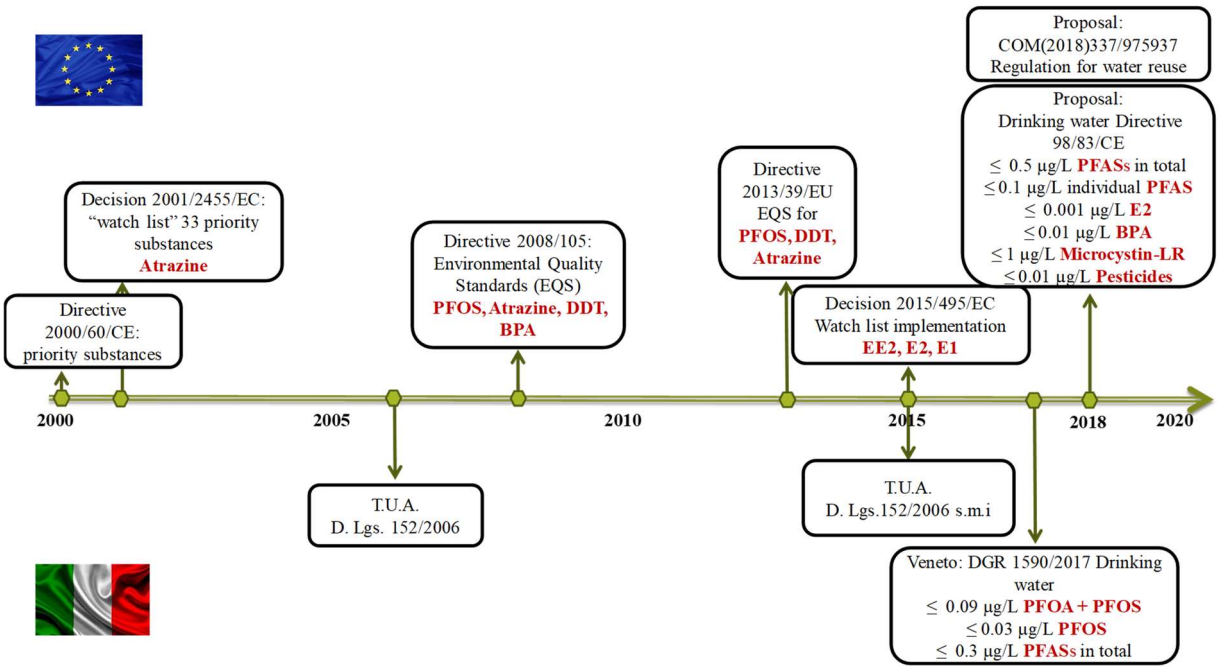

Figure 2 Development of the water policy about emerging pollutants in Europe and in Italy

OMPs detection

The concentration of OMPs in aquatic environment are typically ranged from ng/L to µg/L. Because of the low concentration and the complexity of the environmental matrix, including wastewater, their detection is challenging and entails continuous updates (about new compounds to be detected) and improvements (about required sensitivity) as Noguera-Oviedo and Aga (2016) showed in a review paper (see Figure 3). Analytical techniques include gas chromatography (GC) coupled with mass spectrometry (MS), and liquid chromatography (LC) coupled with MS (Teodosiu et al., 2018). From the analytical point of view, water for human consumption, wastewater and sewage sludge are complex matrices and contain a number of components, such as inorganic anions and heavy metals and other organic compounds that represent potential interferences in the detection of OMPs (Castiglioni et al., 2016). Furthermore, wastewater and sludge composition in the WWTPs changes with time and among the plants (Gerrity et al., 2011; Gómez et al., 2012). In order to obtain a better knowledge of the fate of OMPs in the WWTPs it is of key importance to establish an analytical determination method offering reliability and reproducibility no matter the wastewater and sludge composition. Furthermore, the method must be relatively easy-to-use so as to allow routine measurements for monitoring removal/transformation within the different processes implemented in a WWTP. Due to the high signal

to noise ratio, liquid chromatography coupled with tandem mass spectrometry has been recognized as the method of choice for the detection in aqueous environment of drugs of abuse, pharmaceuticals and most of the other contaminants ascribed to OMPs (Andrés-Costa et al., 2017; Baker and Kasprzyk-Hordern, 2011; Castiglioni et al., 2014).

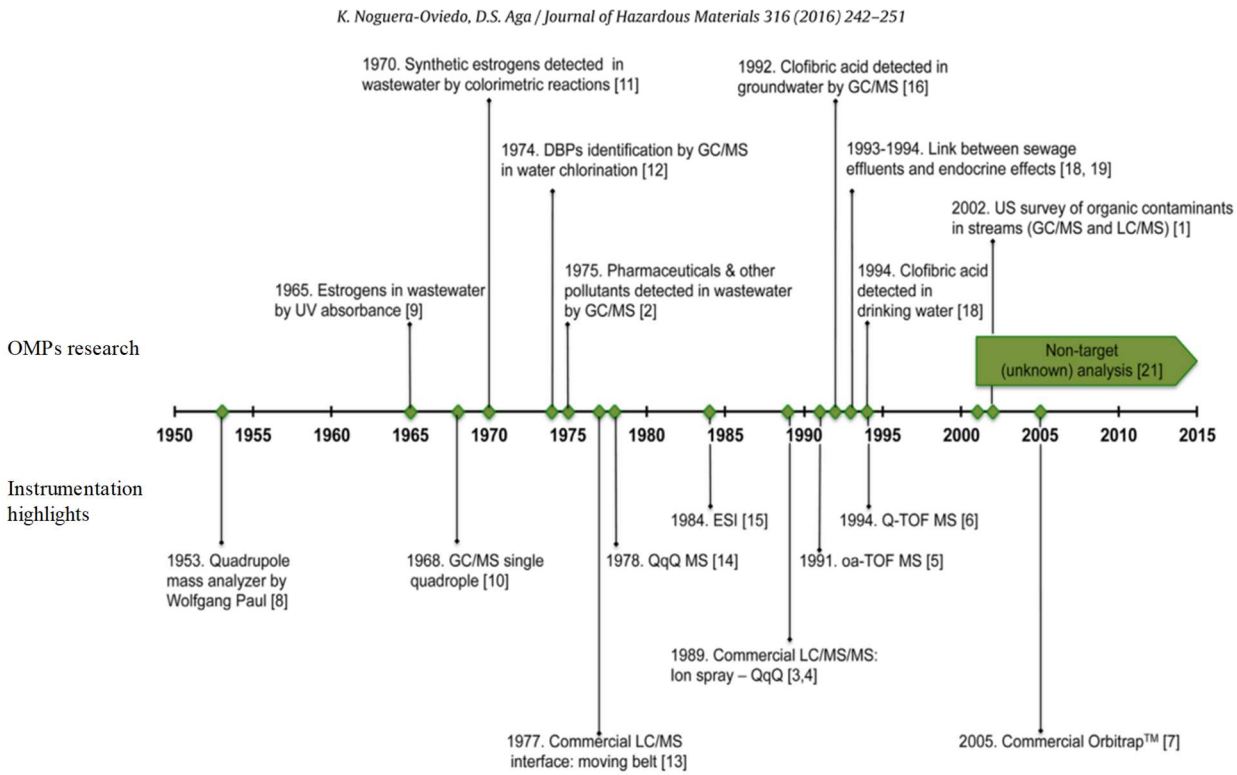

Figure 3 Development of OMPs research and related instrumentation (Noguera-Oviedo and Aga, 2016)

However, our knowledge is still not complete: there is still the need to define the more suitable analytical conditions for the determination of many OMPs in wastewater and sludge samples.

In order to obtain a comprehensive view of water quality and the associated risk, the range of identifiable chemicals must be extended, and the quantification limits are required to be lower. Furthermore, target-based environmental monitoring should be associated with non-target analysis.

Application of non-target screening is promising to characterize unknown peaks in water samples and to determine if unknown, non-target compounds are either removed or formed during water treatment. Numerous studies have shown that liquid chromatography coupled to high-resolution tandem mass spectrometry (LC-HRMS/MS) can be used for the simultaneous analysis of hundreds of known and unknown compounds, including transformation products (Bletsou et al., 2015; Hernández et al., 2016; Little et al., 2012; Schollée et al., 2018). The LC-HRMS/MS is also applied for the analysis of unknown emerging contaminants in water. Additionally, information from HRMS/MS measurement (such as exact mass and isotope information) can be acquired for suspect or non-target compounds and then used for structure elucidation of parent compounds or TPs without reference standards (Schollée et al., 2017).

The major benefit of a full-scan, accurate high-resolution mass spectrometry is that – within a single analytical run – target, suspect and non-target compounds can be analyzed or identified. However, it is still challenging to profile transformation products in environment samples, since they are formed through many possible reactions, and automatic workflows for the identification are not readily available. So manual data inspection, though time consuming, is necessary. The 2000s also saw the advent of free online chemical compound databases such as ChemSpider and PubChem containing structures and properties of millions of natural and synthetic organic chemicals, while the 2010s have yielded an explosion of online mass spectral libraries (e.g., MassBank, METLIN, mzCloud) and software packages aimed at processing the mountains of data generated by these HR-MS/MS instruments. The convergence of these technological developments has led to a fortuitous situation indeed: the analytical capabilities available to the environmental analytical chemist today are finally ready to tackle the complexity of environmental samples. However, a single measurement of a complex environmental sample typically contains many thousands of signals, so that even with the most sophisticated instruments and data analysis workflows, it is currently not feasible to identify all the chemical structures present in such samples (Hollender et al., 2017). More efforts are still needed to improve measurement capability of contaminants in water.

1.1 Target OMPs

Within the wide number of chemicals considered as emerging pollutants, the present study focused on:

- illicit drugs and their metabolites: Benzoylecgonine (BE), 11-nor-carboxy-Δ9-tetrahydrocannabinol (THC-COOH), Amphetamine (AM), Methamphetamine (MET);
- pharmaceuticals: Ketoprofen (KTP), Sulfamethoxazole (SMX), Carbamazepine (CBZ), Trimethoprim (TMT), Lincomycin (LCN), Sulfadiazine (SLD) and Naproxen (NPX);
- steroids: Progesterone (P4), Estrone (E1), 17β Estradiol (E2), 17α Ethynylestradiol (EE2);
- pesticides: Atrazine (ATZ);
- artificial sweeteners: Sucralose (SCL);
- industrial compounds: Perfluorooctane sulfonic acid (PFOS), Perfluorooctanoic acid (PFOA) and Pyrazole (PYZ).

These substances were selected firstly because they are frequently found in the influent of WWTPs (Stevens-Garmon et al., 2011; Tiwari et al., 2017; Trapido et al., 2014), and also for other reasons:

- some are resistant to biological processes, such as CBZ, PFOA, PFOS, PYZ, ATZ and SCL;
- some are included in the list of substances mentioned in the European water framework, such as E1, E2, EE2, PFOA and PFOS;
- some were not often object of studies about water quality and wastewater treatment, such as the group of illicit drugs (BE, THC-COOH, AM, MET), PYZ, LNC;
- some were chosen as lead substances for a particularly interesting class, e.g. SMX for sulfonamide antibiotics (Fischer and Majewsky, 2014);
- some are substances largely used, e.g. SMX and TMT.

The physico-chemical properties of the target compounds and a summary of the scientific literature about their occurrence in WWTPs are reported in Table 1 and Table 2, respectively.

Illicit drugs and their metabolites

According to the European Drug Report 2017, cannabis is the most used drug in both Europe and worldwide (about five times more than other substances), followed by cocaine, amphetamine-group and opiates (EMCDDA, 2017). Some studies indicate that the drugs and drugs metabolites most commonly detected in WWTPs effluents are benzoylecgonine, ecgonine methyl ester, MDMA, methamphetamine, amphetamine and morphine (Pal et al., 2013).

Benzoylecgonine is the major metabolite of cocaine. It is formed by hydrolysis of cocaine in the liver, catalysed by carboxylesterases. It is excreted in the urine of cocaine users. 11-Nor-9-carboxy-Δ9-tetrahydrocannabinol is the main secondary metabolite of tetrahydrocannabinol (THC), which is formed in the body after cannabis is consumed. Amphetamine and methamphetamine are central nervous system stimulants; they are generally manufactured in clandestine laboratories because they are not commercially available and do not have natural sources.

Commonly, illicit drugs are excreted as parent compounds and metabolites through human urine and faeces, and then discharged into the sewage network (Castiglioni et al., 2006; Zuccato et al., 2005). Moreover, clandestine laboratory wastes containing residual parent drugs, unreactive precursors and by-products are disposed of in domestic garbage or discharged on soil or in toilet and then transferred to sewage.

In addition, it is reported that aquatic biota including bacteria, algae, invertebrates and vertebrates has shown susceptibility to illicit drugs exposure, although the concentration of these contaminants necessary to give ecological effects is not completely known (Binelli et al., 2013, 2012; Pal et al., 2015; Parolini and Binelli, 2014; Rosi-Marshall et al., 2015).

Illicit drugs are only partially removed by WWTPs, because they are not specifically designed for that aim (Zuccato and Castiglioni, 2009). Furthermore, removal efficiency depends on many variables, such as the type of technology used in the plant and the operating parameters; chemical-physical characteristics of wastewater and concentration and properties of drugs may also have a high influence. It has been demonstrated that removal takes place mostly during the secondary treatment processes, through adsorption, volatilization, and/or biodegradation (Helbling et al., 2010). However, the real extent and efficiency of these processes is still unknown for many drugs, since most of the previous studies focused on different classes of emerging contaminants (e.g. antibiotics).

Industrial compounds

Among industrial compounds, PerFluoroAlkyl Substances (PFASs) were chosen to investigate because they represent a class of industrial compounds largely employed in the last fifty years due to their high chemical and thermal stability, hydrophobicity and lipophobicity.

The extensive application of PFASs (from plastic polymers to textile fibers and cosmetics industry) has resulted in their environmental ubiquity and worldwide presence in groundwater and sewage as well as in the human body (Ahrens et al., 2011; Castiglioni et al., 2015). Among PFASs, Perfluorooctane sulfonic acid (PFOS) and Perfluorooctanoic acid (PFOA) are those of more concern compounds because of their higher persistence and bioaccumulation capacity in the trophic chain (Castiglioni et al., 2015). Furthermore, scientific research confirmed the endocrine disrupting properties of PFOS and the carcinogenic effect of PFOA, as well as their toxicity to animals and human beings (Persistent Organic Pollutants Review Committee Twelfth Meeting, 2016; United Nations, 2006; White et al., 2011). As a consequence, Environmental Quality Standard (EQS) on PFOS in surface water and biota were fixed; besides, more restricted limit concentrations on PFASs in drinking water were also proposed by the European Community (Directives 2013/39/EU; COM(2017) 753 final), as mentioned above. Since these compounds possess a high stability versus biological and chemical degradation, when they enter the WWTPs through the sewage network the processes here implemented for the removal of carbon and nutrient compounds are unable to achieve also significant reduction of PFOA and PFOS concentrations. Furthermore, potential transformations of precursor compounds to PFOA and PFOS during the same

processes may lead to an increase of their concentrations (Pan et al., 2016). Therefore, the WWTPs become one of the main sources of release into the environment through the effluent and sludge disposal. As highlighted in several studies, physical-chemical properties of these compounds play a relevant role in the removal processes and make its understanding to be more complicated (Buck et al., 2011; Dalahmeh et al., 2019). The molecular structure of PFOA and PFOS is characterized by hydrophobic strong carbon–fluorine bond chain and hydrophilic functional groups, which give them a surfactant property. Similarly to many pollutants such as heavy metals and some organics, also for PFOA and PFOS an important mechanism of removal seems to be their adsorption onto sludge flocs (Quirantes et al., 2017). Therefore, the waste sludge represents the main mass flow coming out from the treatment plant, with concentrations found to be in the range <5-190 ng/g for PFOA and 13-702 ng/g for PFOS (Pan et al., 2016; Yu et al., 2009).

The number of reports examining the biodegradation and biotransformation of PFOS and PFOA by aerobic and anaerobic microbial populations is very limited (Grassi et al., 2013). Furthermore, results found in the scientific literature about the biodegradability of PFOS and PFOA are somehow conflicting (Arvaniti and Stasinakis, 2015). For instance, it was reported that PFOS can be decomposed up to 67% by a specific microorganism present in activated sludge (Kwon et al., 2014). By contrast, other authors concluded that PFOS is microbiologically inert under aerobic conditions (Avendaño et al., 2015). The same authors of the first paper replied that, under the experimental conditions applied in their study, PFOS decomposed to some unknown products due to microbial activity (Kwon et al., 2015). Parsons et al. (2008), after analysing the foregoing literature, affirmed that PFOA is considered biologically inactive under all the examined conditions. Processes other than biodegradation and adsorption are reported to determine PFASs removal from the system, although their specific contribution has not been fully assessed yet (Liou et al., 2010). Despite the high relevance and interest, few and often contradictory are the information available in the scientific literature about the removal and transformation mechanisms involving PFOA and PFOS in the activated sludge reactor, which represents the main stage of wastewater treatment. Therefore, additional understanding is strongly required.

The study focused also on pyrazole, an industrial compound used as an intermediate in the production of various chemicals, including acrylonitrile, pesticides and various pharmaceutical agents. The concern about this compound in water treatments started in 2015, when an incident took place and large quantities of pyrazole were emitted in the river Meuse (The Netherlands) via the effluent coming from the WWTP of an industrial area in the Netherlands. Since the toxicological effect were proved, in 2017 pyrazole was included in the Dutch drinking water directive with a standard of 3 μg/L. The knowledge about its fate and removal in water treatment is limited and therefore needs to be further improved (van der Hoek et al., 2015).

Pharmaceuticals

In the present study, steroids were considered as a separate class of substances.

Pharmaceuticals include substances both for human and veterinary use, such as antibiotics, anti-inflammatories, anti-epileptics, sedatives, antidepressants, steroids, stimulants, disinfectants, antihypertensives, endocrine disruptors.

Pharmaceuticals are often designed to cross biological membranes. Therefore, their rate of uptake and internal concentration are critically important (Miller et al., 2018).

These compounds are discharged into the sewage network by human excretions, after being assumed and then metabolized. Pharmaceutical concentrations in environmental waters are generally considered non-toxic to humans (ng/L to mg/L), but this may not be the case for wildlife. Because of their physico-chemical characteristics and their continuous introduction into the environment, they can cause a bioaccumulation in aquatic organisms, both as active pharmaceutical and as transformation products, even if they are present at low concentrations in water bodies (Gogoi et al., 2018).

First, the bioactive ingredients are subject to the user's metabolism, then the excreted metabolites and unaltered parent compounds can undergo further transformations in sewage treatment facilities. The literature shows that many of these compounds survive biodegradation processes and that metabolic conjugates can even be converted back to their free parent forms, e.g. carbamazepine (Daughton and Ternes, 1999).

It is widely accepted that efficiency in the removal of pharmaceuticals in WWTPs is not only dependent on treatment technologies, but also on other factors, e.g. seasons, operation conditions and nature of the contaminants (Tran and Gin, 2017). Several studies indicated that after the treatment processes, most of the pharmaceuticals were not completely eliminated (Patrolecco et al., 2015).

In the present study 7 pharmaceuticals were chosen as target compounds:

- Ketoprofen, one of the propionic acid class of nonsteroidal anti-inflammatory drugs with analgesic and antipyretic effects;
- Trimethoprim, an antibiotic used mainly in the treatment of bladder infections;
- Sulfamethoxazole, which combined with Trimethoprim, is a fixed antibiotic widely used for mild-to-moderate bacterial infections and as prophylaxis against opportunistic infections. Like other sulfonamide-containing medications, this combination has been linked to rare instances of clinically apparent acute liver injury (PubChem);
- Carbamazepine, an anticonvulsant or anti-epileptic drug.;
- Lincomycin, an antibiotic used to treat severe bacterial infections in people who cannot use penicillin antibiotics;
- Naproxen, a nonsteroidal anti-inflammatory substance used in the management of certain types of arthritis and as a painkiller;
- Sulfadiazine, a sulfanilamide derivative used in the treatment of urinary tract infections, meningitis and malaria.

Steroids

Pharmaceutical products include some hormones that act as endocrine disruptors, or substances able of interacting with the normal hormonal action of humans and other organisms (European food safety authority).

Endocrine-disrupting compounds (EDCs) are chemicals affecting the synthesis, secretion and transport of natural hormones, which are, in turn, involved in the maintenance of homeostasis, reproduction, development and/or behavior of living beings (Spataro et al., 2019).

The main classes of endocrine disruptors are: estrogenic, androgenic and thyroid. Estrogens are the most commonly found in the environment, often used as contraceptive agents. Some recent studies have found that the feminisation of different species of fish is linked to the presence of these estrogenic substances in aquatic environments (Tran and Gin, 2017). These are very active compounds, able to induce the therapeutic effect at very low doses and potentially to remain active even after use, as they are not completely metabolized by the organism and excreted in wastewater. Usually, these micropollutants remain unchanged during the operation of the water treatment plants and are therefore subsequently released into the environment. Thus, they are included in the European water framework directives.

Particularly, progesterone is an endogenous steroid and progestogen sex hormone involved in the menstrual cycle, pregnancy, and embryogenesis of humans and other species.

Estrone is a steroid, a weak estrogen, and a minor female sex hormone.

Estradiol (17β Estradiol) is an estrogen steroid hormone and the major female sex hormone; it is involved in the regulation of the estrous and menstrual female reproductive cycles.

Ethinylestradiol (17α Ethynylestradiol) is an estrogen medication which is used widely in birth control pills in combination with progestins.

Pesticides

Extensive application of pesticides during manufacturing or agriculture practices contributes to the environmental pollution. Atrazine is a persistent organic pollutant in the environment which affects not only terrestrial and aquatic biota but also human health. Due to its rigorous and frequent usage, as well as its perseverance in the environment, it has been often detected in the surface and groundwater bodies. As a consequence, atrazine concentrations exceeded the maximum contaminant level allowed for drinking water in the European Union and USA (Kolekar et al., 2014). Atrazine was found to be persistent in biological treatments (Bertelkamp et al., 2014). The water framework directive (WFD) 2000/60/EC and updates included these chemicals into the list of priority substances, due to their significant risk towards aquatic organism.

Artificial sweeteners

Artificial sweeteners are chemicals used instead of regular table sugar (sucrose). After digestion, artificial sweeteners pass through the human digestive tract largely unaffected and are excreted via urine

or faeces into the sewage system. These artificial sweeteners are not eliminated in WWTPs and are persistent in surface and coastal waters (Loos et al., 2013).

Sucralose is a polar, chlorinated sugar. It was discovered in 1976 by the Tate&Lyle company. At the moment it is used in more than 30 countries. Like other synthetic sweeteners (e.g. aspartame) it replaces sugar in low calorie drinks and food products. Environmental effects of sucralose have not been examined systematically and its fate in water treatments as well (Loos et al., 2009).

Table 1 Main chemical-physical characteristics of the target OMPs. pKa=-log of acid dissociation constant; Log Kow=log of octanol-water partition coefficient; KH=Henry's law constant; logKOC= log of organic carbon-water partition coefficient; S=water solubility; kd=liquid-solid partition coefficient; pv =vapour pressure

OMPs	Class	pK_a	Log K_{ow}	K_H	Log K_{OC}	S	S 25°C	K_d	p_v 25 °C
		/	/	[atm·m³/mol]	[L/kg]	[mg /mL]	[mg /L]	[L/kg]	[mmHg]
EE2	Syntetic estrogen	10.33	3.67	$7.94*10^{-12}$	4.678	0.00677	11.3	/	$1.95*10^{-9}$
E2	Natural estrogen	10.33	3.13	$1.41*10^{-12}$	4.205	0.0213	81.97	/	$6.38*10^{-10}$
E1	Estradiol metabolite	10.33	3.13	$3.80*10^{-10}$	3.13	0.03	30	/	$2.49*10^{-10}$
P4	Natural steroid	18.47	3.87	$6.49*10^{-8}$	3-902	0.00546	8.81	/	$3.39*10^{-4}$
CBZ	Anti-convulsant	13.9	2.45	$1,08*10^{-10}$	3,588	0,152	17,7	/	$1.84*10^{-7}$
SMX	Anti-bacterial	6.16	0.89	$9.56*10^{-13}$	3.185	0.459	3942	/	$3.79*10^{-6}$
TMT	Anti-bacterial	7.12	0.91	$2.39*10^{-14}$	2.957	0.615	2334	/	$5.13*10^{-7}$
KTP	Anti-inflammatory	4.5	3.12	$2.12*10^{-11}$	2.459	0.0213	51 (22°C)	/	$6.81*10^{-7}$
LCN	Antibiotic	7.6	0.2	$3.0*10^{-23}$	1.768	3.02	927	/	$1.34*10^{-17}$
AM	Stimulant	10.1	1.76	$1.08*10^{-6}$	3.045	1.74	$2.81\ 10^4$	/	0.24
MET	Stimulant	9.87	2.07	$2.37*10^{-6}$	3.207	0.928	$1.33*10^{-4}$	/	$5.4*10^{-3}$
BE	Cocaine metabolite	3.15	-1.32	$1.03*10^{-13}$	2.548	3.82	1605	961 - 20	$5.17*10^{-8}$
THC-COOH	Cannabis metabolite	4.21	1.74	$3.87*10^{-12}$	2.794	0.00839	711.9	29100	$3.73*10^{-9}$
PFOA	Industrial compound	<1	6.3	0.0908	2.06	3.4	0.02	150 – 350	$2*10^{-3}$
PFOS	Industrial compound	<1	4.49	$3.09*10^{-9}$	2.57	0.57	680	200 – 4050	$2.4*10^{-6}$
ATZ	Pesticide	<2	0.26	$1.05*10^{-6}$	26-1164	/	33	7.5 – 8.5	$2.89*10^{-7}$
PYZ	Industrial compound	14	0.33	$1.05*10^{-6}$	9.724	0.28 – 1.8	/	/	1.8
NPX	Anti-inflammatory	4.15	3.18	$3.39*10^{-10}$	330	$6.91*10^{-5}$	15.9	/	$1.89*\ 10^{-6}$
SCL	Artificial sweetener	12.52	-1	$3.99*10^{-19}$	10	/	$2.27*10^4$	/	$3.25*10^{-14}$
SLD	Antibiotic	6.36	-0.09	/	/	/	77	/	

Table 2 Scientific literature overview of the influent (IN) and effluent (OUT) concentrations and removal rate (R) of the target OMPs in WWTPs

OMPs	IN [µg/L]	OUT [µg/L]	R [%]	References
BE	0.005 – 4.75	0.0008 – 3.42	(-6) – 99	(Balakrishna et al., 2017; Bijlsma et al., 2014; Castiglioni et al., 2006; Cosenza et al., 2018; Pal et al., 2013; Petrie et al., 2014; Senta et al., 2013; Skees et al., 2018)
THC-COOH	0.015 – 0.10	0.001 – 0.044	68 – 98	(Cosenza et al., 2018; Senta et al., 2013)
AM	0.002 – 4.72	0.0006 – 2.24	(-150) – 96	(Balakrishna et al., 2017; Petrie et al., 2014; Senta et al., 2013)
ME	0.001 – 0.39	0.0002 – 0.50	(-19) – 98	(Balakrishna et al., 2017; Cosenza et al., 2018; D'Alessio et al., 2018; Petrie et al., 2014; Senta et al., 2013)
KTP	0.00013 – 11.24	0.00034 – 0.146	16 – 98	(Behera et al., 2011; Couto et al., 2019; Deblonde et al., 2011; Lishman et al., 2006)
SMX	0.00029 – 4.97	0.02 – 0.45	(-143) - 86	(Balakrishna et al., 2017; Behera et al., 2011; D'Alessio et al., 2018; Deblonde et al., 2011; Petrie et al., 2014)
CBZ	0.043 – 2.59	0.00037 – 3.117	(- 90) – (-3)	(Balakrishna et al., 2017; Behera et al., 2011; D'Alessio et al., 2018; Deblonde et al., 2011; Krzeminski et al., 2019; Petrie et al., 2014; Tran and Gin, 2017)
TMT	0.033 – 0.29	0.013 – 1.152	(-290) - 100	(Balakrishna et al., 2017; Behera et al., 2011; D'Alessio et al., 2018; Deblonde et al., 2011; Petrie et al., 2014)
LCN	0.015 – 19.40	0.043 – 9.089	(-248) – 70	(Balakrishna et al., 2017; Behera et al., 2011; Verlicchi et al., 2012)
P4	0.009	0.0004	55 - 90	(Couto et al., 2019; D'Alessio et al., 2018)
E1	0.0032 – 0.005	0.0003 – 0.024	57 - 100	(Barbosa et al., 2016; Behera et al., 2011; Petrie et al., 2014; Zhang and Fent, 2018)
E2	0 – 0.005	0 – 0.0001	47 - 100	(Barbosa et al., 2016; Behera et al., 2011; Petrie et al., 2014; Zhang and Fent, 2018)
EE2	0 – 0.022	0.00005 – 0.0062	18 - 94	(Krzeminski et al., 2019; Petrie et al., 2014; Zhang and Fent, 2018)
PFOA	0.0002 – 2334.0	0.00016 – 4.30	0 – 90	(Bijlsma et al., 2014; Causanilles et al., 2017; Gómez et al., 2012; Mackuľak et al., 2016; Nefau et al., 2013; Senta et al., 2013)
PFOS	0.001 – 16.00	0.00003 – 0.635	0 - 69	(Bijlsma et al., 2014; Causanilles et al., 2017; Mackuľak et al., 2016; Nefau et al., 2013; Senta et al., 2013)
ATZ	0.001 – 28.00	0.002 – 4.04	24 - 70	(Ahmed et al., 2017; Kim et al., 2018; Loos et al., 2013; Luo et al., 2014)
PYZ	/	/	/	/
NPX	1 – 7.76	0.0082 – 2.7	50 - 91	(Ahmed et al., 2017; Kim et al., 2018; Loos et al., 2013; Patrolecco et al., 2015; Tran and Gin, 2017)
SCL	1.1 – 46.1	0.0017- 48.9	/	(Loos et al., 2013; Tran et al., 2018)
SLD	0.013 – 5.1	0 - 0.164	78 - 100	(Loos et al., 2013; Morlay et al., 2018)

1.2 Removal processes at laboratory scale

The studies of the removal processes of OMPs in activated sludge treatment were carried out through batch tests and continuous feeding tests.

The batch mode was applied to evaluate the contribution of different processes in the removal of not commonly studied OMPs, i.e. benzoylecgonine, 11-nor-9carboxy-Δ9-THC, methamphetamine, perfluorooctanoic acid and perfluorooctanesulfonic acid. Moreover, this test allowed to determine the processes kinetics.

The continuous feeding mode is easier to compare with the functioning of a real scale reactor, even if it is carried out under controlled conditions. In the present work, it was used to study some biological characteristics of the activated sludge treatment, which were enzymes activity and bacteria speciation, in order to find their relations with the removal of 8 different OMPs and to propose a strategy to improve their removals.

1.2.1 Batch tests

Within the wide class of OMPs, the first step of the present study focused on some drugs of abuse, specifically benzoylecgonine (BE), 11-nor-9carboxy-Δ9-THC (THC-COOH) and methamphetamine, and on the most abundant perfluorinated compounds in the environment (perfluorooctanoic acid (PFOA) and perfluorooctanesulfonic acid (PFOS)).

Conventional secondary processes (activated sludge) represent the most extensively used and studied systems for domestic sewage treatment. However, these processes have not been designed to address the presence of OMPs in the wastewater; some removal/transformation of these compounds can also occur in the WWTPs, but their extent is still uncertain and dependent on a number of parameters and conditions. Based on the literature findings, WWTPs are now considered the main source of release of drugs and other OMPs into the environment through both effluent and sludge (Díaz-Cruz et al., 2009).

The double purpose of the study, carried out through laboratory scale investigations, was to optimize the analytical method for the detection of these compounds in wastewater and sludge of a WWTP and also to assess the removal rate through abiotic and biotic processes in the biological reactor of the WWTP. The results obtained allowed to assess the optimal conditions of the analytical method: therefore, under these conditions, the method was suitable for rapid and reproducible measurements, minimizing the interferences due to the other compounds always found in wastewater and sludge. The contribution of biodegradation and other processes (e.g. adsorption and volatilization) were quantified and the kinetic parameters determined. Furthermore, it was evaluated (through a standard respirometric procedure, n. 209 OECD) if the presence of these contaminants at increasing concentrations can negatively affect the microbial activity in the biological reactor, and therefore the nitrification and COD oxidation process.

The experiments were carried out for MET, THC-COOH and BE separately, in order to evaluate their individual effects and processes. PFOA and PFOS were studied using a solution containing both compounds together, because their fate in wastewater is usually linked.

The specific purposes of this part of the Ph.D. research were addressed through the following steps:

- *Validation of the analytical method for OMPs detection:* to investigate and validate the analytical method that allows a rapid detection of the 5 target OMPs in wastewater and sludge samples;
- *Activated sludge tests:* to determine the role of biodegradation and other processes in activated sludge reactors during secondary treatment in WWTPs;
- *Respirometric tests:* to evaluate the response of the biomass in biological reactors to increasing concentrations of contaminants;
- *Equilibrium tests:* to describe the adsorption processes of target compounds on activated sludge flocs;
- *Leaching tests*: to evaluate the amount of the adsorbed contaminants that can be later released from the sludge, when adsorption processes were proved to be relevant.

1.2.2 Continuous feeding tests

Batch tests were useful to assess the removal processes involved in activate sludge treatment. Complementarily, an in-depth analysis of the enzyme biocatalytic processes was carried out in order to enhance the removal rate of the OMPs in biological reactors. This investigation took place at The University of Auckland, New Zealand.

Several approaches have been studied to further enhance the efficacy of the biological processes, particularly in the case of the OMPs showing lower biodegradability. An innovative strategy based on the stimulation of enzyme biocatalytic processes by employing environmental stresses conditions, was proposed by Singhal and Perez-Garcia (2016). More recently, the same research group demonstrated that by a fast change of the dissolved oxygen (DO) concentration inside reactors it is possible to shock the microbial community, which in turn alters the composition of bacterial communities and performance in relation to the OMPs degradation capability (Bains et al., 2019). Further studies confirmed that an oxidative stress can stimulate the production of specific enzymes which allow an increase of OMPs removal rate (Alneyadi et al., 2018a; Gonzalez-Gil et al., 2019). Indeed, certain environmental pressures or genetic defects can induce the cells to produce Reactive Oxygen Species (ROS) (e.g. H_2O_2, $^{\bullet}O^{-}_2$,$^{\bullet}OH^{-}$) in amounts that exceed the management capacity of the cells (Mishra et al., 2005). Therefore, microorganisms alter their metabolism and activate defence strategies in order to avoid damages caused by the oxidative stress. A small change in cellular oxidant status can be sensed by specific proteins which regulate a set of genes encoding antioxidant enzymes, in order to induce the adaptive metabolism including ROS elimination and reparation of oxidative damages (Gambino and Cappitelli, 2016). These enzymes, more specifically oxidoreductase and hydrolase, have been reported to have the ability to catalyse the oxidation and hydrolysis, respectively, of recalcitrant compounds, such

as pharmaceuticals (i.e. Naproxen, Carbamazepine and Sulfamethoxazole) (Naghdi et al., 2018; Tran et al., 2013). Nevertheless, most of the published studies focused on extracted enzymes and to their application as tertiary treatments (Asif et al., 2018; Naghdi et al., 2018). However, the application of extracted enzymes is difficult to implement on a routine-base in full scale WWTPs because it requires high skill operators and a microbiological support, which are usually lacking at the plant; furthermore, employment of tertiary treatment only for the application of extracted enzymes increases costs of construction and operation (Alneyadi et al., 2018b).

In the present study, the strategy proposed by Bains et al. (2019) was further investigated to assess its effectiveness in inducing the synthesis of OMPs degrading enzymes also under different operating conditions. Particularly, the strategy applied is based on exposing microbes in the activated sludge process to cycles of stressing and non-stressing environmental conditions made by acting on the dissolved oxygen. Particularly, the hypothesis is that a fast change of the oxygen concentration (afterwards referred to as a dissolved oxygen perturbation) can determine an oxidative stress on the biomass, which in turn enhances the activity of specific enzymes capable of catalysing the biodegradation reactions of some OMPs (as described in Figure 4). Therefore, controlling the duration of the aeration phase can yield an improvement of the OMPs removal, by stimulating the activity of target enzymes and changing microbial speciation.

In the previous work by Bains et al. (2019), microorganisms were exposed to different temporal DO perturbations, the sludge used as inoculum for the mixed microbial culture came from a dairy wastewater and the mixture of OMPs investigated in the study contained Sulfamethoxazole, Carbamazepine, Tylosin, Atrazine, Naproxen and Ibuprofen. In the present case, inoculum was collected at a full-scale WWTP treating a domestic sewage, and the mixture of OMPs was extended to include a wider range of compounds: pharmaceuticals (Sulfamethoxazole (SMX), Sulfadiazine (SLD), Lincomycin (LNC), Carbamazepine (CBZ), Pyrazole (PYZ) and Naproxen (NPX)), pesticides (Atrazine (ATZ)) and artificial sweeteners (Sucralose (SCL)). These compounds were selected as they are resistant to biological process and are also more frequently found in the influent to WWTPs (Stevens-Garmon et al., 2011; Tiwari et al., 2017; Trapido et al., 2014).

A further step of knowledge with respect to the previous study was also the focus on the nitrogen removal process: particularly, it was investigated if the selected dissolved oxygen perturbations can also affect the nitrification and denitrification rate inside the same biological reactor (A. Chiavola et al., 2017; Han et al., 2018; He et al., 2018; Metcalf & Eddy, 2015). Since the proposed strategy implies a reduction of the aeration duration in the reactor, the simultaneous denitrification-nitrification processes might be stimulated, with an operating-costs saving.

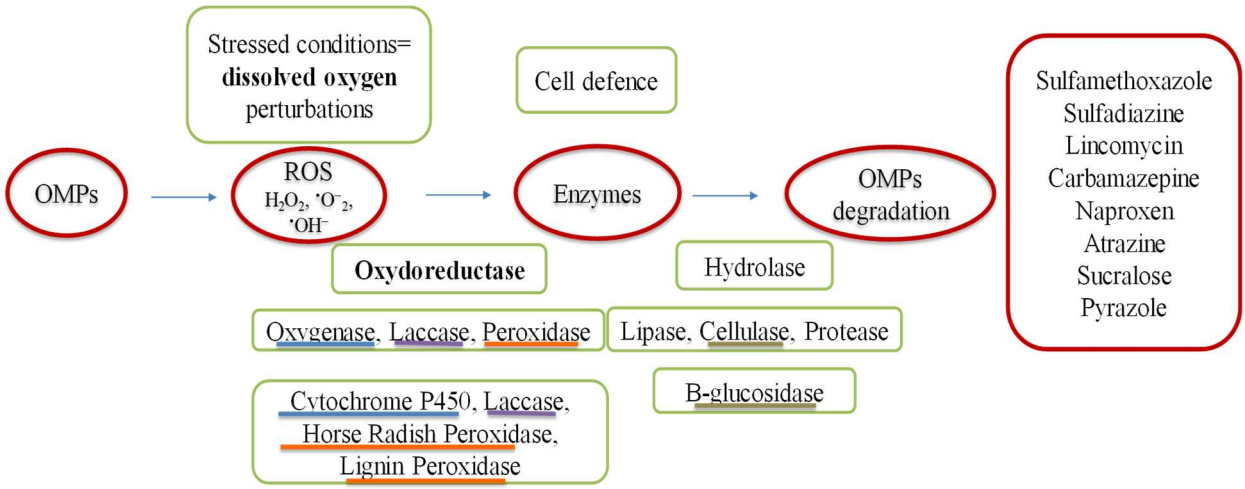

Figure 4 Theoretical approach of the continuous feeding mode test

1.3 Removal processes at real scale

The research included also experimental activity at full-scale plants, in order to validate the experimental results so far obtained in the laboratory scale in the case of more complex real samples. The first full-scale part was about the occurrence, removal and seasonal variation of OMPs in WWTPs, through a wide monitoring campaign carried out in Italy. The second study concerned the monitoring of transformation products formation through biological treatments.

1.3.1 Wastewater Treatment Plants

According to several studies, removal efficiency of OMPs was found to be strongly dependent on the technology implemented at the WWTP (Loos et al., 2013). In Italy, mainly primary and secondary treatments are performed, with the latter being based on conventional activated sludge, while tertiary treatments are less commonly applied (Patrolecco et al., 2015). Primary treatments do not contribute significantly to OMPs removal because they operate only separation of solids particles and somwtimes colloids, while usually OMPs are not hydrophobic enough to be adsorbed by solids and removed in this stage. Several studies proved that biological treatments are effective for biodegradable compounds OMPs, such as illicit drugs (Chiavola et al., 2019);, by contrast, they cannot remove un recalcitrant OMPs while tertiary treatments can be more useful to this purpose (Garcia-Rodríguez et al., 2014; Morlay et al., 2018).

The experimental survey on WWTPs examined influent and effluent streams of 76 plants over about 2 years, and focused on 13 OMPs belonging to the class of illicit drugs, pharmaceuticals and steroids. The illicit drugs and their metabolites consisted of: Benzoylecgonine (BEG), 11-nor-carboxy-Δ9-tetrahydrocannabinol (THC-COOH), Amphetamine (AM), Methamphetamine (ME). Pharmaceuticals included: Ketoprofene (KTP), Sulfamethoxazole (SMX), Carbamazepine (CBZ), Trimethoprim (TMT), Lincomycin (LCN). Steroids included: Progesterone (P4), Estrone (E1), 17β Estradiol (E2), 17α Ethynylestradiol (EE2).

The aim of this part of the study was to assess the occurrence and removal of the target OMPs in a wide set of WWTPs. Additionally, the seasonal variation of the influent concentration was evaluated and the overall efficiency of the plants, according to the treatments level (i.e. due to the combination of primary, secondary and tertiary treatments), was estimated. The results provided an enhancement of the current knowledge about OMPs in WWTPs.

1.3.2 Drinking Water Treatment Plants

As mentioned above, in the past ten years a new issue was highlighted related to OMPs removal: the formation of transformation products (TPs) during wastewater and water treatment processes. Transformation products are often unknown substances and they can be as or more toxic than their precursors, also referred to as parent compounds (PCs) (Li et al., 2017).

Several studies have focused on TPs produced by wastewater treatment and on their environmental risk assessment (Bletsou et al., 2015; Schollée et al., 2018, 2016; Schymanski et al., 2015). However, possible formation of TPs during these drinking water treatments remains to be elucidated (Benner et al., 2013).

Since TPs are often unexpected and unpredictable, an analytical method of detection that can identify compounds for which no previous knowledge is available. A promising method was shown to be the non-target screening (NTS) based on liquid chromatography (LC) coupled to high-resolution tandem mass spectrometry (HR MS/MS). With NTS target, suspect and non-target compounds can be analysed in a single analytical run (Bletsou et al., 2015). However, as a single LC-HRMS sample can result in thousands of so called features, i.e. mass and retention time pairs associated with a signal intensity, prioritization step is needed to limit the number of unknown peaks to be identified (Schollée et al., 2018). The computational workflows to prioritize TPs from NTS data follow two general strategies; the first is a true non-target screening strategy that considers all detected features as mathematical sets and treats them based on statistical tools or relational considerations such as temporal, spatial, or process-related connections (Bletsou et al., 2015; Schollée et al., 2016). The second strategy is based on suspect screening and relies on the prediction of possible TPs through computational tools (Djoumbou-Feunang et al., 2019; Li et al., 2017) (https://envipath.org/, http://biotransformer.ca/). It allows to retrieve a list of potential transformation products for their respective parent compounds under specific conditions (e.g. environmental microbial degradation or human metabolism), the masses of which can then be searched for in the NTS data. Finally, with both strategies, the structures of the prioritized features, i.e. potential TPs, are elucidated based on the match of mass spectrometric information of the full scan (MS1) and fragmentation spectra (MS2), and spectral libraries or *in silico* fragmentation tools, such as MetFrag, ChemSpider or mzCloud (Hollender et al., 2017).

One of the challenges in TPs identification in drinking water treatment is related to the low concentration of the contaminants, both PCs and TPs. To facilitate the identification, some studies focused on laboratory experiments at elevated concentrations. Brunner et al. (2019) studied the TPs of carbamazepine, clofibric acid and metolachlor during rapid sand filtration at lab-scale at initial concentration of 10 µg/L. Kaiser et al. (2014) investigated the transformation of oxcarbazepine, 10-hydroxy-carbamazepine, and 10,11-dihydro-10,11- dihydroxy-carbamazepine during sand filtration at 5 µg/L.

The aim of the present study was to propose a useful workflow for TPs monitoring. The workflow was validated through the application to 8 real scale water treatment plants in The Netherlands and Belgium, particularly to rapid send filters (RSF), since they are one of the most common water treatments employed worldwide. A number of studies have reported the removal of OMPs in rapid sand filters mainly due to biotic processes (Hedegaard et al., 2014; Hedegaard and Albrechtsen, 2014; Zearley and Summers, 2012). For this reason, the treatment was considered interesting to assess how to monitor TPs. The study was carried out at the KWR, Water Research Institute (The Netherland). TPs identification was achieved through a combined data-driven approach based on feature intensity profiles for

prioritization and suspect screening for parent compound identification, TPs prediction with the metabolite prediction tool BioTransformer, suspect screening for predicted TPs and structural elucidation of suspect TPs matches. For the best of our knowledge, this is the first of such an application to real scale drinking water treatment.

Materials and Methods

1.4 Removal processes at laboratory scale

1.4.1 Batch tests

1.4.1.1 Chemicals

Standard (±)-Methamphetamine (ME), 11-nor-carboxy-Δ9-tetrahydrocannabinol (THC-COOH) and benzoylecgonine (BE) solutions were purchased from Sigma-Aldrich Company (Gillingham, UK) at a concentration of 100 µg/mL in methanol. Standard solutions of Perfluorooctane sulfonic acid (PFOS) and perfluorooctanoic acid (PFOA) were purchased from *Ultra Scientific* Italia S.r.l., each one at a concentration of 200 µg/mL in methanol. The solutions were then diluted in methanol at 99% (w/v) to achieve the fixed concentrations required for the batch tests, these solutions were also used to supply the fixed concentration of organic carbon substrate.

Perfluorooctane Sulfonate sodium salt (13C8, 99%) was the isotopically labelled compound used as internal standard (IS) for PFOA and PFOS measurement; it was purchased from Cambridge Isotope Laboratories, Inc. at a concentration of 50 µg/mL. Main characteristics of the contaminants are reported in Table 1 (see page 24).

Activated sludge was collected from the return loop of the secondary settlement tank of a full-scale WWTP treating domestic sewage and stored at 4°C until use for batch tests (storage time less than one week). Biological batch tests were carried out providing the activated sludge with a solution containing both macro- and micro-nutrients needed for the metabolic activity. Particularly, nitrogen and phosphorous solutions were made by dissolving ammonium chloride (NH_4Cl) and sodium dihydrogen phosphate (NaH_2PO_4) into deionized water (MilliQ water), respectively. Micronutrient solution was made according to OECD n. 209 (OECD, 2010), i.e. by dissolving into 1 L deionized water the following components: 0.7g NaCl, 0.4g $CaCl_2 \cdot 2H_2O$, 0.2g $MgSO_4 \cdot 7H_2O$. In some tests, nitrification was inhibited by using a solution of N-allylthiourea in MilliQ water at a concentration of 5.8 g/L (ATU) as inhibitor. Organic carbon substrate was supplied by the methanol solution at 99% (CH_3OH). All the solutions were always kept stored at 4°C.

1.4.1.2 Experimental set-up

Activated sludge tests

The initial concentrations of contaminants in the experiments were as follows: 50, 100 and 200 ng/L of MET, 500, 2000 and 4000 ng /L of BE, 50, 150, 300 and 2000 ng /L of THC-COOH, and 200, 500, 1000, and 4000 ng/L of each PFOA and PFOS. These values were chosen because within the range indicated by the scientific literature as the most commonly measured in real wastewater, as reported in Table 2 (Nefau et al. 2013; Senta et al. 2013; Bijlsma et al. 2014; Mackuľak et al. 2016; Causanilles et al. 2017, Deblonde et al. 2011; Irvine et al. 2011; Baker and Kasprzyk-Hordern 2013).

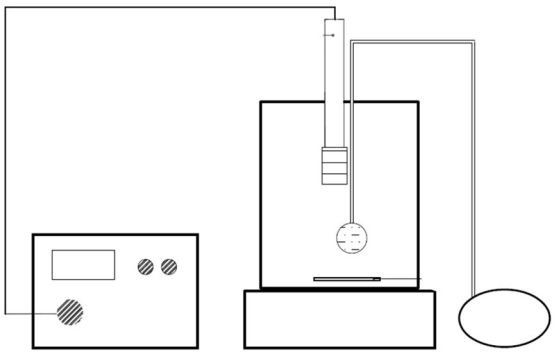

Figure 5 Experimental set-up of batch tests

The potential removal processes were studied using the similar experimental setup as outlined in a previous work by Chiavola et al. (2017). For instance, a series of batch tests was performed in a 600 mL volume glass flask (500 mL operating volume), see Figure 5. Tests were repeated in duplicate, and the results obtained averaged. Each flask was placed on a jar tester to provide a mechanical stirring in order to maintain the content under completely mixed and aerated conditions; the flasks were covered with aluminium foils to avoid photo-degradation phenomena while the temperature was maintained within the range 22±2 °C. Through the addition of NaOH 30% (w/v), it was possible to maintain pH within 7.2-8.0, which is the range that ensures optimal conditions for nitrification (Metcalf and Eddy, 2013).
Prior to the addition of the contaminant solution and nutrients, the activated sludge was kept under completely mixed and aerated conditions for 24 h in order to bring the biomass into the endogenous respiration state. Tests were started (t=0) when the Oxygen Uptake Rate measurements were at about 0.1 mg/L·min. The overall duration of each test was fixed at 24 h based on preliminary tests, with the aim to guarantee the achievement of equilibrium conditions. During the tests, the concentration of the contaminants in the flasks was measured at fixed time intervals (i.e. 0, 3, 5, 6 and 24 h) to determine kinetics of the removal process.
Nitrification and carbon removal were also monitored, by analysing the following parameters at different sampling times: Chemical Oxygen Demand (COD), NH_3-N, NO_2-N and NO_3-N, Mixed Liquor Suspended Solids (MLSS) and Mixed Liquor Volatile Suspended Solids (MLVSS) concentrations. The sample volume at each contact time was equal to 20 mL, considered enough for all the analytical determinations mentioned above. Sampling was carried out under stirring conditions, in order to collect each compound and phase in the same proportion. OMPs concentration was also measured in the solid phase at the beginning and at the end of the tests.

Five series of batch tests were carried out for each contaminant concentration. The series differed based on the type of mixed solution used in the batch, with the aim to evaluate contribution of each of the following processes to OMPs removal:

1) *overall biological process tests:* biodegradation by heterotrophic and autotrophic biomass;

2) *heterotrophic process tests:* biodegradation by heterotrophic biomass;

3) *inactivated sludge tests:* adsorption onto sludge flocs;

4) *control tests*: other abiotic processes (e.g. ionization, hydrolysis and volatilization);

5) *blank tests:* biological processes in absence of contaminants.

Details of each series are reported below.

Series A - Overall biological process tests

This test was accomplished with the aim to evaluate the overall biological process, i.e. involving both heterotrophic and autotrophic bacteria. The flasks were filled by a mixed solution containing a sample of activated sludge taken from the oxidation tank of a full-scale WWTP for domestic sewage, the OMPs-contaminated solution and micro- and macro-nutrients, in order to simulate the main components of the mixed liquor in the biological reactor of the WWTP. The initial concentrations inside the flasks were set as follows: 3000 mg/L MLSS, 300 mg/L COD (including methanol added through OMPs solution), 30 mg/L NH_3-N, 6 mg/L P and 50 mL of micronutrients solution (according to OECD n. 209). These concentrations allowed to obtain inside the reactors a value of the C:N:P ratio equal to 100:10:2, considered suitable for the microbial activity.

Series A_{he} - Heterotrophic process tests

The aim of this series of tests was to evaluate only the heterotrophic biomass activity in the presence of OMPs. The mixed solution was the same as in *Series A*, except for the addition of 23.2 mg/L ATU (10^{-4}mol/L) in order to cause 100% inhibition of nitrifying activated sludge (ISO 8192) (OECD, 2010).

Series S - Inactivated sludge tests

This series of tests was performed with the aim to evaluate only adsorption of OMPs onto sludge flocs. To this purpose, the test was carried out using inactivated sludge (by adding sodium azide 0.2% w/v or by maintaining the sludge for 30 min at 120°C in autoclave) and the OMPs-contaminated solution. Sludge inactivation was considered successful if DO concentration, monitored inside the flasks, never decreased throughout the duration of the test (Ying and Droste, 2015).

Series C - Control tests

Each flask was filled with OMPs-contaminated solution and MilliQ water only, in order to evaluate contribution of abiotic processes such as ionization, hydrolysis and volatilization.

Series B - Blank tests

Blank tests were conducted under the same conditions as in *Series A* and *Series A_{he}* as above described, and without OMPs addition. This type of test was performed with the aim to compare the biomass activity in the presence and absence of OMPs.

Respirometric tests

The potential inhibition of effects of OMPs on biomass activity were studied by using the same experimental setup and the type of batch tests as above described. The studies were performed by following the Activated Sludge, Respiration Inhibition Test, Carbon and Ammonium Oxidation OECD 209 method (OECD 2010). This method, through the oxygen uptake rate (OUR) measurements, allows to determine how different concentrations of a test compound may affect microorganisms' activity.

The test method indicates to measure SOUR at least after 3 h since the beginning; in the present study, SOUR was measured after 3 h and in some test also 6 h. Particularly, the flasks were continuously aerated for 3 h; then, aeration was turned off and DO(t) was recorded every minute for a fixed time interval of 10 minutes. The linear regression of DO(t) data allowed to determine the average OUR (and SOUR) within the interval of 10 minutes. The linear fitting was considered acceptable when the correlation coefficient, R^2, was above 0.95. The same procedure was repeated after 6 h since the beginning of the batch test.

The Respiration Inhibition Test allows to determine the value of ECx, which represents the concentration that reduces the oxygen uptake rate by X(%). At the end of the test, the inhibition percentage is calculated by comparing the SOUR values measured in presence of the test compound and in absence (blank test).

The effect on carbon oxidising microorganisms only was also determined by measuring (according to the method) the SOUR after inhibition of nitrifiers bacteria through the addition of an inhibitor such as N-allylthiourea.

Equilibrium tests

Equilibrium tests were performed with the aim to identify the isotherm model of the contaminant adsorption onto the inactivated sludge.

The tests were performed using sludge samples from the *inactivated sludge test* when the adsorption process have shown to be relevant, i.e. in the case of PFOA, PFOS and THC-COOH.

In the experimental set-up for PFOA and PFOS equilibrium tests, initial concentrations were fixed at 1000 ng/L each one, which was considered representative of the average value in the range tested in the present study. Five different dosages of sterilized sludge were added to the flasks: 1, 2, 3, 4 and 5 g/L TS (total solids). The duration of the test was fixed at the time corresponding to equilibrium of the mass transfer process. At the beginning (t=0) and at the end of the tests (t=24h), concentrations of TS, PFOA and PFOS in the liquid and sludge phases were measured. pH was maintained within the 7.2-8.0 range, as in the activated sludge tests, through the addition of NaOH 30% (w/v). The following isotherm models were applied to the experimental data of the equilibrium tests: Langmuir, Freundlich, Brunauer–Emmett–Teller (BET), Dubinin-Radush Kevich (DRK), Tempkin and Harkins-Jura (Erhayem et al., 2015; Foo and Hameed, 2010; Saad et al., 2017; Shanavas et al., 2011). The best fitting model was considered that one providing the highest value of the correlation coefficient (R^2) between the experimental and modelled data, based on the linear form of the model equation.

Leaching tests

The release of contaminants adsorbed on the sludge is considered mechanism potentially responsible of environmental risks. When the adsorption process was proved to be relevant, particularly for PFOA and PFOS, leaching tests according to standard UNI EN 12457-2 procedure were performed in order to evaluate the potential release of contaminants adsorbed on the sludge.

The sludge samples were collected at the end of the equilibrium tests conducted at 4 and 5 g/L TS. Prior to the use, they were centrifuged at 4000 rpm for 10 minutes, in order to eliminate the supernatant. The leaching agent used for the test was deionized water in accordance to the standard procedure (UNI EN 12457-2). A proper volume of leaching agent (33 mL and 41 mL for the tests performed at 4 and 5 g/L TS, respectively) was added to the sludge in order to obtain a liquid/solid ratio L/S=10 L/kg. The content of the flasks was maintained under mixed conditions using a magnetic stirrer, for t=24 h. At the end of the tests, contaminant concentration in the liquid phase was measured and the mass of contaminants leached by the sludge was determined, as required by the UNI EN 12457-2 procedure.

1.4.1.3 Analytical methods

Detection of control parameters

The concentrations of the following parameters were determined according to APHA methods (Eaton et al., 2005): COD, NH_3-N, NO_2-N, NO_3-N, MLSS and MLVSS. pH, temperature and dissolved oxygen (DO) were measured using standard probes (Hanna Instruments).

Detection of OMPs concentration

The analytical technique chosen for the quantitative analysis of the contaminants in the liquid and solid phases was Ultra-Performance Liquid Chromatography coupled to tandem Mass Spectrometry (UPLC–MS/MS).

Each contaminant required specific analytical method conditions, described as follow:

Methamphetamine

The UPLC was an Ultimate 3000 RS Thermo, equipped with two pumps, degasser, column oven compartment and auto sampler. The MS/MS was the type 5500 AB Sciex Q-Trap, equipped with Atlas Copco FS2 compressor, FX1 dryer, 270 litres tank and nitrogen generator Zephyr Zero 16 LC-MS. The liquid sample preparation included only a filtration step by using a 0.2 μm membrane filter of regenerated cellulose, followed by direct injection. This procedure makes the method more suitable for routine and rapid analysis.

The applied analyser and instrumental conditions were as follows:

-UPLC-MS/MS Chromatography column Phenomenex Kinetex 2.6µm Biphenyl 100A, 50x2.1 mm with security-guard column at 30°C. Mobile phase A: Milli-Q Reference A+ water with a chromatography column acidified with 0.1% formic acid; mobile phase B: LC-MS methanol acidified with 0.1% formic acid. The gradient elution conditions were from 95% A and 5% B to 0% A and 100% B in 10 min. Flow was 0.4 mL/min. Each drug was quantified by Multiple Reaction Monitoring ratio (MRM) using the two most abundant precursor/product ion transitions.

-Analytical determination of drug concentration in the solid phase was carried out by following the Ultrasound assisted Extraction (USE) procedure, adding 10 mL of 50% Methanol and 50% MilliQ water, for 15 min at room temperature. After this pre-treatment, the sample was filtered using a 0.2 µm membrane filter and then injected as described above for the liquid phase. The recovery of the method was > 75% (as reported in Table 5).

11-nor-9carboxy-Δ9-THC and benzoylecgonine

The analytical method for the detection of THC-COOH and BE in wastewater is based on WARC, TZV, NIAES, OCWD, 2008 (Chiavola et al., 2016). The liquid sample pre-treatment consists only of a filtration step using 0.2 µm membrane filter of regenerated cellulose. The method was designed in order to avoid internal standards use due to the complexity of their supply and because the direct quantification showed to be reliable. This procedure makes the method more suitable for routine and rapid analysis.

According to the method, filtration is followed by a direct injection in the UPLC-MS/MS system with the instrumental conditions reported below:

1) UPLC: Ultimate 3000 RS Thermo, with two pumps, degasser, column oven compartment and auto sampler; Chromatography column was Phenomenex Kinetex 2.6µm Biphenyl 100A, 50x2.1 mm with security-guard column at 30°C. Mobile phase A: 100 % Milli-Q water acidified with 0.1% formic acid; mobile phase B: 100 % LC-MS methanol acidified with 0.1% formic acid. The gradient elution conditions were from 95% A and 5% B to 0% A and 100% B in 8 min. Flow was 0.3 mL/min. Injected volume was 20 µL.

2) Mass spectrometer: 5500 AB Sciex Q-Trap with Atlas Copco FS2 compressor, FX1 dryer, 270 L tank and nitrogen generator Zephyr Zero 16 LC-MS. The applied UPLC-MS/MS parameters are reported in supplementary materials (Table S.M. 1).

Each drug was quantified by MRM (Multiple Reaction Monitoring ratio) using the two most abundant precursor/product ion transitions. The overall response time for each liquid sample was below 30 min.

The solid sample pre-treatment was carried out by following the Ultra-Sound assisted Extraction (USE) procedure as described below:

50 mL of wastewater samples (50 mL) were centrifuged at 4000 rpm for 15 min in order to separate the solid phase from the supernatant;

10 mL of 50% methanol and 50% MilliQ water were added to centrifuged solids. The samples underwent the USE for 15 min at room temperature; then, they were filtered at a 0.2 µm using a

membrane filter and injected as described above for the liquid phase. The recovery of the method was > 75% (as reported in Table 6).

The extraction method was selected based on recent scientific studies and previous tests of the same authors, where two different extraction procedures were compared: Accelerated Solvent Extraction (ASE) and Ultrasound assisted extraction (USE). The USE method provided better results; furthermore, it was considered preferable also because the temperature is maintained at room level while the investigated molecules (mainly THC-COOH) might be unstable at high temperature and pressure (Álvarez-Ruiz et al., 2015; Gago-Ferrero et al., 2015).

Perfluorooctane sulfonic acid and perfluorooctanoic acid

The EPA method 537 was followed, amended so as to be suitable for wastewater analyses (Chiavola et al., 2020; Kwon et al., 2014).

For calibration and quantification, the internal standard (IS) approach was followed. The liquid sample pre-treatment consisted only of a filtration step by using a 0.2 µm membrane filter of regenerated cellulose. Before the injection in the HPLC-MS/MS system, 800 µL of supernatant was spiked with 10 µL of IS for the analytes quantification. The instrumental conditions applied are reported below:

1) HPLC: Perkin Elmer Series 2000 equipped with chromatography column Phenomenex Kinetex 2.6 µm F5 100A, 100x2.1 mm and security-guard column. Mobile phase A: 95% LC-MS water and 5% LC-MS methanol with ammonium acetate 20mM. Mobile phase B: 100 % LC-MS methanol with ammonium acetate 20mM. The gradient elution conditions were from 60% A and 40% B to 10% A and 900% B in 9 min. The injected volume was 50 µL, the temperature was 40°C and the flow rate equal to 0.25 mL/min.

2) Mass spectrometer: Applied Biosystem – API 2000 LC-MS-MS System. The applied HPLC-MS/MS parameters are reported in Table S.M. 2.

The overall response time for each liquid sample was below 20 min.

Each contaminant was quantified by MRM (Multiple Reaction Monitoring ratio) using the two most abundant precursor/product ion transitions of the two analytes and the IS.

The solid sample pre-treatment was carried out by following the Ultra-Sound assisted Extraction (USE) procedure: 50 mL of wastewater samples were centrifuged at 4000 rpm for 15 min in order to separate sludge from supernatant; 10 mL of 50% methanol and 50% MilliQ water were added to centrifuged solids. The samples underwent the USE for 15 min at 30°C; then, they were filtered at a 0.2 µm using a membrane filter, spiked with the IS and injected in the HPLC-MS/MS system, as described above for the liquid phase. The USE extraction method was selected since recent scientific studies and previous tests by the same authors showed to be superior to the Accelerated Solvent Extraction (ASE) (Álvarez-Ruiz et al., 2015; Boix et al., 2016; Chiavola et al., 2019; Gago-Ferrero et al., 2015).

1.4.1.4 Validation of the analytical method for OMPs detection

Methamphetamine

The expanded uncertainty of the method was calculated as described below for the two ion transitions:

$$Uexp = K\sqrt{S_A^2 + S_B^2 + S_C^2 + S_D^2} \qquad \text{Eq. 1}$$

The coverage factor (K) used was equal to 2 which gives a level of confidence of approximately 95 % for four degree of freedom.

The four degree of freedom (S_A, S_B, S_C, S_D) considered were:

- Repeatability: instrument precision. Average RSD% was calculated on 5 replicates of three validation concentrations, of the respective integrated areas of the chromatographic peak.
- Bias uncertainty: bias variability in different matrices. It was calculated as RSD% on MET concentrations of 4 solutions defined in the following sections.
- Accuracy: represents the calibration accuracy and was defined by the data processing software Multiquant as RSD% of the experimental point of the calibration curves.
- Pre-treatment uncertainty: derived from the use of micropipettes as RSD % on 10 measurements.

Determination of the limit of detection (LOD) and of quantification (LOQ) was done according to the following procedure: 5 times injection of a sample at a concentration close to the expected LOQ (i.e. 19 ng/L); integration of analyte peaks; calculation of signal-to-noise ratios and their averages values; concentrations calculation; definition of LOQ as the concentration that gives signal to noise ratio equal to 10 multiplication of LOD for a precautionary factor (equal to 2).

Matrix effect tests

A series of tests was carried out using four reference solutions containing the main components typically present in a domestic wastewater, i.e. ammonia, phosphorous and micronutrients, and a fixed MET concentration. For instance, the solutions had the following compositions and were prepared according to the indications provided in section Chemicals:

Solution P: 50 ng/L MET, 25 mg/L P

Solution N: 50 ng/L MET, 60 mg/L NH_3-N

Solution MN: 50 ng/L MET, micronutrients

Solution ATU: 50 ng/L MET, 23.2 mg/L N-allylthiourea (ATU)

The effect of carbon compounds was not investigated since MET solutions are provided diluted in methanol, which is a carbon source.

Tests with Solution ATU were performed in order to check if the addition of ATU, used in some batch experiments described afterwards, could also interfere the analytical determination of MET.

The matrix effect was evaluated by measuring MET concentration in each solution. Then, based on the comparison between the expected (as calculated) and the measured concentration, it was possible to

determine if the detection of MET was compromised by the interaction with the other components of the tested solutions. From a statistical point of view this test coincides with Bias test. Its significance was also evaluated by the Fisher's exact test (F-test): this is a partial test and it is appropriate for the determination of non-random associations between two categorical variables. For instance, the F-test allows to compare the variances of two data sets (S_A^2 and S_B^2). The value of F was calculated as reported below:

$$F_{calc} = \frac{\sigma_A^2}{\sigma_B^2} \qquad \text{Eq. 2}$$

where σ_A^2 is the variance of the difference between the detected concentration in each solution and the expected one, whereas σ_B^2 stands for the repeatability of the analytical method.
The F calculated value was compared to the printout value for n-1, m-1 degrees of freedom representing a significance level equal to 95% (Skolnik, 2009). In this case, n and m were equal to 4. The test is considered valid if:

$$F_{calc} \leq F_{3,3} \qquad \text{Eq. 3}$$

11-nor-9carboxy-Δ9-THC and benzoylecgonine

This part of the study aimed to validate the detection method of BE ad THC-COOH with respect to the effects of the main wastewater components, i.e. carbon, nitrogen, phosphorus and micro-nutrients.
The expanded uncertainty (Uexp) of the method was calculated as described in Eq. 1 for the two ion transitions.
The four elements (S_A, S_B, S_C, S_D) considered were:

- Repeatability: instrument precision. Average RSD% was calculated on the integrated areas of the chromatographic peak of 5 injections, using the concentration of validation as reported in Table S.M. 1. Average RSD% was calculated on 5 replicates of the validation concentration, of the respective integrated areas of the chromatographic peak.
- Bias uncertainty: bias variability was calculated as RSD% of contaminant concentration in different solutions simulating the main components of a typical domestic sewage; particularly, the solutions always contained 50 ng/L of THC-COOH or BE and (1) 25 mg/L P, (2) 60 mg /L NH3-N (3) micro-nutrients, or (4) 900 mg/L COD. The value of 50 ng/L was chosen being near the limit of quantification (LOQ) value of the analytical method.
- Accuracy: represents the calibration accuracy and was defined by the data processing software Multiquant as RSD% of the different points of the calibration curves.
- Pre-treatment uncertainty: derived from the use of micropipettes as RSD% on 10 measurements.

The coverage factor (K) gave 95% as a confidence level. It was determined as the average value of Two Tails T Distribution factor, for the degrees of freedoms (df) calculated with the Satterthwaite formula

(Bettencourt Da Silva et al., 1999). The Satterthwaite formula, shown below, was applied to the most relevant elements of the uncertainty (Repeatability and Bias):

$$df = \left(\frac{S_A^4}{m}\right) + \left(\frac{S_B^4}{n}\right) \Big/ \left(\frac{S_A^4}{(m-1)\cdot m^2}\right) + \left(\frac{S_B^4}{(n-1)\cdot n^2}\right) \quad \text{Eq. 4}$$

where SA and SB stand for the variance of Repeatability and Bias distributions, respectively, whereas (m-1) and (n-1) indicate the degrees of freedom of the same distributions.

The Satterwaite formula is used to estimate the effective degrees of freedom of a Normal distribution when the number of random measurements is small, in order to overvalue the uncertainty, in a precautionary approach (Bettencourt Da Silva et al., 1999).

The limit of detection (LOD) was defined as the concentration that gives signal-to-noise ratio of 10. The limit of quantification (LOQ) was calculated by multiplying LOD for a precautionary factor of 2.

Perfluorooctane sulfonic acid and perfluorooctanoic acid

The analytical method was validated based on the criteria of the 2002/657/EC Commission Decision (Decision 2002/657/EC). The validation parameters were defined and calculated as follows:

Minimum required performance limit (MRPL), determined as the concentration which gives a signal/noise ratio ≥ 10; the test was performed on n. 6 replicates using MilliQ water (MRPLW) and the experimental matrix (MRPLm);

Repeatability (Rep), calculated as the relative standard deviation percentage (RSD%) on the measured concentration of n. 6 injections; the samples were made by spiking 68 µg/L PFOA and PFOS and 10 µL of IS in MilliQ water (Rep_W) and the experimental matrix (Rep_m);

Linearity, expressed as R^2 of the calibration curves;

Recovery from the liquid (REC_L) and sludge (REC_S) phase, obtained by spiking 68 µg/L PFOA and PFOS and 10 µL of IS in the experimental matrix sample using glass flasks; the test was performed in triplicate and the results compared with the initial concentration; the REC values were also used to correct the concentrations, in both liquid and sludge phases, of the experimental samples in order to discard all the errors; Recovery was calculated based on the mass balance, as follows:

$$REC_S\,[\%] = \frac{M_{sludge}}{M_{spiked} - M_{liquid}} \cdot 100 \quad \text{Eq. 5}$$

$$REC_L\,[\%] = \frac{M_{liquid}}{M_{spiked}} \cdot 100 \quad \text{Eq. 6}$$

where M_{spiked}, M_{sludge} and M_{liquid} represent the mass of PFOA and PFOS that was spiked, measured in the sludge and measured in the liquid, respectively.

1.4.1.5 Calculation methods

Removal processes

Contaminants removal percentage in each series of batch tests was calculated based on the following equation:

$$\text{Removal } (\%) = \frac{C_0 - C_e}{C_0} \cdot 100 \qquad \text{Eq. 7}$$

where C_0 and C_e represent OMPs concentration at the beginning and at the equilibrium time of the batch test, respectively.

In *Series A* and *Series A_{he},* all the processes, i.e. abiotic and biodegradation, were likely to take place. In *Series S,* all abiotic processes were reasonable to occur, while biodegradation was absent since activated sludge was maintained chemically inhibited. In *Series C*, the removal was assumed to be only due to abiotic processes.

Indicating with RB_T, RB_{he}, RA and RO percentage removal due to either only biodegradation, heterotrophic biodegradation (i.e. under inhibited nitrification), adsorption and other abiotic processes, respectively, total removal in the four tests was assumed to be equal to:

$$A(\%) = RB_T + RA + RO \qquad \text{Eq. 8}$$

$$A_{he}(\%) = RB_{he} + RA + RO \qquad \text{Eq. 9}$$

$$S(\%) = RA + RO \qquad \text{Eq. 10}$$

$$C(\%) = RO \qquad \text{Eq. 11}$$

where A(%), A_{he}(%), S(%) and C(%) stand for the total percentage removal measured in *Series A, A_{he}, S and C,* respectively.

The liquid-solid partition coefficient (k_d), calculated as follows:

$$k_d\,[L/kg] = C_S/C_L \qquad \text{Eq. 12}$$

where C_S and C_L represent the concentrations of OMPs in the solid phase (ng/kg) and in the liquid phase (ng/L) (Stasinakis et al., 2013).

Inhibition of biomass activity

The specific oxygen uptake rate (SOUR) was also calculated, by normalizing the OUR to the MLSS content in the batch test, as reported below:

$$SOUR(t) = \frac{DO_0 - DO(t)}{\Delta t \cdot MLSS} \quad \text{Eq. 13}$$

where DO_0 and DO(t) stand for the dissolved oxygen concentration measured at the beginning and at time t, respectively, of the test, while MLSS represents the average solid concentration.

The effect on biomass activity of each tested concentration was expressed as percentage inhibition and calculated as described in OECD n.209 for the total oxygen consumption (I_T%), the heterotrophic oxygen consumption (I_{he}%) and the oxygen consumption due to nitrification (I_N%):

$$I_T\% = [1-(SOUR_T/SOUR_{TB}] \cdot 100\% \quad \text{Eq. 14}$$

$$I_{he}\% = [1-(SOUR_{he}/SOUR_{heB}] \cdot 100\% \quad \text{Eq. 15}$$

$$I_N\% = [1-(SOUR_T - SOUR_{he})/(SOUR_{TB} - SOUR_{heB})] \cdot 100\% \quad \text{Eq. 16}$$

where SOUR and $SOUR_B$ indicate the specific respiration rates in each of the tested conditions and in the corresponding blank test, respectively.

Mass balances of PFOA and PFOS

Experimental data from PFOA and PFOS in the Activated sludge tests and Sterilized sludge tests were analysed by following the mass balance approach, as reported by previous studies (Jelic et al., 2011; Pan et al., 2016). Percentage mass proportions of each contaminant in the liquid and sludge phases (Liquid [%] and Sludge [%], respectively), were calculated at the end of the tests (t=24h) with respect to the mass added at the beginning (t=0). The difference between the mass found in the liquid and sludge phases was referred to as "loss" (Loss [%]) and ascribed to a series of processes and transformations not identified. Calculations were performed as follows:

$$Liquid\ [\%] = \frac{M_L}{M_T} \cdot 100 \quad \text{Eq. 17}$$

$$Sludge\ [\%] = \frac{M_S}{M_T} \cdot 100 \quad \text{Eq. 18}$$

$$Loss\ [\%] = \frac{M_T - M_S - M_L}{M_T} \cdot 100 \quad \text{Eq. 19}$$

where M_L and M_S stand for the mass of contaminant found in the liquid and sludge phases, respectively, at the end of the tests, whereas M_T indicates the mass added to the tests at the beginning. All the values of PFOA and PFOS concentration used for the mass balance calculations were already corrected by the recovery values obtained from the analytical method validation. As a result, the mass not detected due to the analytical method was excluded from the "loss" and considered to represent the effect of the transformation processes.

Leaching potential

The leaching potential of the sludge was calculated as follows:

$$Leached\ mass\ [\%] = \frac{M_l}{M_0} \cdot 100 \qquad \text{Eq. 20}$$

where M_l is the mass of contaminant measured in the liquid phase at the end of the Leaching tests (t=24h) o and M_0 is the mass of contaminant found on the sludge at the end of the Equilibrium tests, which was also the beginning of the Leaching tests.

Kinetic models

The experimental data collected from *activated sludge tests (*both *overall biological* and *inactivated sludge*) were fitted considering different kinetic models. The linear form of each equation, as reported below, was used to find out the best fitting model. For instance, the model providing the higher value of the correlation coefficient, R^2, between experimental and modelled data, was considered as the best fitting one.

The values of the kinetic constants were calculated based on the amount of contaminant removed from the liquid phase during *activated sludge tests*. The following equations were used to this purpose:

Zero-order

$$C(t) = C_0 - k_0 \cdot t \qquad \text{Eq. 21}$$

First-order

$$\ln C(t) = \ln C_0 - k_1 \cdot t \qquad \text{Eq. 22}$$

Second-order

$$\frac{1}{C(t)} = \frac{1}{C_0} + k_2 \cdot t \qquad \text{Eq. 23}$$

k_0, k_1 and k_2 represent the rate constants of the zero, first, second order models, respectively, and C_0 and C(t) indicate concentrations of the contaminants in the liquid phase at the beginning and at any time t of the test, respectively.

$$q_e = \frac{M_{ads}(e)}{MLSS} = \frac{(C_0 - C_e)}{MLSS} \quad \text{Eq. 24}$$

$$q(t) = \frac{M_{ads}(t)}{MLSS} = \frac{(C_0 - C(t))}{MLSS} \quad \text{Eq. 25}$$

Where q_e and q(t) stand for the amount of contaminants per unit mass of adsorbent (i.e. sludge solids) at the equilibrium time and at any time t, respectively (Plazinski et al., 2013).
In Eq. 24 and Eq. 25, $M_{ads}(e)$ and $M_{ads}(t)$ represent the mass of contaminant adsorbed on the sludge at equilibrium time and at any time t before, respectively, during the tests. Measurements of solid concentration at the beginning and at the end of each contact time showed that microbial growth during the tests was negligible. Therefore, the MLSS concentration in Eq. 24 and Eq. 25 was considered equal to the average concentration measured throughout the tests.

Pseudo-first order

$$\ln(q_e - q(t)) = \ln q_e - k'_1 \cdot t \quad \text{Eq. 26}$$

Pseudo-second order

$$\frac{t}{q(t)} = \frac{1}{k'_2 \cdot q_e^2} + \frac{t}{q_e} \quad \text{Eq. 27}$$

Where k'_1 and k'_2 represent the rate constants of the pseudo-first and pseudo-second order models, respectively.
Elovich model

$$q(t) = \frac{1}{b}\ln(ab) + \frac{1}{b}\ln t \quad \text{Eq. 28}$$

Where a is the initial adsorption rate [ng/g/h] b is the desorption constant [mg/g] (Wei et al., 2017).
Intraparticle diffusion model (IDM)

$$q(t) = k_{id} t^{0.5} + C \quad \text{Eq. 29}$$

Where k_{id} represents intraparticle diffusion rate constant [ng/g], C is a coefficient which provides an indication of the thickness of the boundary layer [ng/g] (Saad et al., 2017).

The liquid-solid partition coefficient (k_d), calculated as follows at each concentration, confirmed this result:

$$k_d\,[L/kg] = C_S/C_L \quad \text{Eq. 30}$$

where C_S and C_L represent the concentrations in the solid phase [ng/kg] and in the liquid phase [ng/L] (Stasinakis et al., 2013).

Adsorption isotherms models

The following linear isotherm models were applied to the experimental data of the equilibrium tests (Erhayem et al., 2015; Foo and Hameed, 2010; Saad et al., 2017; Shanavas et al., 2011). The best fitting model was considered that one providing the highest value of the correlation coefficient (R^2) between the experimental and modelled data, based on the linear form of the model equation.

Langmuir

$$\frac{C_e}{q_e} = \frac{1}{k_L \cdot q_m} + \frac{C_e}{q_m} \quad \text{Eq. 31}$$

where k_L is the equilibrium constant [L/g], q_m is the maximum adsorption capacity [ng/g].

Freundlich

$$logq_e = logK_F + \frac{1}{n} logC_e \quad \text{Eq. 32}$$

where K_F is the Freundlich adsorption coefficient and n is the Freundlich exponent.

Brunauer–Emmett–Teller (BET)

$$\frac{C_e}{q_e(C_S - C_e)} = \frac{1}{q_S C_{BET}} + \frac{C_{BET} - 1}{q_S C_{BET}} \frac{C_e}{C_S} \quad \text{Eq. 33}$$

where C_{BET}, Cs and qs are the BET adsorption isotherm [L/ng], adsorbate monolayer saturation concentration [ng/L], theoretical isotherm saturation capacity [ng/g], respectively.

Dubinin-Radush Kevich (DRK)

$$lnq_e = lnq_m - \beta\varepsilon^2 \quad \text{Eq. 34}$$

Where β is a coefficient related to the adsorption energy and ε is the Polanyi's adsorption potential, i.e. $\varepsilon = \mathrm{RT} \ln\left(1 + \frac{1}{C_e}\right)$

Tempkin and Harkins-Jura

$$\frac{1}{q_e} = \frac{B}{A} + \frac{1}{A} log C_e \qquad \text{Eq. 35}$$

Where A and B are the Harkins-Jura constants.

1.4.2 Continuous feeding tests

1.4.2.1 Chemicals

The certified standards of the eight selected OMPs were purchased from Sigma Aldrich and Merck at purities > 99% and dissolved in LC-MS methanol to obtain the OMPs solution at 1000 mg/L of each one. The isotopically labelled (> 99% purity) Carbamazepine-d_{10} (CBZ-d_{10}), Naproxen-d_3 (NPX-d_3) and Atrazine–d_5 (ATZ-d_5) supplied by Sigma-Aldrich were used as internal standards (IS). High purity analytical LC-MS grade solvents (Methanol, Acetonitrile and tert-Butyl methyl ether) were purchased from Merck. Sigma Aldrich also provided oxidoreductases, used as standards, such as lignin peroxidase (LiP), horseradish peroxidase (HRP), laccase (Lacc) derived from cultures of *Trametes versicolor*, cytochrome P450 (Cyt P450) from human 3A4 isozyme microsomes and beta-glucosidase (β-glu) from *Aspergillus niger* as well as their respective enzyme substrates (Methylene Blue (MB), Azure B (AB), 3,4-Dihydroxy-L-phenylalanine (L-DOPA), 2,2'-Azino-bis-3-ethylbenzothiazoline-6-sulfonic acid (ABTS), Sudan Orange G (SO), 4-nitrophenyl-dodecanoate (PNP-D), Indole (INDOLE) and 4-Aminoantipyrine (4-AAP), 4-nitrophenyl N-acetyl-β-D-glucosaminide (PNP-A) and 4-nitrophenyl-β-D-glucopyranoside (PNP-G)). Sodium acetate trihydrate, glacial acetic acid (≥ 99% purity), di-potassium hydrogen phosphate, potassium di-hydrogen phosphate, dextrose and magnesium chloride hexahydrate of ≥ 99% purity were (by Sigma Aldrich) used to prepare enzyme buffers at pH=5 and pH=7, respectively.

A synthetic wastewater (SyWW) was used as a feed to the batch tests. It was made according to Bassin et al. (2011), properly modified in order to have a C:N:P ratio equal to 100:5:1. Sodium acetate trihydrate was the main source of soluble organic carbon (81% of the total amount); besides, also the OMPs solution, made in methanol, provided easy biodegradable organic carbon (19% of the total concentration of COD purchased to the reactors). The SyWW was obtained by dissolving in MilliQ water the following ingredients: 1 mg/L of each OMP; 15.84 g/L $NaCH_3COO{\cdot}3H_2O$; 0.89 g/L $MgSO_4{\cdot}7H_2O$; 0.4 g/L KCl; 1.53 g/L NH_4Cl; 0.30 g/L K_2HPO_4; 0.12 g/L KH_2PO_4; 10 mL/L trace elements. The trace elements solution contained the following components: 50 g/L EDTA; 22 g/L $ZnSO_4{\cdot}7H_2O$; 5.54 g/L $CaCl_2$; 5.06 g/L $MnCl_2{\cdot}4H_2O$; 4.99 g/L $FeSO_4{\cdot}7H_2O$; 1.1 g/L $(NH_4)6Mo_7O_{24}{\cdot}4H_2O$; 1.57 g/L $CuSO_4{\cdot}5H_2O$; 1.61 g/L $CoCl_2{\cdot}6H_2O$ (Bassin et al., 2011). All the solutions were stored at 4°C until their use.

1.4.2.2 Experimental set-up

The activated sludge sample used for the experimental activity was collected from the sludge recycle loop of the secondary settlement tank of the Mangere municipal WWTP in Auckland, New Zealand. Before the use, it was rinsed several times using tap water to remove residual soluble compounds from the previous treatments and then stored at the temperature T= − 20°C.

The tests were performed in bioreactors of 1 L volume. A sample of activated sludge at a concentration of 3000 mg/L MLVSS was added to each reactor, along with 50 mL of 0.2 M PBS solution (Phosphate buffered saline, made according to Stoll and Blanchard (1990) and tap water. Prior to each experimental test, biomass was acclimatized by maintaining it under aerobic conditions for at least t=24 h at room temperature, fed with the same synthetic wastewater (SyWW) as that used in the experimental tests without OMPs (Figure 6). The acclimatization period was considered completed when steady state conditions of nitrogen and carbon removal were achieved. At the end of the acclimatization phase, the experimental tests were started: a proper volume of OMPs solution was firstly added in order to obtain an initial concentration of 0.1 mg/L of each OMP inside the reactor. Then, the supply of the synthetic wastewater (containing 1 mg/L of each OMPs and nutrients as above described) was started in a continuous mode (at a flow rate equal to 0.0347 mL/min) and continued throughout the duration of the tests (t=48 h).

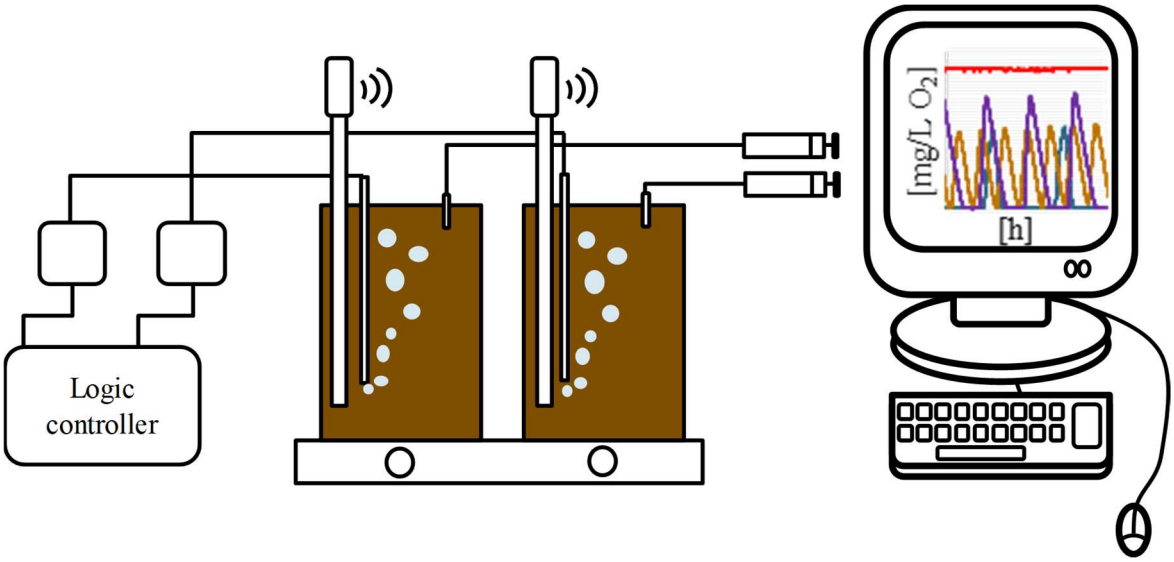

Figure 6 Experimental set-up of continuous feeding tests

The pH value inside the reactors was maintained within the optimal range for nitrification, i.e. 7.2-8, through the addition of the PBS buffer solution at the beginning of the test (Metcalf & Eddy, 2015). The oxygen perturbations were performed by a Millenium 3 CD 20 logic controller connected to solenoids valves, setting the ON and OFF times of the aeration system. The oxygen monitoring system was composed by a Hamilton Device Manager 1.0.0 software equipped with a wireless sensor which was connected to VisiFerm DO sensors. Tests were performed in duplicate and the results obtained averaged. Samples were collected at the following times: t=0, 5, 24 and 48 h. This sampling schedule was designed in order to obtain information during all the conditions of reactor operation. At each contact time, the OMPs concentrations and enzymes activity in the liquid phase were measured.

The target enzymes to be investigated were selected according to previous studies (Alneyadi et al., 2018a; Karigar and Rao, 2011). Nitrification and carbon removal were monitored by measuring the following parameters: acetate (the main source of carbon in the system), NH_3-N, NO_2^--N and NO_3^--N concentration.

During the periods of active aeration (ON cycle), the dissolved oxygen (DO) concentration was maintained in the range 0->5 mg/L by controlling the air flow rate provided through a pump.

The duration of ON-OFF cycles was controlled in order to have different values of the perturbation frequency, f (1/h), defined as the inverse of the duration of an ON-OFF aeration cycle per hour (Eq. 37). Particularly, during each cycle, duration of the ON phase (i.e. presence of aeration) was maintained the same (tON=11 min) whereas the OFF phase (i.e. absence of aeration) was changed accordingly to establish the following frequencies: E1) f=0.6 1/h (tOFF=83 min); E2) f=0.9 1/h (tOFF=53 min); E3) f= 1.8 1/h (tOFF=23 min). A non-perturbed condition test (C) was also run as a control where oxygen concentration was constantly maintained at DO≈7 mg/L O_2.

1.4.2.3 Analytical methods

Detection of acetate and nitrogen species

Analytical determination of nitrates, nitrites and acetate was performed by using the Thermo Scientific Dionex ICS-2100 Ion Chromatography System, following APHA methods 4110 B. NH_3-N was measured by the Thermo Scientific Orion 4 ammonia ion selective electrode, following the APHA methods 4500-NH3 D (APHA methods, 2005).

Detection of OMPs concentration

OMPs concentrations in the liquid phase were measured by a first solid phase extraction (SPE) on OASIS HLB cartridges (Waters, Milford, MA, USA) following the method described by Vanderford et al. (2003). Particularly, 20 mL of sludge sample were collected from the reactor and centrifuged to separate suspended particles (20400 x g for 20 min at T= - 4°C) and stored for less than one week at T= − 20°C. The supernatant was spiked with 100 µg/L of internal standard, IS_1 (ATZ-d_5), and filtered through the cartridge (pre-conditioned with 5 mL of tert-methyl butyl ether, 5 mL of methanol and 5 mL of deionised water). Then, the cartridge was rinsed with water and air-dried for 30 min. The OMPs were eluted in 5 mL 90/10 MTBE/MeOH (v/v) and 5 mL MeOH under a vacuum system. Total evaporation of the extracts was performed at T=40°C and 1200 rpm rotation speed using a rotary evaporator RVC 2-25 CO plus Christ. The dried phase was dissolved in 1 mL of MeOH and then filtered with a 0.2 µm membrane filter of regenerated cellulose. Just before the injection, other two internal standards, IS_2 (CBZ-d_{10} and NPX-d_3 at 100 µg/L), were added and used for the concentration quantification.

Quantitative analysis of OMPs was carried out by liquid chromatography coupled with mass spectrometry (LC-MS) using a Shimadzu 8040 Series LC-MS (Shimadzu, Japan) with an Agilent ZORBAX Eclipse Plus C18 column (2.1 mm × 100 mm, particle size 1.8 µm, Agilent Technologies, Germany). Two specific analytical methods were developed, one in negative mode for Naproxen and one in positive mode for all the other OMPs, based on EPA Method 1694 (Imma Ferrer, 2008). A binary gradient system of mobile phase A, 0.1% formic acid in deionised water, and mobile phase B, 0.1% formic acid in acetonitrile, were used to separate analytes in positive ESI mode, while 5 mM ammonium acetate, pH-5.5 (mobile phase A) and methanol (mobile phase B), were used for analysis in negative ESI mode. The solvent gradient programme for positive ESI mode was as follows: 5% B held for 4 min., increased linearly to 50% by 5 min and then to 90% in 6 min and then dropped to 5% for 2 min. A 3 min equilibration step at 5% B was used at the end of each run to bring the total run time per sample to 17 min. For negative ESI mode, the gradient started with 30% B, and was increased linearly to 100% B over 8 min and held for 3 min., then maintained at 40% B for 3 min. The flow rate was 0.3 mL/min in the former and 0.2 mL/min in the latter mode and the injection volume was set to 3 µL and 10 µL for +/- polarity modes, respectively. Limits of detection and limit of quantification (LOD and LOQ, respectively) were determined using signal/noise ratios of 3 and 10, respectively. The quality assurance and quality control were checked within each measurement series by recovery experiments both in deionized water (Recovery in Water) and SyWW (Recovery SyWW) spiking at 100 µg/L OMPs solution ($n \geq 3$) and with 5 repeated injections of matrix recovery samples (Repeatability). The analytical method was also validated in terms of linearity (R^2 of the calibration curves). The validation results are summarized in Supplementary materials (Table S.M. 2).

Enzyme activity assays

The activity of oxidoreductases and hydrolase target enzymes (Lignin peroxidase (LiP), Horseradish peroxidase (HRP), Laccase (Lac), β-glucosidase (β-glu), Cytochrome P450 (Cyp450)) in culture biomass samples was determined spectrophotometrically by measuring the degradation (oxidation and hydrolysis) of various chromogenic substrates used as surrogate xenobiotics (details in Table S.M. 6 of Supplementary materials). Specifically, 2 mL aliquots of microbial culture samples were centrifuged at 16000 x g for 3 min in Eppendorf tubes. Ultrasonication (physical disruption) was applied as a standard method for the disruption of microbial cells from activated sludge. The pellets from each tube were individually homogenized by sonication in 600 µL of EDTA buffer (1 mM EDTA, 0.1% Surfact-Amps, 50 mM ammonium bicarbonate, pH 8) at 12 Hz for 30 seconds thrice. Sonication was performed with a sonication microtip (Qsonica Q-125, Alphatech Systems, New Zealand) to the ice-cold homogenised samples. Cell debris was removed by centrifugation at 16000 x g for 10 min and the supernatant was used for the analysis of enzyme activity. Each well of a 96 well microplate was filled with 50 µL aliquots of buffers (50 mM acetate buffer, 50 mM sodium acetate trihydrate adjusted to pH-5 with glacial acetic acid), 100 mM phosphate buffer(80 mM di-potassium hydrogen phosphate, 20 mM potassium dihydrogen phosphate, 10 mM dextrose, 6 mM magnesium acetate adjusted to pH-7.4), 50 µL

chromogenic dye and 50 µL culture supernatant. Dyes and samples resuspended in double the amount of buffer served as controls. To start the reactions of the sample enzymes with assay dyes, 10 µL of 0.3% H_2O_2 at 30% was added to the Methylene Blue, Azure B, L-DOPA and ABTS dye wells and 10 µL of 1M NaOH added to the para-nitrophenol dye wells (to stop the reaction) and vortex mixed. Changes in absorbance caused by chromogenic reactions were read on a Victor X3 Multimode Plate Reader (PerkinElmer, USA) at different wavelengths for 1 h with incubation at 30˚C.

Microbial DNA isolation and bacterial species identification

A PowerSoil DNA isolation kit (MoBio, Carlsbad, USA) was used for the isolation of bacterial total genomic DNA extracted from sludge samples (1 mL) following the manufacturer's protocol. All the extractions were performed in duplicate. Bacterial community composition was characterised by amplifying and sequencing a fragment of the bacterial 16S ribosomal RNA (rRNA) gene following a standard protocol (Illumina 2013). The V3 and V4 regions of 16S rRNA genes were amplified from individual DNA extracts with the universal 16S Amplicon PCR Forward Primer (5'-TCGTCGGCAGCGTCAGATGTGTATAAGAGACAGCCTACGGGNGGCWGCAG-3') and 16S Amplicon PCR Reverse Primer (5'-GTCTCGTGGGCTCGGAGATGTGTATAAGAGACAGGACTACHVGGGTATCTAATCC-3'). These primers have been validated to provide good bacterial phylum coverage as they are also modified to include Illumina adapter overhang sequences (in bold) required for downstream DNA sequencing. DNA amplification was conducted as follows: (i) 94˚C for 3 min; (ii) 30 cycles of 94˚C for 30 s, 55˚C for 30 s, 72˚C for 30 s; (iii) 72˚C for 5 min. Following amplification, PCR products were purified using the AMPure XP beads kit (Beckman Coulter Inc., Brea, CA, USA) according to the manufacturer's instructions. The concentrations of purified amplicons were finally measured and recorded using a Qubit® dsDNA HS Assay Kit (Life technologies, Carlsbad, CA, USA) and submitted to New Zealand Genomics Ltd for sequencing by Illumina MiSeq machine. The resulting paired-end read DNA sequence data were merged and quality filtered using the USEARCH sequence analysis tool (Edgar, 2013). Data were dereplicated so that only one copy of each sequence was reported, and 'singleton' sequences represented by only one DNA sequence in the database were removed. Sequence data were then checked for chimeric sequences and clustered into groups of operational taxonomic units based on a sequence identity threshold equal to or greater than 97% (thereafter referred to as 97% OTUs) using the clustering pipeline UPARSE in QIIME v.1.6.0 as described in (Ramirez et al., 2014). After that, prokaryote phylotypes were classified to their corresponding taxonomy by implementing the RDP classifier routine in QIIME v. 1.6.0 to interrogate the Greengenes 13˙8 database. All sequences of chloroplast and mitochondrial DNA were removed. Finally, DNA sequence data were rarefied to a depth of 5,600 randomly selected reads per sample and two samples per treatment to achieve a standard sequencing reads across all samples.

1.4.2.4 Calculation methods

Based on the concentrations, removal efficiency was calculated using the following Equation:

$$R\%(t)=\frac{M_f-M_m(t)}{M_f}\cdot 100 \quad \text{Eq. 36}$$

where M_f and $M_m(t)$ stand for the mass of OMPs in the feeding and measured at time t inside the reactor, respectively.

The perturbation frequency, f (1/h) was defined and calculated as follow:

$$f=\frac{1}{ON+OFF} \quad \text{Eq. 37}$$

where ON and OFF represent the durations (h) of the active aeration phase and of the phase conducted in the absence of aeration, respectively.

The Pearson's correlation coefficient (ρ) was calculated by the software R using the following equation (Mu et al., 2018):

$$\rho = \frac{\sigma_{xy}}{\sigma_x \cdot \sigma_y} \quad \text{Eq. 38}$$

where σ_{xy} is the covariance, σ_x and σ_y are the standard deviations of the two variables, i.e. the removal efficiency of each OMP (x) and the activity of the target enzymes (y) measured at the end of the test, respectively.

The specific nitrogen removal rate (SNRR) calculation was done according to the following equation:

$$SNRR(t) = \frac{\Delta([NH_4^+-N]+[NO_2^--N]+[NO_3^--N])}{\Delta t \cdot X} \quad \text{Eq. 39}$$

where $\Delta([NH_4^+$-N]+ [NO_2^--N]+ [NO_3^--N]) is the difference of the total nitrogen concentrations (mg/L N) measured inside the reactor at time t=0 h and t (either 24 h or 48 h as above detailed), respectively; Δt is the time interval (d); X is the MLVSS concentration inside the reactor (mg/L MLVSS).

1.5 Removal processes at real scale

1.5.1 Wastewater Treatment Plants (WWTPs)

1.5.1.1 Chemicals

Standard solutions of the analysed OMPs (CBZ, THC-COOH, AM, MET, KTP, SMX, CBZ, TMT, LCN, P4, E1, E2, EE2) and of the internal standard Carbamazepine-d10, were purchased from Sigma-Aldrich Company (Gillingham, UK) at a concentration of 100 µg/mL each in methanol. Main characteristics of the contaminant are reported in Table 1 (Williams et al., 2017).

1.5.1.2 WWTPs sample collection

Influent and effluent samples were collected from 76 different WWTPs located in central Italy. The study was conducted for about 2 years, from March 2017 to May 2019. Because of the long hydraulic retention times of the WWTPs, it was decided to perform wastewater collection through grab sampling; the data were then statistically analysed in order to obtain representative results. During the first year, the monitoring campaign included a total number of 1296 measurements and focused on selected illicit drugs and steroids. In the second year, the total number of measurements was reduced to 1012, whereas the list of monitored compounds was enriched by adding also pharmaceuticals to illicit drugs and steroids. The number of sampling days varied from 1 to 7 depending on the WWTP. Supplementary Materials reports the main lay-out of each WWTP and the number of samples (Table S.M. 8). Since the characteristics of the WWTPs were different, these were grouped into 4 classes based on the increasing complexity of the treatment level: 1) only secondary treatment (ST); 2) primary treatment followed by the secondary treatment (PT+ST); 3) secondary and tertiary treatments (ST+TT); 4) primary, secondary and tertiary treatment (PT+ST+TT). Table 3 shows a summary of the classes considered in the study, the corresponding number of WWTPs (n.) belonging to each one and the number of measurements carried out for each class of contaminant.

Table 3 Summary of the entire data set about WWTP at real scale

Treatments	WWTPs [n.]	Illicit drugs	Pharmaceuticals [n. measurements]	Steroids
ST	29	336	140	328
PT+ST	6	200	140	188
ST+TT	39	396	140	392
PS+ST+TT	2	24	0	24
Total	76	956	420	932

1.5.1.3 Analytical methods

The analytical technique chosen for the quantitative analysis of the OMPs in the samples was the Ultra-Performance Liquid Chromatography coupled to tandem Mass Spectrometry (UPLC–MS/MS). The analytical method is based on EPA 538 (Boni et al., 2018; Chiavola et al., 2019; Daughton and Ternes, 1999). For calibration and quantification, the internal standard (IS) approach was followed and the IS used was Carbamazepine-d10. The liquid sample pre-treatment consisted only of a filtration step by using a 0.2 μm membrane filter of regenerated cellulose.

Each contaminant was quantified by MRM (Multiple Reaction Monitoring ratio) using the two most abundant precursor/product ion transitions of the two analytes and the IS.

According to the method, filtration is followed by a direct injection in the UPLC-MS/MS system with the instrumental conditions reported below:

1) UPLC: Ultimate 3000 RS Thermo, with two pumps, degasser, column oven compartment and auto sampler; Chromatography column was Phenomenex Kinetex 2.6μm Biphenyl 100A, 100x2.1 mm with security-guard column at 30°C. Mobile phase A: 100 % Milli-Q water acidified with 0.1% formic acid; mobile phase B: 100 % LC-MS methanol acidified with 0.1% formic acid. The gradient elution conditions were from 95% A and 5% B to 0% A and 100% B in 8 min. Flow was 0.3-0.4 mL/min. Injected volume was 50 μL.

2) Mass spectrometer: 5500 AB Sciex Q-Trap with Atlas Copco FS2 compressor, FX1 dryer, 270 L tank and nitrogen generator Zephyr Zero 16 LC-MS. The applied UPLC-MS/MS parameters are reported in Table S.M. 7.

The overall response time for each liquid sample was below 30 min.

Limits of detection (LOD) were determined using signal/noise ratios of 10, for 7 replicates. Furthermore, Minimum Reporting Level (MRL) was defined as the LOD rounded to the second decimal, according to EPA method. MRL values of each OMPs were reported in supplementary materials and they also correspond with the minimum values of the concentration detected in the experimental samples (Table 3).

The quality assurance and quality control were checked within each series of measurement with the following criteria: the linearity coefficient (R^2) and relative standard deviation (RSD%) of the calibration curves were up to 0.990 and 10%, respectively. The bias was lower than 30%. The repeatability of the measurements in the samples matrix (wastewater) was lower than 20%. The expanded uncertainty (U_{EXP}) of the analytical method was lower than 39% with a confidence level of 95%.

1.5.1.4 Calculation methods

The frequency of detection (F_D) was calculated as outlined below:

$$F_D[\%] = \frac{n}{N} \cdot 100 \qquad \text{Eq. 40}$$

where N is the total number of samples, and n is the number of samples with a concentration above the MRL concentration, for a given contaminant.

All the boxplot graphs presented in this study were built using R software and they display different statistical elements, as reported below.

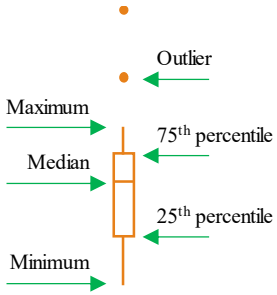

For instance, the box shows the interquartile range (IQR), which represents the difference between the upper (Q3, the 75th percentile) and lower quartiles (Q1, the 25th percentile). The bar inside the box indicates the median value (the 50th percentile). The dots represent the outlier. The whisker (extreme lines) are the maximum and minimum values in the data which cannot be considered outliers and are defined as (Wickham, 2016):

Q3+ 1.5×IQR for maximum;
Q1- 1.5×IQR for minimum.

The percentage removal efficiency (R) was calculated as indicated by below:

$$R\ [\%] = \frac{C_{in} - C_{ef}}{C_{in}} \cdot 100 \qquad \text{Eq. 41}$$

where C_{in} and C_{ef} stand for the influent and effluent concentrations for a contaminant.
The removal was not calculated if the influent and effluent concentration were both equal to the MRL.

The standardized removal efficiency (SRE) was calculated by following the equation below:

$$SRE = \frac{x - \mu}{\sigma} \cdot \frac{n}{N} \qquad \text{Eq. 42}$$

where x represents each individual removal efficiency for a given contaminant in a specific WWTP and sampling day, μ is the average removal efficiency for the contaminant over all WWTPs, σ is the standard deviation of the removal efficiencies for a contaminant over all WWTPs, n is the number of

measurements for the contaminant in the WWTPs class which the plant considered is belonged and N is the number of measurements across all WWTPs (Ben et al., 2018).

1.5.2 Drinking water treatment plants (DWTPs)

1.5.2.1 DWTPs sample collection

Rapid sand filters are a common treatment employed to remove inorganic compounds and residual particles remaining after pre-treatments (Cakmakci et al., 2008; Clasen, 1998; Sharma et al., 2005). Moreover, the filter's medium is colonized by native microbial populations, which use the organic compounds present in the water, including OMPs, as an energy source (Benner et al., 2013).

Seven full-scale rapid sand filters at different locations spread over The Netherlands and Belgium were selected, see Figure 7 and Table 4. The complete treatment schemes are provided in the Supplementary materials (

Table S.M. 9). Two measuring campaigns were performed, one in May 2018 and one in September 2018. For all filters, 1 litre of influent and 1 litre of effluent water were sampled for OMP target screening and non-target analysis.

In the spring sampling campaign, samples were collected during two consecutive days in all the locations (23th and 24th May 2018) and analyzed simultaneously. By contrast in the autumn sampling campaign, the samples were collected 19th September in the locations 4., 5., 6., 1.and and 26th September in 7., 3., 2. The HR MS/MS spring data were thus more comparable, e.g. in term of retention time, and they were considered more appropriate to validate the workflow proposed. Consequently, TP formation was monitored in the spring sampling campaign data.

Figure 7 Locations of the 7 studied drinking water treatment plants

Table 4 Characteristics of the selected RSFs

Name	Type of RSF	Nr. of filters [-]	Surface area filter [m^2]	Bedheight [m]	Filter medium [mm]
1.	Downflow	12	7.9 x 5.1	2.0	1.0 – 1.6 sand
2.	Downflow	4	9 x 4	1.2	0.71 – 1.25 sand, 1.4 – 2.5 hydroanthracite
3.	Dual media downflow	12	36	2.2 (0.7 grind, 0.7 sand, 0.8 anthracite)	0.8-1.25 sand, 1.6 – 2.5 anthracite
4.	Downflow	80	4 x 12	1.25	0.70 – 1.40 sand
5.	Upflow	18	15 x 2.6	1.75	1.0 – 2.5 sand
6.	Downflow	24	4 x 12	1.20	0.8 – 1.25 sand
7.	Downflow	24	6 x 12	0.85 (0.25 anthracite, 0.60 sand)	0.8 – 1.25 sand, 1.6 – 2.5 anthracite

1.5.2.2 Analytical methods

LC HR MS/MS

Non-target screening (NTS) based on liquid chromatography (LC) coupled to high-resolution tandem mass spectrometry (HR MS/MS) were carried out to analyse the samples. The sample preparation included only a filtration step, followed by direct injection.

A Tribrid Orbitrap Fusion mass spectrometer (ThermoFisher Scientific, Bremen, Germany) provided with an electrospray ionization source was interfaced to a Vanquish HPLC system (ThermoFisher Scientific). For the chromatographic separation an XBridge BEH C18 XP column (150 mm × 2.1 mm I.D., particle size 2.5 µm) (Waters, Etten-Leur, The Netherlands) preceded by Phenomenex Security Guard Ultra column (Phenomenex, Torrance, USA) maintained at a temperature of 25 °C was used. The gradient started with 5% acetonitrile, 95% water and 0.05% formic acid (v/v/v), increased to 100% acetonitrile with 0.05% formic acid in 25 min, and was held constant for 4 min at a flow rate of 0.25 mL/min. Prior to LC-HRMS analysis, atrazine-d5 was added to the water samples as internal standards with a final concentration of 1 µg/L; this allowed LC-HRMS performance evaluation and quality control based on their signal intensities, peak shapes, exact mass and retention times. Subsequently, samples were filtered using Phenex™-RC 15 mm Syringe Filters 0.2u (Phenomenex, Torrance, USA). 100 µL of filtered sample was used for injection. Blank samples of internal standards spiked into ultrapure water were run every 5-10 samples to check for carry-over and contamination. With every batch run mass calibration was performed using Pierce ESI positive and negative ion calibration solution to ensure a mass error smaller than 2 ppm. The vaporizer and capillary temperature were maintained both at 300 °C. Sheath, auxiliary and sweep gas was set to arbitrary units of 40, 10 and 5, respectively. The source voltage was set to 3.0 kV in the positive mode. The RF lens was set to 50%. Full scan high accuracy

mass spectra were acquired in the range of 80-800 m/z with the resolution set at 120,000 FWHM and quadruple isolation were used for acquisition. Data dependent MS/MS acquisition was performed for the eight most intense ions detected in the full scan, using a High Collision Dissociation (HCD) energy at 35% and an FT resolution of 15,000 FWHM.

1.5.2.3 Calculation methods

The internal standard equivalent concentration (IS-eq conc.) was calculated as follow:

$$\text{IS} - \text{eq Conc.} = \frac{A_f}{A_{IS}} \cdot C_{IS} \qquad \text{Eq. 43}$$

where A_f is the peak area of the unknown feature, A_{IS} is the peak area of the IS (atrazine-d5) and C_{IS} is the concentration of IS spiked in each sample (1 µg/L).

The internal fold change (log2FC) was calculated as follow

$$\text{log2FC} = \log_2 \frac{A_E}{A_I} \qquad \text{Eq. 44}$$

where the change between influent and effluent (FC) is expressed as base-2 logarithm of the ratio of peak area of the unknown feature in the effluent (A_E) and in the influent (A_I). The log2FC is negative if the intensity of the feature decreases during the treatment (removal) and it is positive if the intensity increases (formation).

1.5.2.4 Methodology

The aim of the present study was to identify TPs from real scale RSF as well as to propose a workflow for this goal. Therefore, in this section only the tools, databases and software used are described. The identification workflow was considered an integral part of the results.

Parent compound identification

The identification of PCs was carried out with a "known unknown" approach also called suspect screening that focuses on compounds that are known in the chemical literature. In the suspect screening, the features detected in the NTS data were searched for matches in monoisotopic mass and/or fragmentation spectra in different databases in the following order of priority:

1) in-house suspect list of 127 water relevant chemicals that were also quantified (see Table S.M. 11, for full list of chemicals);

2) the mass spectral library mzCloud (www.mzcloud.org). Identification with mzCloud was based on MS1 and MS2 information;

3) the chemical structure databases EAWAG Biocatalysis/Biodegradation Database, the EPA DSSTox, and the EPA Toxcast via ChemSpider. Identification with these databases was based on MS1 information only, i.e. elemental composition and monoisotopic mass of the candidates (Little et al., 2012).

Transformation product prediction

The key step of the workflow proposed in this study is the prediction of TPs through BioTransformer, an open access web service for *in silico* metabolism prediction and metabolite identification (Djoumbou-Feunang et al., 2019). The software consists of two components: a metabolism prediction tool (BMPT), and a metabolite identification tool (BMIT). BMPT generates predicted metabolite structures in standard electronic formats. The input required by the software is the SMILE code of the PC. The BMPT consists of five independent prediction modules (transformer):

(1) the Enzyme Commission based (EC-based) transformer; (2) the CYP450 (phase I) transformer; (3) the phase II transformer; (4) the human gut microbial transformer; (5) the environmental microbial transformer.

For the prediction of metabolites, BioTransformer implements two approaches, a rule-based or knowledge-based approach, and a machine learning approach. BioTransformer's knowledge-based system consists of three major components:

1) a biotransformation database (called MetXBioDB) containing detailed annotations of experimentally confirmed metabolic reactions. MetXBioDB is a database that consists of a manually curated collection of >2000 experimentally confirmed biotransformations derived from the literature. Each biotransformation in MetXBioDB includes as input a starting reactant (structure and identifiers), as output a reaction product (structure and identifiers), the name or type of the enzyme catalyzing the biotransformation, the type of reaction, and one or more citations.

2) a reaction knowledgebase containing generic biotransformation rules, preference rules, and other constraints for metabolism prediction. This component contains chemical reaction descriptions and rules encoded by SMARTS (a language that allows to describe part of molecular structures using rules that are extensions of SMILES) and SMIRKS (a language for generic reactions, and it is an hybrid of SMILES and SMARTS) strings that are used by the reasoning engine to make biotransformation predictions (Daylight Chemical Information Systems, 2008). This knowledgebase encodes information about, and contains mapping data between, five different concepts: a) the biosystem, as the environmental microbiome; b) the metabolic enzyme; c) the metabolic reaction: it is a single chemical reaction that modifies the structure of a molecule generating one or more products; d) the metabolic pathway: it is a linked series of chemical reactions that occur in a specific order in the cell or within an organism; e) the chemical class: they are group of chemicals that share a common structural feature or a group there of as defined using a web-based application for automated structural classification of chemical entities (ClassyFire) (Djoumbou Feunang et al., 2016).

3) a reasoning engine that implements both generic and module-specific algorithms for metabolite prediction and selection. This component merges the reaction knowledgebase and the biotransformation database to select the most likely of the applicable metabolic pathways. To predict the metabolites two type of reasoning are applied: the absolute reasoning (it is based on the likelihood of a biotransformation to occur with an occurrence ratio above a given threshold), and relative reasoning (it compares the likelihood between two independents but competing reactions). The attributes used for the prediction are both qualitative (e.g. chemical class) and quantitative (e.g. mass, LogP). The qualitative attributes are helpful to select the most likely biotransformations, on the other hand the quantitative ones are needed to identify a specific substrate for various enzymes if the physico-chemical properties of a molecule can fit the proposed reaction.

In the present study the environmental microbial module of the BMPT was used. The products of environmental microbial degradation (TPs) are predicted using a set of rules provided by the EAWAG-BBD/PPS system (Ellis et al., 2008).

Transformation products identification

TP identification was achieved through suspect screening based on accurate mass with suspect lists consisting of both the detected PCs from 2.3.1 and the potential TPs from the BioTransformer prediction step. Subsequently, the level of confidence of identification (Schymanski et al., 2014) of the detected suspects was further increased using the BioTransformer metabolite identification tool (BMIT) and fragmentation spectra information (as described in section *Parents compound identification*), or the suspect candidate rejected.

The BMIT is a successive step of BMPT designed for metabolite identification based on PubChem suspect screening. BMIT takes as input the chemical structure of the starting molecule (the parent compound) and the mass or molecular formula of the metabolite (usually obtained from BMPT) and performs searches in PubChem for the metabolites. The results are a list of identified metabolites including their structures, identifiers (InChIKey, InChI, SMILE and synonyms from PubChem), reaction types, and enzymes (Djoumbou-Feunang et al., 2019).

Spectral similarity

Confirmation of the TPs detected with the suspect screening was performed through spectral comparison between the experimental fragmentation spectrum of the suspect and the respective library and/or *in silico* spectrum of the compound. *In silico* fragmentation was performed with both the open source software MetFrag (https://ipb-halle.github.io/MetFrag/) and the commercial software Compound Discoverer. While MetFrag uses a bond disconnection approach (Ruttkies et al., 2016), Compound Discoverer uses a rule based fragmentation prediction called fragment Ion search (FISh) (i.e. fragmentation pattern obtained following a set of general ionization, fragmentation, and rearrangement rules). Both output a score based on the assignment of m/z fragment peaks to fragment-structures, that

indicates how well the candidate matches the given MS/MS spectrum and that can be used for suspect ranking.

Furthermore, the spectral similarity between PC and TP spectra were calculated using the R package "OrgMassSpecR" (http://OrgMassSpec.github.io/). Head-to-tail plots of the two mass spectra were generated and a similarity score calculated as the dot product between the aligned intensity vectors of the two spectra.

Results and Discussions

1.6 Removal processes at laboratory scale

1.6.1 Batch tests

1.6.1.1 Validation of the analytical method for OMPs detection

Methamphetamine

The second transition of MET was chosen for the quantitative determination due to the best result of statistical parameters of the analytical method, as shown in Table 5 in terms of calibration curves linearity (MET-1 R^2=0.9997; MET-2 R^2=0.9999). Other results of the method validation are also reported in Table 5.

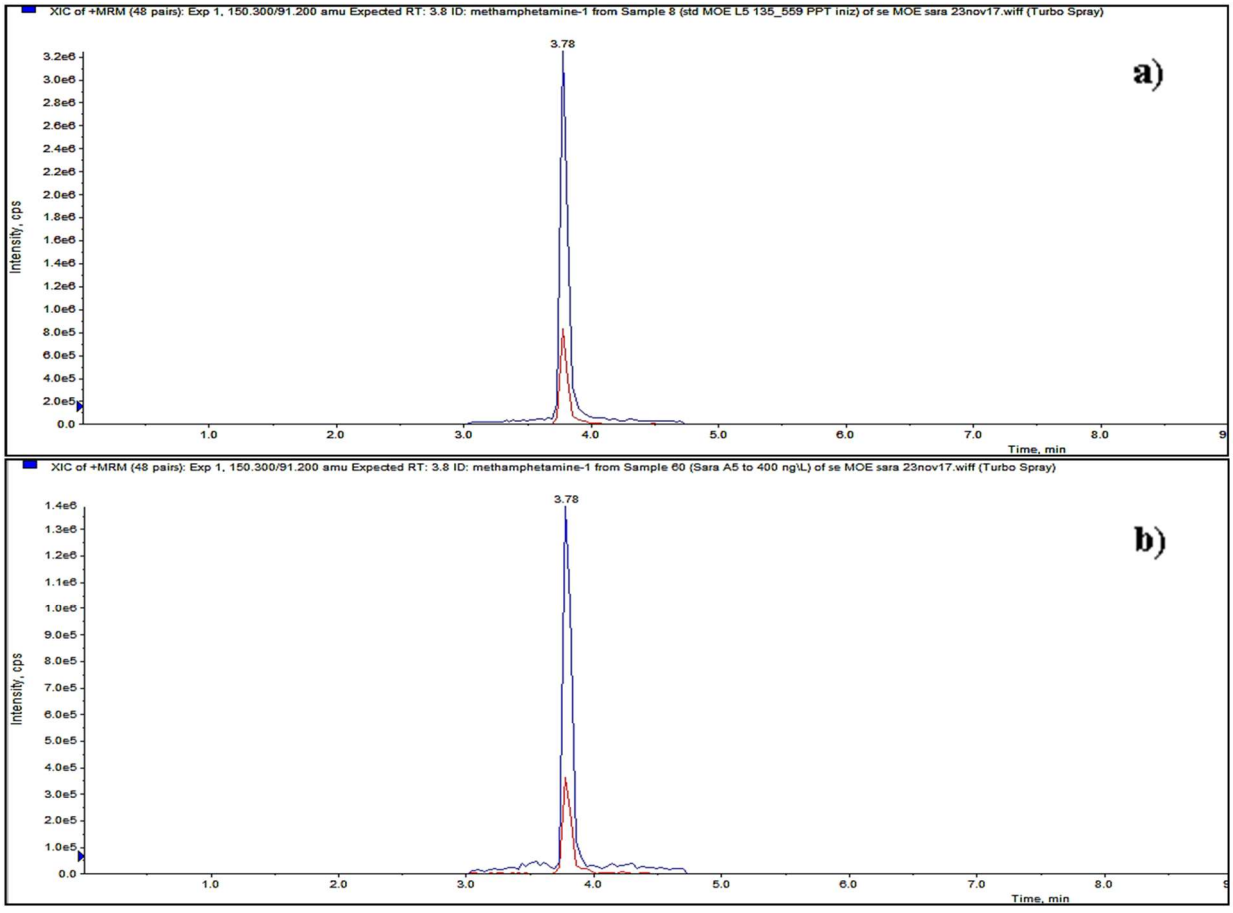

Figure 8 Chromatograms related to (a) a standard solution and (b) a sample collected from one of the overall biological process tests

Figure 8 shows two chromatograms representing the detection of MET in the standard solution used for calibration and in a sample collected from one of the overall biological process tests. It is possible to notice how the two chromatograms are perfectly comparable and that the effects of the complex matrix in sample (b) do not increase consistently the base noise.

Based on these results, shown in Table 5, it was considered to be addressed the objective of the study, i.e. to assess an analytical method for MET determination in the liquid and solid phase of a WWTP to be repeatable and reliable (recovery>75%; repeatability<10-15%; bias uncertainty<30%), and relatively easy-to-use, and therefore suitable for measurements on routine base.

Table 5 Validation parameters of the analytical method for MET detection (UPLC-MS/MS) in liquid and solid phases for the two ion transitions

OMP	Conc. validation [ng/L]			Rep [%]	Bias [%]	R^2 [%]	Accuracy [%]	Uexp [%]	LOD_L [ng/L]	LOQ_L [ng/L]	LOQ_S [ng/gTSS]	REC [%]
MET-1	19	105	429	2.7	21.9	0.9997	12.7	51	7.4	14.8	2.8	>75%
MET-2	19	105	429	3.3	13.3	0.9999	-3.0	28	4.9	12.2	2.4	>75%

Matrix effect tests

In order to evaluate the effect of the matrix components on MET determination, the Fisher's extract test was conducted. The results of this test are as follows:

$F_{calc} = 4.08$

and $F_{3,3} = 9.27$ (Skolnik, 2009)

so $F_{calc} \leq F_{3,3}$

This result allows to confirm that the variances were statistically equivalents, so the matrix effects are statistically not relevant.

Furthermore, it is useful to observe the results of two replicates of MET concentration measured in the matrix effect tests for the different solutions, as shown in Figure 9.

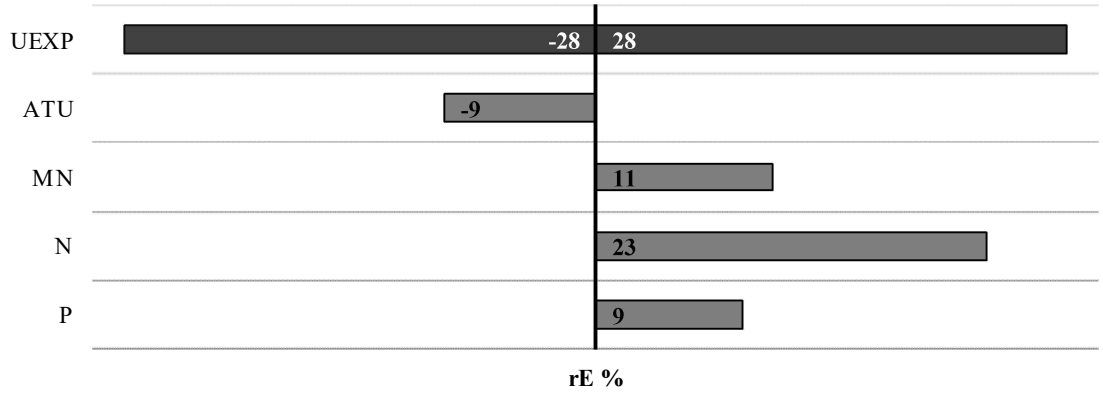

Figure 9 Relative error of matrix effect tests compared with expanded uncertainty (UEXP) of the analytical method

The results are reported as relative error (rE %) compared to the expected concentration (nominal concentration, Cn, equal to 50 ng/L). In the same figure, the expanded uncertainty of the analytical method is also reported. It is possible to note that the deviation (bias) measured in the different analysed matrices is included in the uncertainty of the method, and that the measured values are statistically distributed around the true value (bias = 0).

Therefore, it can be concluded that the adopted method for the analytical determination of MET is not statistically affected by the interaction with the tested wastewater components. The method results to be reliable and suitable for carrying measurements in the WWTPs. However further tests on other matrices are needed as confirmation.

11-nor-9carboxy-Δ9-THC and benzoylecgonine

From a statistical point of view, Bias effect, that represents the matrix effect, was evaluated by the Fisher's exact test (F-test): this is a partial test which is appropriate for the determination of non-random associations between two categorical variables. For instance, the F-test allows to compare the variances of two data sets (S_A^2 and S_B^2). The value of F was calculated as reported below:

$$Fcal = \sigma_A^2 / \sigma_B^2 \qquad \text{Eq. 45}$$

where σ_A^2 is the variance of the difference between the detected concentration in each solution (of Bias test) and the expected one, whereas σB2 stands for the repeatability of the analytical method.

The F calculated value was compared to the printout value for (n-1) and (m-1) degrees of freedom representing a significance level equal to 95% (Skolnik, 2009). In this case, n=4 and m=5. The test is considered valid if:

$F_{cal} \leq F_{3,4}$

The method was considered valid if the followed conditions were respected: repeatability<10% and bias uncertainty<10%.

The second transition for BE and THC-COOH was chosen for the quantitative determination of concentrations due to:

- the statistics results of calibrations curves for BE ($R^2_{BE\text{-}2}$=0.9996);

- for THC-COOH, the first transition, which had the best correlation coefficient ($R^2_{THC\text{-}COOH\text{-}1}$= 0.9995), presented another chromatographic peak with a retention time neighbouring THC-COOH. This peak hinders the correct and undoubted integration of the contaminant's area. The second transition presented a peak that allowed simple and reliable area integration valley-to-valley (chromatograms of the peaks related to standard solutions are shown in

Figure S.M. 2 of Supplementary materials); besides, the correlation coefficient was considered high ($R^2_{THC\text{-}COOH\text{-}2}$= 0.9961).

The coverage factor (K=2.509) was determined as the average value of Two Tails T Distribution factors of BE and THC-COOH, for the degrees of freedoms equals to 6 and 5, respectively, calculated by Eq. 4.

Other results of the method validation are reported in Table 6 for the transitions used for quantification. In order to evaluate the effects of the matrix components on drug determination, the Fisher's extract test was conducted. The results of the test are as follows:

$F_{calc,BE} = 0.60$

$F_{calc,THC\text{-}COOH} = 1.80$

and $F_{3,4} = 6.59$ (Skolnik, 2009)

so $F_{cal} \leq F_{3,4}$

These results confirm that the variances were statistically equivalents, so the matrix effects can be considered not statistically relevant.

Based on these results, as shown in Table 6, it was considered to be addressed the objective of the study, i.e. to assess an analytical method for BE and THC-COOH determination in the liquid and sludge phase of a WWTP to be repeatable and reliable (recovery>75%; repeatability<10%; bias uncertainty<10%). The recovery value above 75% was considered acceptable because falls within the recovery range reported by previous studies, i.e. 31-196 %, regarding extraction, clean-up and detection techniques for the determination of organic pollutants in sewage sludge (Álvarez-Ruiz et al., 2015).

The method also demonstrated to be relatively easy-to-use, and therefore suitable for measurements on a routine base. Nevertheless, for THC-COOH further investigations are needed concerning the effects of emphasis and inhibition of the electronic response, due to the highest values of Bias uncertainty, and consequently the expanded uncertainty (Uexp=34%) achieved. Similar issues associated to the determination of THC-COOH in wastewater have been highlighted also by other analytical studies (Causanilles et al., 2017; Hernández et al., 2016).

Table 6 Validation parameters of the analytical method for BE and THC-COOH detection (UPLC-MS/MS) in liquid and sludge phases the transitions used for the quantification

OMPs	Conc. of validation [ng/L]	Rep_L [%]	Bias [%]	R^2 [%]	Accuracy [%]	Uexp [%]	LOD_L [ng/L]	LOQ_L [ng/L]	LOQs [ng/gTSS]	RECs [%]
BE-2	100	6.1	3.4	0.9996	3.4	20	5	10	0.3	>75%
THC-COOH-2	100	5.4	9.8	0.9961	-7.6	34	10	20	1.1	>75%

Perfluorooctane sulfonic acid and perfluorooctanoic acid

Results of the validation phase are reported in Table 7 (MRLW= minimum reporting level for liquid samples; MRLm= minimum reporting level for sludge samples; RepW= repeatability in water; Repm= repeatability in experimental matrix; R2= calibration curves linearity; RECL= recovery from liquid samples; RECS= recovery from sludge samples).

Table 7 Validation parameters of the analytical method for PFOA and PFOS detection (UPLC-MS/MS) in the liquid and sludge phases for the transitions used for the quantification

OMPs	MRL_W	MRL_m	Rep_w	Rep_m	R^2	REC_L	REC_S
	ng/L	ng/g	%	%		%	%
PFOA	20	>6.7	5	2	0.999	100	30
PFOS	10	>3.3	19	14	0.998	101	34

1.6.1.2 Fate and removal of methamphetamine

Activated sludge tests

Figure 10a, Figure 11a and Figure 12a show removal efficiency of MET and the corresponding COD profiles in the activated sludge test in absence (A) and in the presence of nitrification inhibition (A_{he}) (i.e. measured during the overall biological and heterotrophic batch tests, respectively) conducted at 50 ng/L, 100 ng/L and 200 ng/L MET. The figures show also the standard deviation calculated on the removal efficiency values of two replicates.

Figure 10b, Figure 11b and Figure 12b show ammonia, nitrate and nitrite nitrogen concentrations versus time during the same tests, respectively.

MET profiles indicate that the drug is removed progressively during the tests. The highest reduction is occurring in the first 3-4 h, while afterwards removal becomes much lower. COD time-profiles follow very closely MET pattern, with the main removal also observed in the first 3-4 h of the tests. The behaviour of MET and COD remain basically the same at all the tested drug concentrations, and the removal efficiency increases as the concentration rises.

Comparison of the processes in the absence (A) and presence of nitrification inhibition (A_{he}) shows higher values of removal in the former case, i.e. in the presence of both carbon and ammonia oxidation. This pattern is observed at all the tested concentrations, and particularly at 50 ng/L and 100 ng/L of MET.

Measurements of ammonia during the overall biological tests (A) show its continuous conversion into nitrate, as reported in Figure 10b, Figure 11b and Figure 12b: nitrification in the presence of MET proceeds regularly with no significant difference with respect to the processes observed in the blank tests (reported as supplementary material, Figure S.M. 1). Nitrite production is very low in all the cases, thus indicating complete nitrification into nitrate. Therefore, it can be concluded that nitrifiers bacteria provide a contribution to the removal of MET, whereas nitrification is not negatively affected by the presence of the drug. It is noteworthy that MET is a

nitrogenous compound: therefore, the presence of MET in the mixed liquor might be able to stimulate autotrophic biomass activity, without compromising other reactions such as observed in previous study Chiavola et al. (2017).

Furthermore, within the 6 h contact time and at a concentration of activated sludge which is similar to the average found in the WWTPs, almost complete removal of MET is achieved even starting from the highest value, i.e. 200 ng/L of MET. This is in a good agreement with the work of Baker and Kasprzyk-Hordern (2013) and the review of Nefau et al. (2013) where a total removal and a removal from 50 to 100 % of MET in activated sludge treatment plants was reported, respectively.

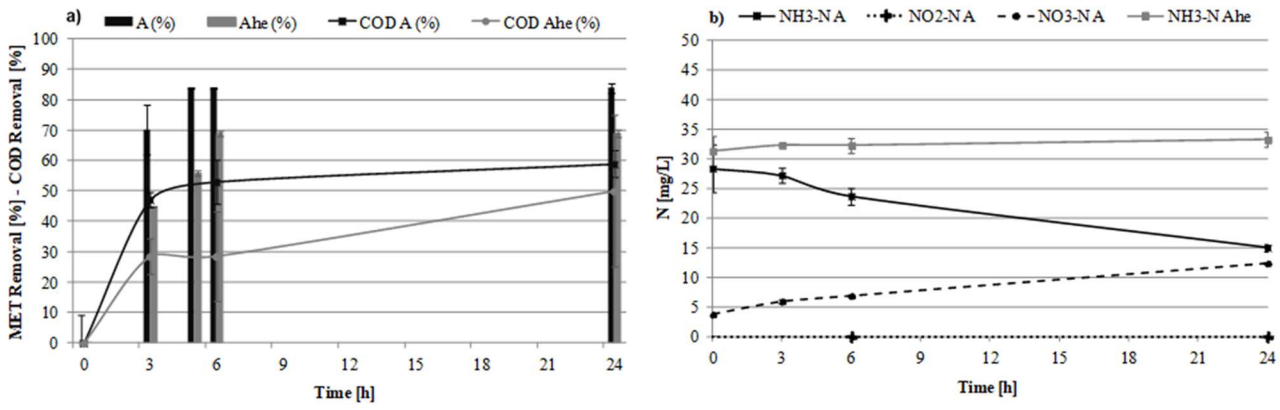

Figure 10 Results of the batch tests at initial MET concentration of 50 ng/L. Time-profiles of (a) MET and COD removal efficiency and (b) ammonia, nitrate and nitrite concentrations (error bars indicate the standard deviation)

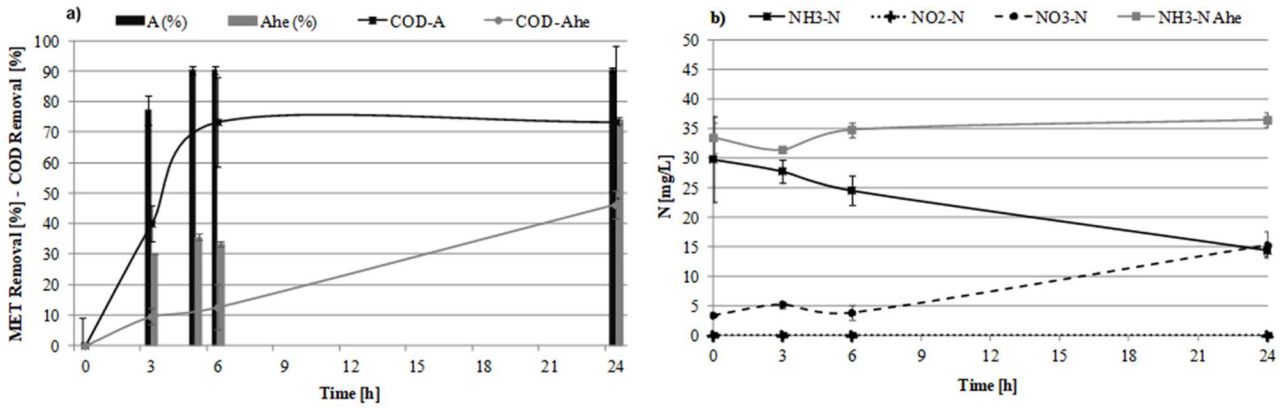

Figure 11 Results of the batch tests at initial MET concentration of 100 ng/L. Time-profiles of (a) MET and COD removal efficiency and (b) ammonia, nitrate and nitrite concentrations (error bars indicate the standard deviation)

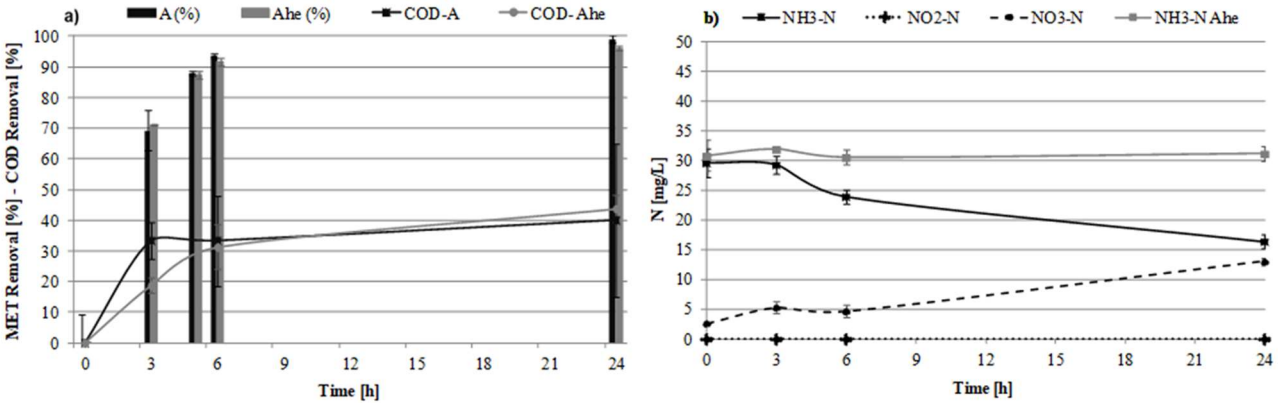

Figure 12 Results of the batch tests at initial MET concentration of 200 ng/L. Time-profiles of (a) MET and COD removal efficiency and (b) ammonia, nitrate and nitrite concentrations (error bars indicate the standard deviation)

Table 8 Average results of removal efficiency measured in the biological tests at different MET initial concentration: T=Total. RB_T=removal for biodegradation. RB_H=removal for heterotrophic biodegradation. RA=removal for adsorption. RO=removal for other abiotic

C_0 [ng/L]	T	RB_T	RB_H [%]	RA	RO
50	84	81	66	0	3
100	90	86	70	3	2
200	96	96	94	0	0

Table 8 reports average removal efficiency measured in the batch tests, where T stands for the total removal, while RB_T and RB_H refer to the values ascribed to the biological processes, either overall or only heterotrophic, respectively, calculated after reduction of the contribution due to adsorption (RA) and to other abiotic processes (RO) (as outlined in Eq. 8, Eq. 9, Eq. 10, Eq. 11). As above outlined, the total removal improves at increasing MET concentrations, from 84% to 96% at 50 ng/L and 200 ng/L, respectively. Contributions of adsorption and other abiotic processes are always negligible, as highlighted by Bagnall et al. (2013) and the main removal can be ascribed to the biological activity. These results agree with the high solubility and the hydrophilic characteristics of MET (K_{OW}=2.95, $S=1.33 \cdot 10^4$), as reported in Table 1. Furthermore, concentrations detected in the solid phase were always lower than LOQ (2.4 ngMET/gTSS) either at the beginning and at the end of the tests. Thus, it is confirmed the reduced tendency of the contaminant to be adsorbed, according to the values found for $\log K_{OC}$ and $\log K_{OW}$.

The results obtained by the application of the selected kinetic models to the data from the overall biological processes are summarized in Table 9. The same table shows the equilibrium time, T_e, and the corresponding MET concentration, C_e. It is possible to observe that the experimental data fit better the pseudo-first order kinetic model for all the tested concentrations of MET (highlighted in bold). The

values of C_e are always below the detection limit, thus indicating complete removal, whereas the equilibrium time does not change significantly with concentration.

Table 9 Kinetics models and parameters of the overall biological process tests at different MET initial concentration (in bold the best fitting)

C_0	**50 ng/L**					**100 ng/L**					**200 ng/L**				
T_e [h]	5					5					6				
C_e [ng/L]	<LOQ					<LOQ					<LOQ				
Kinetic order	0	I	II	**Pseudo I**	Pseudo II	0	I	II	**Pseudo I**	Pseudo II	0	I	II	**Pseudo I**	Pseudo II
R^2	0.24	0.25	0.23	**1.00**	0.12	0.28	0.47	0.74	**0.99**	0.44	0.36	0.84	0.98	**0.99**	0.40
Kinetic constant	0.86 [ng/L·h]	0.04 [1/h]	0.00 [L/h·ng]	**0.66 [1/h]**	0.00 [1/h]	1.66 [ng/L·h]	0.07 [1/h]	0.00 [L/h·ng]	**0.58 [1/h]**	0.00 [1/h]	3.24 [ng/L·h]	0.16 [1/h]	0.00 [L/h·ng]	**0.47 [1/h]**	0.00 [1/h]

Respirometric tests

Figure 13 shows the corresponding SOUR values determined at time t=0, 3 h and 6 h, where the first value refers to the endogenous respiration SOUR. The same figure also displays the SOUR measured in the blank tests (i.e. in the absence of MET).

It can be noted that at all the tested drug concentrations, SOUR is always higher when MET is present: it seems that the drug is capable of stimulating the biological activity, although its concentration remains significantly lower than COD and ammonia. Based on the Respiration inhibition tests procedure, it can be assessed that inhibition effects are completely absents either on heterotrophic or autotrophic biomass activity. Therefore, the percentage inhibition indices reported Eq. 14, Eq. 15, Eq. 16 cannot be calculated.

Since the tested concentrations of MET fall within the typical values found in the influent to WWTPs, the results here obtained indicate that the presence of this drug does not negatively affect the biological activity in the reactor.

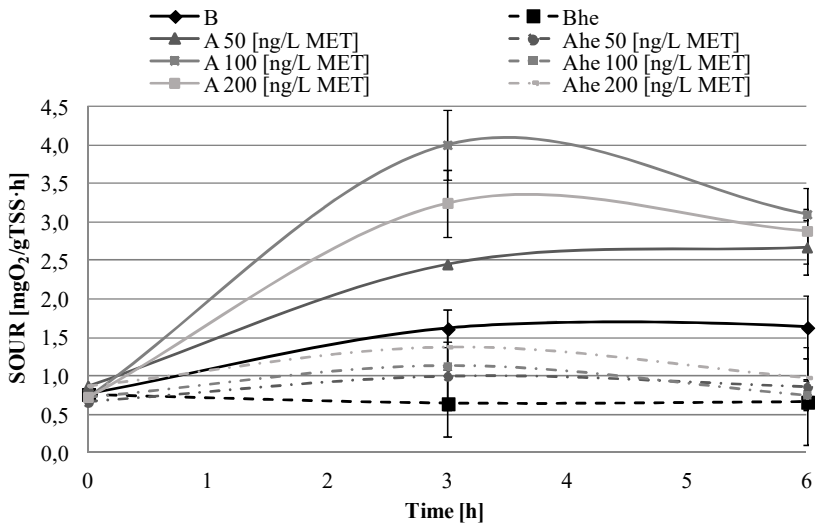

Figure 13 Time-profiles of SOUR in the biological tests and in the blank tests (error bars indicate the standard deviation)

1.6.1.3 Fate and removal of benzoylecgonine

Activated sludge tests

BE removals with time in the Overall biological and Inactivated sludge tests are shown in Figure 14a and Figure 14b, respectively; error bars indicate RSD% calculated on the removal efficiency values of two replicates.

In the Overall biological tests (Figure 14a), removal increased with time and reached 100% between 6 and 24 h of contact time for all the initial concentrations. This is in good agreement with previous works and the review of Nefau et al., (2013) where a removal greater than 90% of BE in activated sludge treatment plants is reported (Castiglioni et al., 2006; Gerrity et al., 2011; Subedi and Kannan, 2014). The Heterotrophic biological tests showed the same removal with time (i.e. 100% between 6 and 24 h) (data shown in Figure S.M. 3Figure S.M. 3 of Supplementary materials), indicating that the nitrification process did not appreciably contribute to the BE biodegradation. The removal in the Inactivated sludge tests (Figure 14b) also increased with time, but it did not exceed 9%; accordingly, the low value of the sludge-water partition coefficient, K_D, of BE indicates the difficulty of this compound to be adsorbed onto sludge flocs. Furthermore, removal measured in the Control tests (conducted in the absence of sludge) was less than 8%: therefore, contributions due to ionization, hydrolysis, volatilization and other abiotic processes can be considered negligible. These results are also confirmed by the high solubility (S=1686 mg/L) and the small value of Henry's constant ($H=7.9\cdot10^7$ atm·m^3 mol) which indicate the low volatility of this compound, as reported in Table 1.

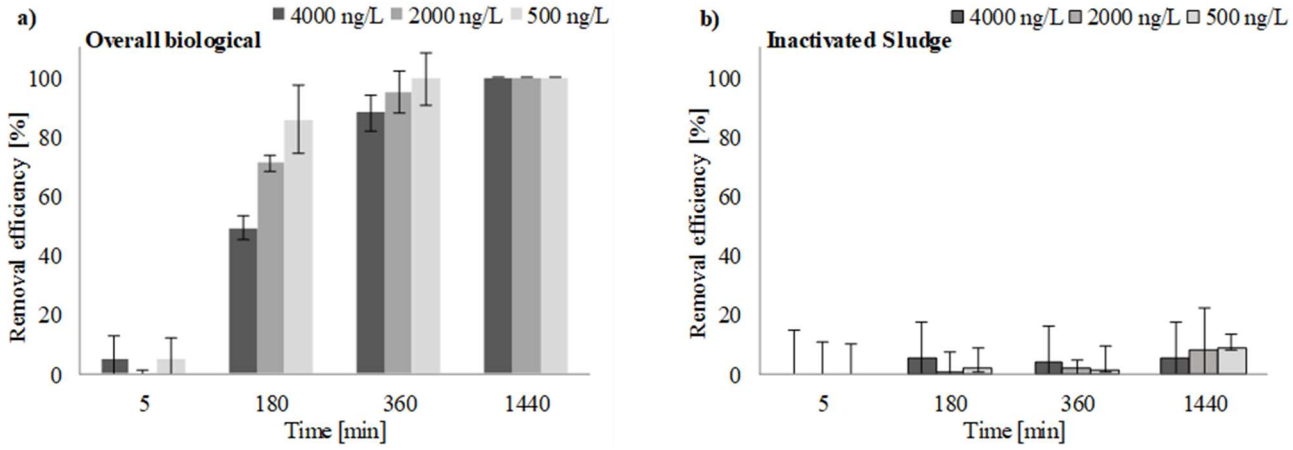

Figure 14 Time-profiles of BE removal efficiency in the liquid phase during (a) the Overall biological tests and (b) the Inactivated sludge tests (error bars indicate the SDR%)

As outlined above, a total removal of 100% due to all the processes taking place within the reactor was observed at all the initial concentrations tested: since contributions due to adsorption and other abiotic processes were always low, the main removal was ascribed to the biological activity (between 91% and 95% at increasing BE concentrations). Furthermore, concentrations detected in the sludge phase were always lower than LOQ (0.3 ngBE/gTSS) either at the beginning or at the end of the tests. The reduced tendency of BE to be adsorbed is consistent with its values of $\log K_{OC}$ and $\log K_{OW}$. Similar results were also reported by other experimental works where a low concentration of BE in the sludge of different WWTPs was measured (<4 ng/g) (Álvarez-Ruiz et al., 2015).

Table 10 summarizes the results obtained by the application of the selected kinetic models to the experimental data of the Overall biological tests. The best fitting model was found to be the first order for all the tested concentrations of BE, providing the highest value of R^2. Figure 15 shows the experimental data and the curves predicted by the model.

Table 10 also displays the equilibrium time, T_e, which is the time required for the concentration in the liquid solution to become stable. The corresponding BE concentration in the liquid and sludge phases ($C_{e,liquid}$ and $C_{e,sludge}$, respectively) were always below the detection limit, thus indicating complete removal. These results indicate that BE at the tested concentrations can be efficiently removed in the biological reactor of a WWTP. The sludge concentration was equal to about 3 g/L MLSS, which falls within the range commonly found in the full-scale plants, while the required contact time was less than 24 h.

Table 10 Kinetics models and parameters of the Overall biological tests of BE

C_0	4000 ng/L	2000 ng/L	500 ng/L
T_e [h]	<24	<24	>6

$C_{e,liquid}$ [ng/L]	< LOQ			< LOQ			< LOQ		
$C_{e,sludge}$ [ng/g]	< LOQ			< LOQ			< LOQ		
Kinetic order	0	I	II	0	I	II	0	I	II
R^2	0.599	0.992	0.952	0.426	0.993	0.851	0.337	0.980	0.781
Kinetic constant	123.38 [ng/L·h]	0.28 [1/h]	0.01 [L/h·ng]	58.78 [ng/L·h]	0.52 [1/h]	0.001 [L/h·ng]	12.30 [ng/L·h]	0.87 [1/h]	0.06 [L/h·ng]

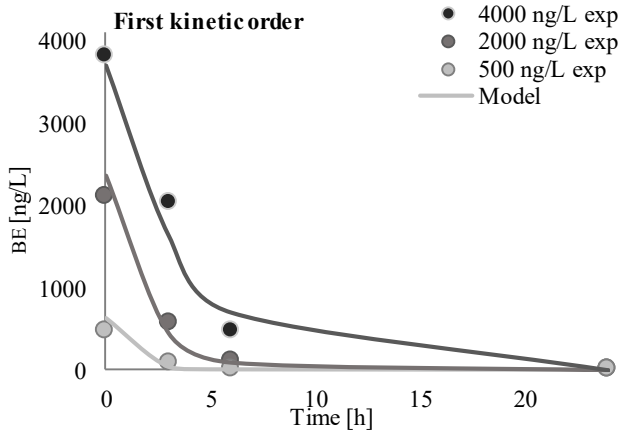

Figure 15 First kinetic order plots for the biodegradation of BE in the Overall biological tests at different initial concentrations

Respirometric tests

Figure 16 shows the efficiency of COD removal and nitrification in the Blank and Overall biological tests conducted at 500 ng /L, 2000 ng /L and 4000 ng /L BE; the same figure also highlights the maximum inhibition of heterotrophic and autotrophic biomass activity obtained through the Respiration inhibition tests.

It can be observed that at the lowest concentration tested (500 ng /L BE), neither COD removal nor nitrification processes were inhibited by the presence of BE. Increasing concentrations, both processes became inhibited and the removal efficiency decreased progressively with respect to the value measured in the Blank test. Particularly, COD removal efficiency decreased from 70% to 60% at 2000 ng /L BE and to 45% at 4000 ng /L BE. The corresponding percentage inhibitions of the heterotrophic biomass activity were calculated to be 49% and 55%, respectively. Similarly, in the test at initial concentration of 2000 ng /L the percentage inhibition of the autotrophic biomass activity was found to be equal to 48% and a reduction of the nitrification efficiency was observed. At 4000 ng /L BE, nitrification efficiency was further reduced and percentage inhibition reached 50%.

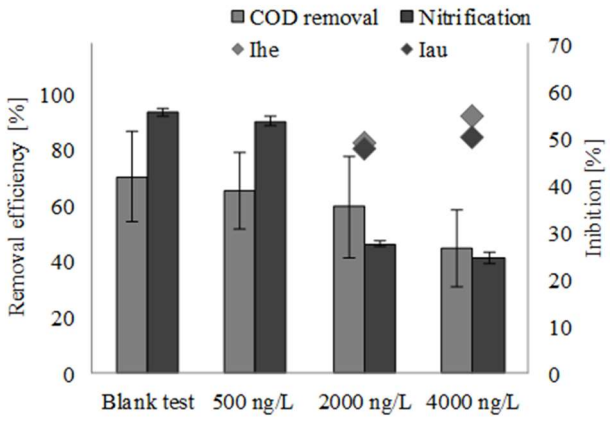

Figure 16 Efficiency of COD removal and nitrification and percentage inhibition of heterotrophic biomass activity (Ihe) and autotrophic biomass activity (Iau) at different BE concentration and in the blank test (error bars indicate the SDR%)

It must be pointed out that the operating parameters of the process, such as DO, pH and temperature, were always maintained within the optimal range indicated for the biological reactions to take place regularly (i.e. DO≈6 mg /L, pH =7.2-8.0, and T=22±2 °C) (Metcalf and Eddy, 2013). Therefore, the inhibition effects could be ascribed only to the presence of high concentrations of BE. The presence of BE does affect oxidation of nitrogen compounds and also COD removal, although only at the higher concentrations.

1.6.1.4 Fate and removal of 11-nor-9carboxy-Δ9-THC

Activated sludge tests

Figure 17a and Figure 17b show removal efficiency of THC-COOH in the Overall biological and Inactivated sludge tests, respectively, conducted at 50 ng/L, 150 ng/L, 300 ng/L and 2000 ng/L THC-COOH. The figures show also the RSD calculated on the removal efficiency values of two replicates.
It can be noted that for concentration of 50 ng/L, 150 ng/L and 300 ng/L, the removal reached about 100% in the first 5 minutes and did not change appreciably afterwards. For the highest concentration, i.e. 2000 ng/L, the following removal efficiencies were calculated with time: 75.23% at t=5 minutes, 98.69% at t=180 minutes, 99.38% at t=360 minutes and 99.6% at t=1440 minutes. Time profiles indicate that THC-COOH was totally eliminated within 24 h at all the tested concentrations. Looking in details at the Overall Biological tests, it can be noted that the main removal occurred in the first 5 minutes. Therefore, the equilibrium time can be considered less than 5 minutes for the tests at 50 ng/L, 150 ng/L and 300 ng/L initial concentrations. By contrast, in the test conducted at 2000 ng/L THC-COOH removal continued to take place afterwards.

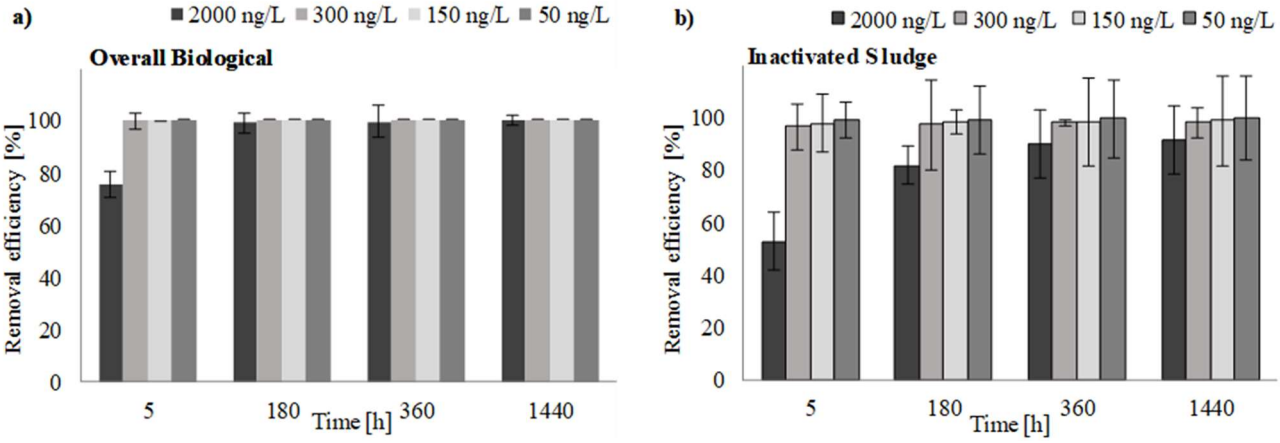

Figure 17 Time-profiles of THC-COOH removal efficiency in the liquid phase during (a) the Overall biological tests and (b) the Inactivated sludge tests (error bars indicate the SDR%)

The concentrations in the sludge phase at the end of the biological test were also measured and the values found were: 1.6 ng/gTSS at 2000 ng/L, 0.9 ng/gTSS at 300 ng/L, 1.1 ng/gTSS at 150 ng/L and 1.2 ng/gTSS at 50 ng/L. The Heterotrophic biological tests provided very similar results (data shown in Figure S.M. 4 of Supplementary materials) to those determined in the Overall biological tests: therefore, contribution of nitrification seemed not to be relevant for biodegradation of THC-COOH.

The Inactivated sludge tests provided very similar profiles: main removal took place during the first 5 minutes, while afterwards it increased appreciably only at the highest concentration of 2000 ng/L. Determinations on the sludge phase showed THC-COOH concentration ranging from 28 to 11 ng/g at the end of the tests, depending on the initial concentration in the liquid phase.

Results of Control tests conducted in the absence of biomass showed a removal percentage about 25% for all the initial concentrations. This removal could be ascribed to the drug dissociation in water because THC-COOH is a weak acid with pKa=3.15-2.15; besides, ionization processes might have also provided a contribution because THC-COOH molecule is weak volatile according to the Henry's constant value ($9.21 \cdot 10^{-10}$ atm·m^3/mol). Therefore, several abiotic processes were likely to occur giving rise to transformation of THC-COOH into different products which could not be detected.

Comparison of the results obtained through all the tests highlights the relevance of adsorption as compared to the other abiotic processes and to biodegradation. The high values of K_D and log K_{OW} (29100 L/kg and 5.63, respectively) (Table 1) confirm the low tendency of THC-OOH to dissolve in the liquid phase and its inclination to be adsorbed to suspended solids and organic matter (Postigo et al., 2010). Additionally, biodegradation contributed to the contaminant removal in both the liquid phase and the sludge phase.

As outlined above, THC-COOH was totally removed within 24 h, and the main responsible removal mechanism was a combination of adsorption and biodegradation. Although scientific literature on the removal of THC-COOH in WWTP is very scarce, the few available data are in agreement with the

results of the present study referring complete removal in the activated sludge treatment (Castiglioni et al., 2006; Racamonde et al., 2012).

Data obtained in the Inactivated sludge tests were fitted by different kinetic models. Table 11 shows the results of the fitting process, the equilibrium time, T_e, and the corresponding THC-COOH concentration, C_e, in the liquid and sludge phases. The experimental data were best fitted by the pseudo-second order kinetic model for all the tested concentrations as proved by the highest R^2 value. Experimental data and the modelled curve are reported in Figure 18.

Table 11 Kinetics models and parameters of the Inactivated sludge tests of THC-COOH

C_0	**2000 ng/L**		**300 ng/L**		**150 ng/L**		**50 ng/L**	
T_e [h]	<24		<24		<24		<3	
$C_{e,liquid}$ [ng/L]	183		41		30		16	
$C_{e,sludge}$ [ng/g]	11.6		28.1		18.1		15.4	
q_e [ng/g]	261.6		10.9		6.1		5.8	
Kinetic	Pseudo	**Pseudo**	Pseudo	**Pseudo**	Pseudo	**Pseudo**	Pseudo	**Pseudo**
order	I	**II**	I	**II**	I	**II**	I	**II**
R^2	0.993	**0.999**	0.923	**0.957**	0.731	**0.990**	0.865	**0.905**
Kinetic	0.564	**0.005**	0.300	**0.013**	0.174	**0.044**	0.426	**0.020**
constant	[1/h]	**[g/ng·h]**	[1/h]	**[g/ng·h]**	[1/h]	**[g/ng·h]**	[1/h]	**[g/ng·h]**
K_D [L/kg]	1428		263		200		358	

Table 11 also displays the value of K_D experimentally calculated. Only one data was found in the scientific literature (Table 1) and shows a higher value of K_D (29100 L/kg): this difference is likely due to the fact that in the latter case the value was estimated by a software and is related to adsorption onto soils, while in the present study it was calculated for sludge solids.

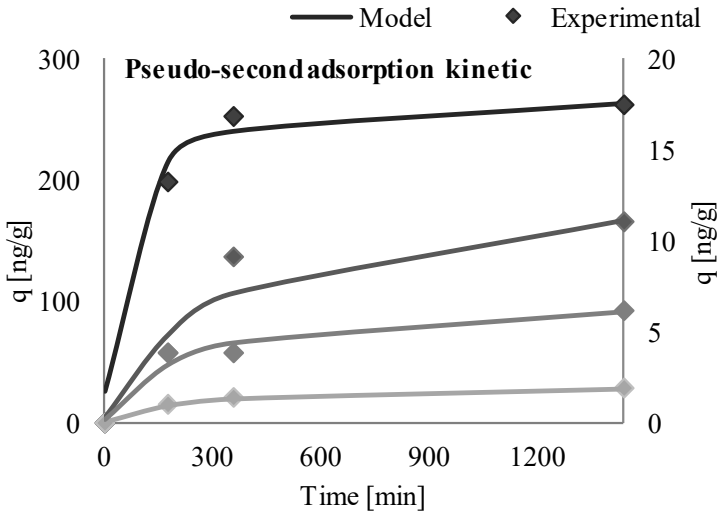

Figure 18 Pseudo-second order kinetic plots for adsorption of THC-COOH onto inactivated sludge at different initial concentrations

Respirometric tests

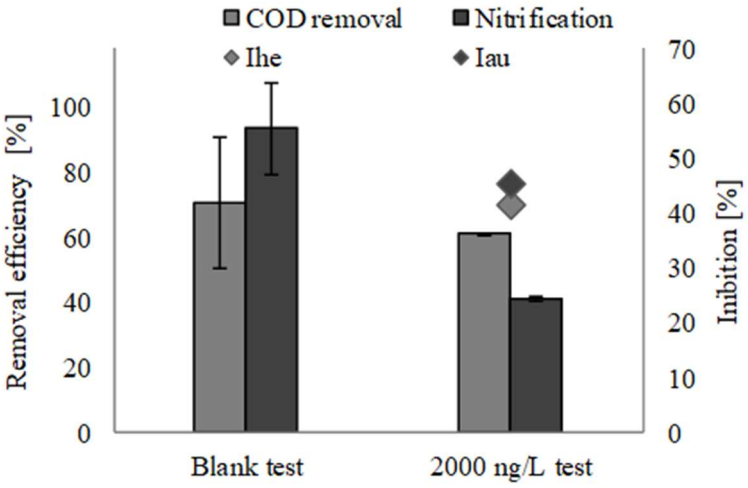

Figure 19 Efficiency of COD removal and nitrification at 2000 ng/L TH-COOH, and percentage inhibition of heterotrophic biomass activity (Ihe) and autotrophic biomass activity (Iau) (error bars indicate the SDR%)

The Respirometric tests provided results only at 2000 ng /L THC-COOH, when a residual concentration was still present at 3 and 6 hours of contact time when the test has to be carried out according to the procedure. Figure 19 shows the efficiency of COD removal and nitrification in Blank and Overall biological tests and the percentage inhibitions in this case. It can be noted that both COD and ammonia oxidation proceeded continuously during the tests (data not here shown), but the efficiency was lower as compared to that measured in the blank test; accordingly, activity of both heterotrophic and autotrophic biomass was partially inhibited as a consequence of THC-COOH presence (percentage inhibition of 41 and 45%, respectively).

Equilibrium tests

Freundlich and Langmuir isotherm models were applied to fit the results of the Inactivated sludge tests. The Freundlich's model provided the best agreement with the experimental data (Figure 20). This model indicates the existence of weak adsorption forces at the first adsorbed layer between the adsorbent and the adsorbed compound; however, with increasing C_e, the adsorption amount becomes more relevant.

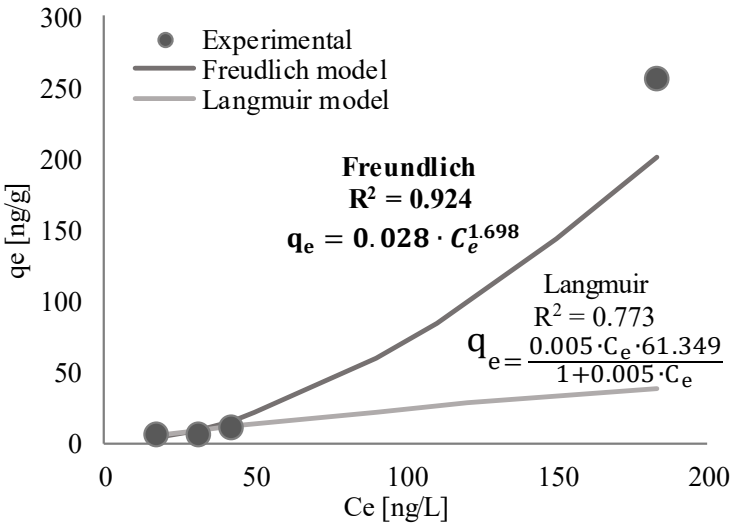

Figure 20 Fit of Freundlich and Langmuir adsorption isotherm of THC-COOH onto Inactivated sludge (in bold the best fitting)

1.6.1.5 Fate and removal of perfluorooctane sulfonic acid and perfluorooctanoic acid

Activated sludge tests

Figure 21a and Figure 21b depict the time profiles of PFOA and PFOS concentration in the liquid phase, respectively, measured in the Activated sludge tests, for the different initial concentrations (C_0): 200 ng/L, 500 ng/L, 1000 ng/L and 4000 ng/L of each compound.

The figures show for PFOA a continuous decrease of the concentration in the liquid solution throughout the tests can be observed at all the initial concentrations. More in details, the main removal took place in the first 3 h, whereas afterwards it continued at a slower rate. At the end of the tests, total PFOA removal accounted, as average, for 59%, 68%, 63% and 68% at 200 ng/L, 500 ng/L, 1000 ng/L and 4000 ng/L, respectively. Therefore, it can be highlighted an increasing trend with the concentrations.

In the case of PFOS, shown in Figure 21b, main reduction occurred rapidly at the beginning of the tests for all the concentrations. The PFOS removal observed in the following hours was very low, and at the end of the tests it reached 66%, 85%, 90% and 96%, as average, at 200 ng/L, 500 ng/L, 1000 ng/L and 4000 ng/L, respectively. Therefore, it is confirmed an increasing trend with the concentrations also in the case of PFOS. However, the removals values were always higher than those measured for PFOA.

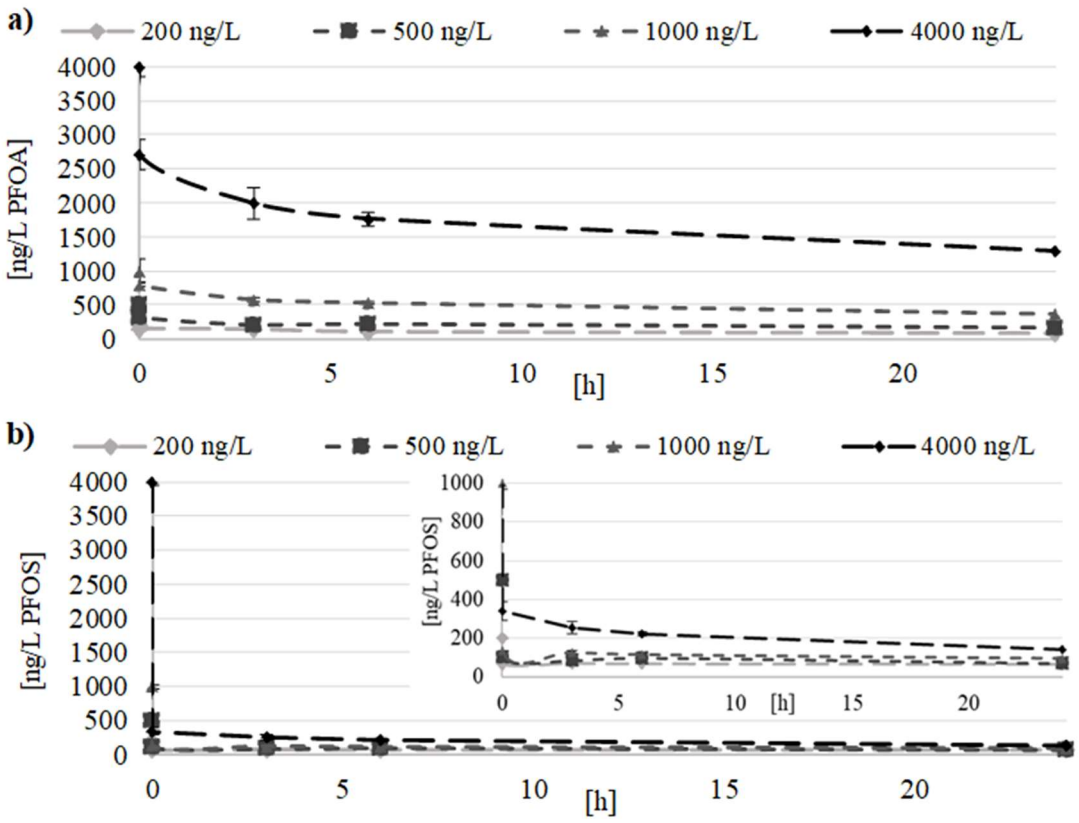

Figure 21 Time-profiles of (a) PFOA and (b) PFOS concentrations in the Activated sludge tests (error bars indicate the standard deviation)

These results do not fully agree with most of the scientific studies, where negative or much lower removal were referred (<30%). The difference has to be ascribed to the fact that these studies were mainly carried out at full scale WWTPs with a real wastewater having a more complex composition and containing other compounds; furthermore, more processes take place in the biological reactor which may interfere with the removal of PFOA and PFOS. For instance, it is known that municipal wastewaters contain also precursors, e.g. fluorotelomer alcohols, perfluoroalkyl phosphates, fluorotelomer sulfonates and other compounds not completely identified, which are being transformed into PFOA and PFOS during the processes taking place in the WWTPs (Arvaniti and Stasinakis, 2015; Pan et al., 2016). Furthermore, PFOA and PFOS are subjected to processes which may give rise to by-products (Arvaniti and Stasinakis, 2015; Becker et al., 2010; Dauchy et al., 2017; Loganathan et al., 2007; Xiao, 2017; W. Zhang et al., 2013). By contrast, in order to obtain a better understanding of the processes, the current study was conducted in laboratory under controlled conditions; besides, the feeding solution of the tests was a synthetic wastewater containing only selected compounds, that were PFOA, PFOS and nutrients.

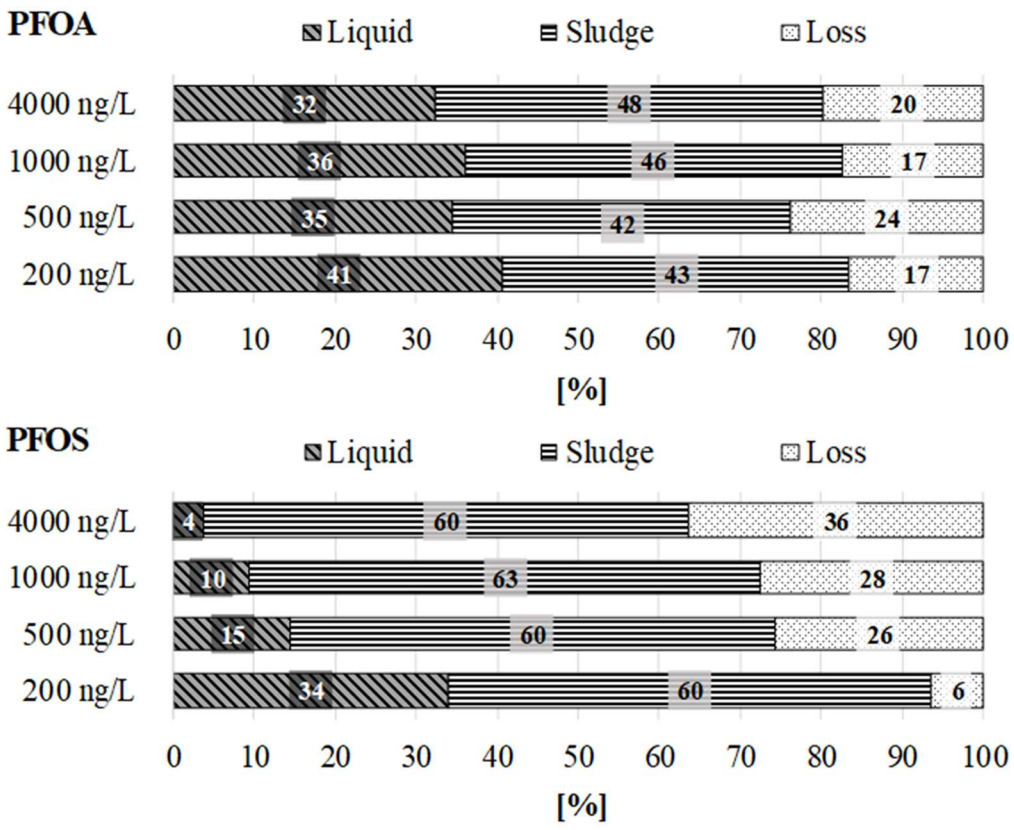

Figure 22 Normalized mass of PFOA and PFOS remaining in the liquid and sludge phases and the loss measured at the end of the Activated sludge tests

Based on the residual concentrations measured at the end of the Activated sludge tests in the liquid and the sludge phases, it was possible to carry out a mass balance on the contaminants. The results obtained are shown in Figure 22.

Normalized mass in the liquid and sludge phases and the loss were computed with respect to the mass of each contaminant initially added to the tests. The loss represents the fraction of contaminant that could not be found neither in the liquid nor in the sludge phase at the end of the tests. It was computed as the difference between the fractions measured in solution and on the sludge. This loss of PFOA and PFOS from the system cannot be completely attributed to the uncertainty of the analytical method of detection: indeed, concentrations used in the mass balances were previously corrected based on the recovery percentage determined in the method validation.

The mass of PFOA found in the liquid phase ranged from 32% to 41%, at decreasing concentration. An inverse trend was observed for the mass remaining on the sludge, which increased from 42% to 48% with the concentration. The total loss was accounted to be from 17% to 24%.

Arvaniti et al. (2014), using the same solid concentration as in the present study, found a similar mass percentage adsorbed on the secondary sludge (about 50%). Pan et al. (2016) observed a similar mass loss, below 25%, in a real scale WWTPs study; however, the residual concentration in the effluent was much higher, i.e. about 75% of the initial load, likely due to the presence of precursors in the real wastewater which gave rise to transformation processes increasing the final concentrations. The

different percentages reported with respect to the present work are likely due to the fact that most of the previous studies were carried out at full-scale, whereas in this case the behaviour of PFOA and PFOS was investigated in the activated sludge reactor at laboratory scale, in absence of precursor compounds. Considering that PFOA is reported not to be biodegradable, these results seem to indicate that adsorption was the main responsible of the removal from the liquid phase. However, the uptake capacity of the sludge was unable to determine the complete mass transfer from the liquid solution.

Values of k_d, listed in Table 12, resulted to be in the range 345-466 L/kg, and confirm the moderate sorption potential of the sludge (Tran et al., 2018). These results are in agreement with other studies as shown in Table 1 (Zareitalabad et al., 2013).

Table 12 Results of the Activated sludge tests: removal efficiency (R); experimental adsorption capacity ($q_{e,exp}$); liquid-solid partition coefficient (k_d); pseudo-second order kinetic model parameters (R^2, $_{qe,calc}$, k_2')

	Unit	**PFOA**				**PFOS**			
C_o	ng/L	200	500	1000	4000	200	500	1000	4000
k_d	L/kg	344.71	465.72	401.82	431.02	946.64	1946.23	3143.71	4681.54
$q_{e,exp}$	ng/g	49.04	143.33	265.41	1150.86	54.76	181.50	384.27	1636.88
R^2		0.98	1.00	0.99	1.00	1.00	1.00	1.00	1.00
$q_{e,calc}$	ng/g	52.04	145.91	275.43	1215.52	54.89	182.28	385.34	1640.86
k_2'	g/ng·h	0.01	0.01	0.003	0.001	0.23	0.03	0.03	0.01

In the case of PFOS, the main fraction found at the end of the tests (up to 63%) was that adsorbed on the sludge. The residual mass in the liquid phase decreased proportionally at increasing concentration: it varied from 34% in the test at 200 ng/L up to 4% for 4000 ng/L. The PFOS mass loss showed exactly an opposite trend. Since biodegradation is reported to be very low for this contaminant, adsorption was considered to be the main removal mechanism (Kwon et al., 2014).

It is likely that during the tests there was a mass transfer from the liquid to the sludge phase or to the interface, since molecules of PFOA and PFOS are partly hydrophilic and partly hydrophobic; however, processes other than adsorption and biodegradation were likely responsible for the definitive leaving of the compounds from the system (referred to as loss). Biodegradation was excluded from the responsible processes because no reliable evidence of biodegradability of PFOA and PFOS under aerobic conditions was reported in the scientific literature (Parsons et al., 2008; Tjanowiczro et al., 2018). Indeed, although microorganisms can remove non-fluorinated functional groups, they are unable to successfully attack and remove PFASs fluorine substituents to achieve mineralization of perfluorinated molecules (Parsons et al., 2008). For this reason, the strength of the carbon–fluorine bond is generally considered the main factor that limits biodegradability of PFASs.

To explain the loss, it must be also taken into account that volatilization from water cannot be considered as a relevant mobility mechanism for PFOA and PFOS due to the low values of the Henry's constant

(H) and the vapour pressure (p_v) as highlighted in Table 1 (Johansson et al., 2017). Values of the water solubility of PFOA and PFOS are relatively high (3.4 g/L for PFOA and 0.52 g/L for PFOS), due to the presence of the two hydrophilic functional groups (Zhang et al., 2013). However, the compounds have also hydrophobic properties related to the C-F long chains; this turns out to be more relevant for PFOS, and suggests that the hydrophobic interaction represents a key mechanism in the sorption process (Zhou et al., 2010). Furthermore, being pKa < 0, they exist in a dissociated form at the typical pH of aquatics systems, which means as positively charged cation and negatively charged anion, carboxylate or sulfonate, indicating that they are strong acids (Smith et al., 2016). Another reason of mass loss might be considered their irreversible adsorption to glass (Martin et al. 2004; Ferrey et al. 2012; Zhang et al. 2013a). However, this loss contribution has been already taken into account in the tests used for the definition of the recovery percentage of the two compounds in the analytical method validation. These tests were performed using glass flasks in the presence of all the elements which were also contained in the experimental reactors. Due to the high polarity of PFASs molecules, a specific test involving only water, glass and contaminants was considered not reliable and maybe misleading, since in that case PFASs would have had high affinity with the only available phase other than water.

Time-profiles concentrations measured in the Activated sludge tests were best fitted by the pseudo-second order kinetic model at all the tested concentrations and for both contaminants, since it provided the highest value of R^2 with respect to the other models. Table S.M. 3 summarizes the results obtained by the application of all the selected kinetic models.
The values of the parameters found for the best model are shown in Table 12, where $q_{e,exp}$ and $q_{e,calc}$ stand for the equilibrium adsorption capacity experimentally calculated and predicted by the model, respectively. It can be noted that values of $q_{e,exp}$ and $q_{e,calc}$ do not differ appreciably for all the tested concentrations (for example at 200 ng/L, they were 49 ng/g and 52 ng/g, respectively): this confirms the good quality of the kinetic results fitting. Similar results for PFASs were also found by other authors (Zhou et al., 2010).

During the Activated sludge tests, ammonia, nitrates, nitrites and COD concentrations were also monitored in order to evaluate if the presence of PFOA and PFOS can affect the biomass activity.

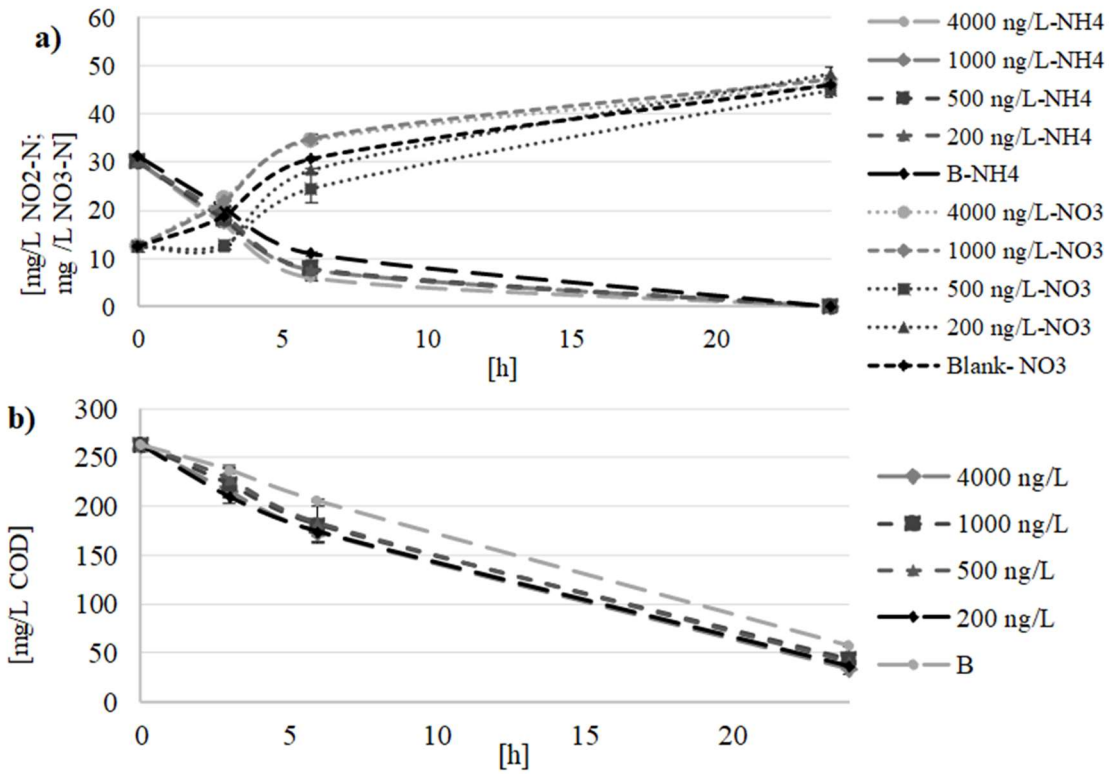

Figure 23 Time-profiles of ammonia and nitrate concentrations (a) and COD concentration (b) in the Activated sludge tests (error bars indicate the standard deviation)

Figure 23a shows ammonia and nitrate nitrogen concentrations measured with time at the different initial concentrations of PFOA and PFOS, and in the absence of these contaminants (Blank tests, B). It can be noted that ammonia was continuously converted into nitrate at all the tested concentrations of PFOA and PFOS, with removal efficiency of about 100% measured at the end. Furthermore, the difference with the blank tests in the rate of conversion was negligible. Nitrite concentration (not here shown) was always under the detection limits. These results indicate that complete nitrification was taking place without any inhibition by PFOA and PFOS.

Figure 23b shows carbon removal with time in the presence and in the absence (Blank test, B) of PFOA and PFOS. Reduction of COD occurred continuously at a similar rate as that observed in the Blank test. COD oxidation reached final values above 80% for all the concentrations, which were comparable with those measured in the absence of PFOA and PFOS (Blank test). Therefore, it can be deemed that these contaminants do not affect the main biological processes taking place in the activated sludge reactor.

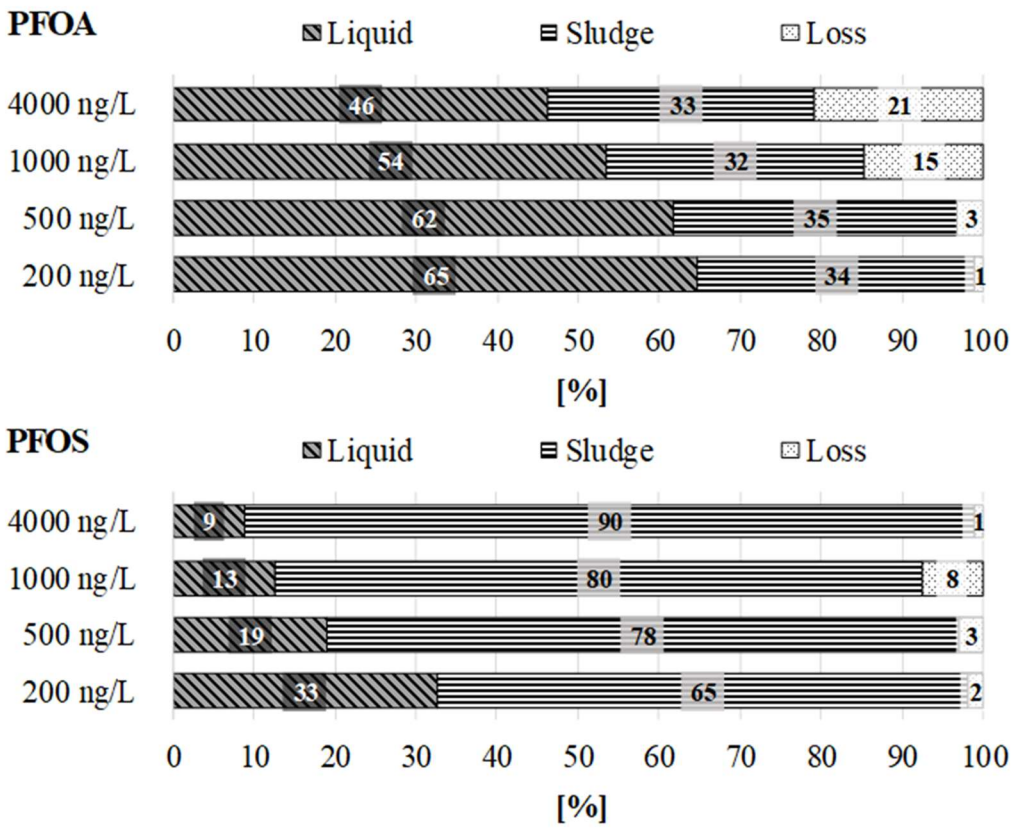

Figure 24 Normalized mass of PFOA and PFOS in the liquid and sludge phases and the loss measured at the end of the Sterilized sludge tests

Figure 24 shows the results obtained at the end of the Sterilized sludge tests in terms of mass of PFOA and PFOS measured in the liquid and sludge phases and the total loss. The fraction of PFOA found in the liquid phase varied from 46% to 65% as the initial concentrations decreased from 4000 ng/L to 200 ng/L, respectively. This trend is similar to that observed in the Activated sludge tests; however, now the residual concentrations are always higher. The mass adsorbed on the sludge slightly decreased at the higher concentration, as observed in the Activated sludge tests. By contrast, trend of loss was different, with an important decrease with the concentrations (from 21% to 1% at 4000 ng/L and 200 ng/L, respectively). These results confirm that adsorption was the main responsible of PFOA removal.

At the higher concentrations (4000 ng/L and 2000 ng/L), the mass loss of PFOA due to processes other than biological and adsorption was comparable in the Activated and Sterilized sludge tests, whereas it decreased significantly at the lower concentrations in the presence of inactive biomass (Figure 22 and Figure 24). This seems to indicate that these other processes were likely mediated by activated sludge bacteria when they were not inhibited.

As far as PFOS is concerned, at the end of the Sterilized sludge tests the residual mass was found mainly adsorbed on the sludge, with values ranging from 65% at 200 ng/L up to 90% at 4000 ng/L. It is confirmed the high tendency of PFOS to be adsorbed onto the sludge. The mass remaining in the liquid phase showed the same profiles as observed in the Activated sludge tests, with an increase at lower concentrations. The amount accounted as loss was very low (few percentages) and much smaller than

that measured in the presence of active biomass. It is noteworthy that both PFOA and PFOS showed a higher loss in the presence of biomass activity, highlighting some role of the biological processes or the effect of an active biosorption of microorganisms, as also highlighted by Zhou et al. (2010a).

Respirometric tests

To further investigate the potential inhibition, respirometric tests were also conducted by following a standard procedure (OECD n. 206). These tests allowed to determine the inhibition index of the biomass activity at t=3h contact time for all the concentrations. The values found for this index resulted to be always zero, except at the highest concentration (4000 ng/L) when the index was calculated to be equal to 14%.

Based on these results, it can be assessed that PFOA and PFOS are capable of negatively affecting biomass activity only at the highest load: however, the inhibition still remains quite low.

Equilibrium tests

In accordance with other studies, the adsorption process of both PFOA and PFOS was better represented by the Freundlich model, which provided the higher value of the R2 between the experimental and modelled data (Arvaniti and Stasinakis, 2015; Hu et al., 2017; Zareitalabad et al., 2013; C. Zhang et al., 2013). Supplementary Materials show the results of the application of the other isotherm models (Table S.M.4).

Figure 25 shows the experimental data and the fitting obtained by the application of the linear form of the Freundlich equation.

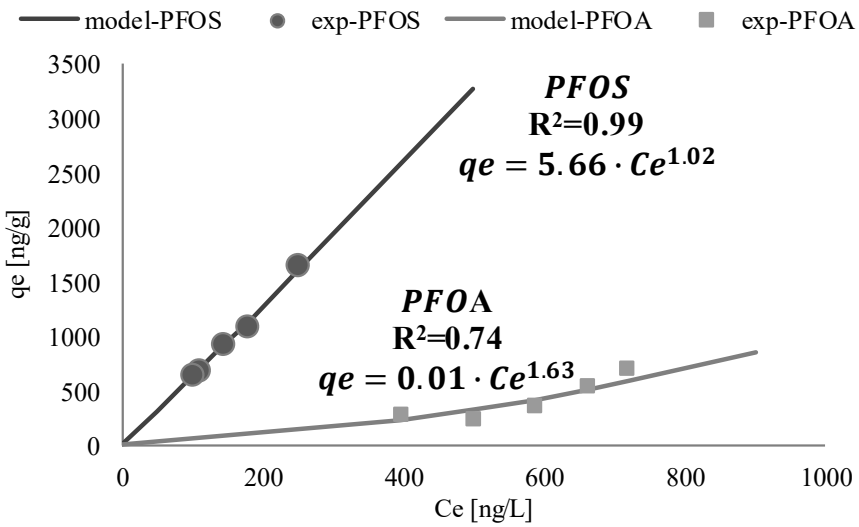

Figure 25 Experimental data and Freundlich isotherm modelling of the Equilibrium tests

The Freundlich model usually applies to heterogeneous surface energy systems (non-uniform distribution of sorption heat), when more than one sorption mechanism is exhibited. This hypothesis

seems to fit the double behaviour of the molecules having a hydrophilic head group and a hydrophobic perfluorinated chain, such as PFOA and PFOS. Values found of the Freundlich model parameters are reported in Figure 25. The maximum adsorption capacity, q_{max}, can be extrapolated posing $C=C_0$, where C_0 is the initial concentration of the contaminant in solution (Eskandarpour et al., 2008). In the present case, being C_0= 1000 ng/L, it resulted to be q_{max}=1004 ng/g for PFOA and 6624 ng/g for PFOS.
Values of K_F, which represents the adsorption capacity, was higher for PFOS than PFOA (5.66 ng/g and 0.01 ng/g, respectively): this confirms the stronger sorption potential of PFOS on the sludge, as also reported by previous studies (Zhou et al., 2010). PFOA was mainly found distributed between the aqueous and the sludge phases, while PFOS showed higher accumulation on the sludge. This different behaviour is also due to the shorter chain (C<8) of the PFOA molecule, while PFOS has a longer chain (C≥8) (Pan et al., 2016).
The magnitude of the value of 1/n is a measure of the adsorption intensity or the surface heterogeneity, becoming more heterogeneous as its value approaches zero. When 1/n assumes a value above unity, the adsorption is described to be cooperative: this means that adsorbate already present on the surface of the adsorbent material, facilitates the adsorption of others molecules from the solution, due to the steric interaction and the interaction between the same compounds in solution (Liu, 2015). In the present case, 1/n was found to be equal to 1.63 and 1.02 for PFOA and PFOS, respectively, thus indicating the cooperative nature of the adsorption process. These values are comparable to those reported by Zhang et al., (2013) which found 1/n=0.88-1.22 and 1/n=0.78-1.09 for PFOS and PFOA, respectively.

Leaching tests

A further series of tests was carried out with the aim to evaluate the stability of the adsorption process of the contaminants on the sludge; this would allow to determine the eventual risk associated to the reuse/disposal of the sludge loaded by PFOA and PFOS in the biological reactor and then wasted by the WWTP. The Leaching tests were performed on the sludge collected at the end of the Equilibrium tests carried out at the initial concentration of 1000 ng/L PFOA and 1000 ng/L PFOS, at two different solid contents. The released mass of PFOA at the end of the Leaching tests was found to be 1.2% and 0.6% (mass/mass) at 4 g/L TS and 5 g/L TS, respectively, with respect to the load present on the sludge at the beginning of the tests. For PFOA, the released mass was equal to 0.3% and 0.2%, at 4 g/L TS and 5 g/L TS, respectively. These results highlight that these contaminants, once transferred on the sludge, remain strongly adsorbed and cannot be leached out under the conditions of the standard tests. Therefore, disposal of waste sludge does not pose a serious risk due to leaching processes.

1.6.2 Continuous feeding test

1.6.2.1 OMPs removal

Figure 26 depicts the average removal efficiency (R%(t)) of each compound as measured at t=48 h for the different DO perturbation strategies. Concentrations of OMPs measured inside the reactors at each sampling time during the tests are reported in Supplementary materials Figure S.M. 5.

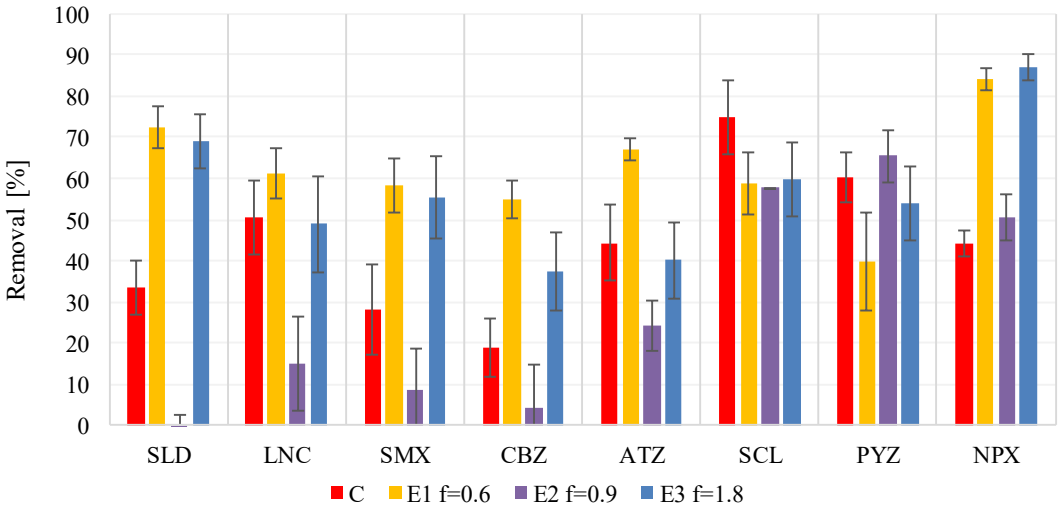

Figure 26 Removal efficiency measured t=48 h for each DO perturbation and each OMP (error bars indicate the standard deviation of the replicates)

It can be noted that the perturbation strategies affected in a different way and extent the removal of each OMP. With the exception of SCL, there was always a perturbed condition capable of improving the removal efficiency with respect to the control test (C). At the end of the experiments (t=48 h), the best effect for most of the contaminants (i.e. SLD, LNC, SMX, CBZ and ATZ) was obtained by applying the E1 frequency (i.e. f=0.6 1/h), with removals ranging from 40% (for PYZ) up to 84% (for NPX), for an average value measured on all the investigated OMPs of about 62%. With respect to the control, an increase of the removals by 39%, 11%, 30%, 36%, 23%, for SLD, LNC, SMX, CBZ and ATZ, respectively, was obtained. This indicates that the longer the DO OFF phase (i.e. absence of aeration) the higher the achieved removal; therefore, facultative aerobic bacteria or anoxic bacteria (being nitrate present in the reactor) were likely responsible of the observed improvement. This result is consistent with other scientific studies where biotransformation of some OMPs, such as NPX and Trimethoprim, were observed under anaerobic conditions (Gonzalez-Gil et al., 2019). Better removals, with respect to the control, were also measured in the case of SLD, SMX, NPX and CBZ during the tests conducted at the E3 frequency (i.e. f=1.8 1/h) with an increase accounting for 36%, 28%, 43%, 19% respectively. Therefore, the two extreme conditions of DO perturbation among those tested in the present study were both capable of boosting degradation of many of the considered OMPS. Only PYZ showed a better degradation in the test at E2 frequency, i.e. at f=0.9 1/h.

Considering the average removal value of all OMPs calculated in each type of test, it can be deemed that the E1 strategy provided the best improvement; furthermore, a reduced variability of the data was observed at this frequency as compared to the others.

Since the duration of the ON aeration phase was maintained unchanged in all the tests as well as the volume and composition of the reactors, therefore the minimum amount of oxygen supplied to the biomass was always the same. Thus, the observed changes in the removal efficiency were likely due to the applied DO perturbation frequency instead of the amount of available oxygen. Consequently, the DO concentration range can be considered a less relevant parameter for this enhancing strategy. The same observation was also reported by Stadler and Love (2019) which showed that a reduced DO concentration, from 6 to 0.5 mg/L O_2, did not decrease appreciably the pharmaceuticals biotransformation rate.

The lower perturbation frequency (which was f=0.25) was also found by Bains at al. (2019) to be capable of a better removal of SMX, CBZ, ATZ and NPX. Particularly, with respect to the control, the observed percentage increase for CBZ, ATZ and NPX was comparable to the values obtained in the present study, whereas in the case of SMX the enhancement achieved at f=0.25 was much higher (about 80%). These results confirm that the lowest perturbation frequency which implies longer absence of aeration is the more effective strategy for OMPs degradation.

1.6.2.2 Activity of target enzymes

During the same tests conducted at the different DO perturbations, the activity of target enzymes was also measured.

Figure 27 shows the values obtained at the end of the experiments, i.e. at t=48 h, whereas the data determined at each sampling time are reported in Supplementary materials Figure S.M. 6.

Data of Figure 27 show that DO perturbations affected in a different way the activity of each of the investigated enzymes. Specifically, Lignin Peroxidase (LiP) was favourably stimulated at both E1 and E3 frequency, with an increase of its activity as compared to the control test, for both dyes. By contrast, HRP and Lacc were negatively affected whereas negligible differences were observed in the case of Cyt P450 and β-glu.

Similarly to the finding by Bains et al. (Bains et al., 2019), Lignin peroxidase (AB, MB) activity was evident in all DO conditions (perturbed and non-perturbed). By contrast, the effects of the DO perturbed conditions on the other investigated enzymes were different For instance cultures perturbed with f=0.25 1/h and f=0.5 1/h showed significantly higher Cyt P450 and HRP compared to constant DO control, whereas in the present study they were less active under DO perturbed conditions. It is important to notice that the activity of the target enzymes differed also between the control tests used in the two studies.

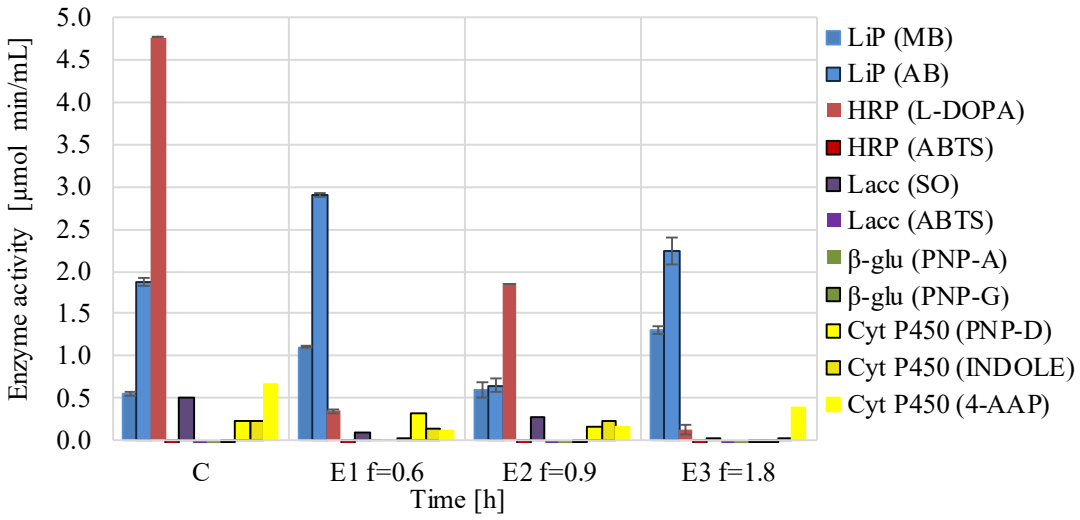

Figure 27 Target enzyme activity measured at t=48 h for each DO perturbation (error bars indicate the standard deviation of two replicates)

Comparing these results with those obtained on OMPs removal highlights that the same DO perturbation strategies were capable of enhancing both enzyme activity and OMPs degradation. The two effects were then correlated in order to find out if one or more of the target enzymes played a more relevant role. Figure 28 shows the matrix of correlation coefficient between the removal efficiency of each OMP at the end of the tests and the activity of the target enzymes. Correlation was quantified based on the value of the Pearson's coefficient (ρ, see Eq. 38). HRP (ABTS) was excluded from the statistical evaluation because no activity was detected in all the tests.

A positive correlation was obtained for the activity of LiP, β-glu and Lacc (only with ABTS dye) and LNC, SLD, CBZ, SMX, NPX and ATZ removals. Particularly, a very strong correlation (ρ ≈1) was observed with the LiP activity, thus highlighting that this enzyme plays a sensitive role in the degradation processes. The results are in accordance with the observations reported by Naghdi et al. (2018), who carried out different studies about the Lip capability to degrade several recalcitrant aromatic pollutants (such as some pharmaceuticals like Diclofenac, Tetracycline, Oxytetracycline, endocrine-disrupting compounds and dyes). A study by Jelic et al. (2012) also showed an efficient removal of carbamazepine due to the presence of laccase and peroxidase enzymes.

β-glu showed a slightly less correlation coefficient value (ρ ≈0.5) as compared to LiP for the same OMPs, also due to the really low values of its activity. Since β-glu is the only enzyme belonging to the class of hydrolase, particularly cellulose, this shows that hydrolysis reaction plays some roles in the OMPs removal. Previous studies demonstrated that hydrolysis is a key step in the degradation of persistent micro-pollutants also under anaerobic conditions (Tiwari et al., 2017). Regarding the other investigated enzymes, i.e. Lacc (SO), HRP (L-DOPA), Cyt P450 (INDOLE and 4-AAP), a positive

correlation was only found with PYZ and SCL removals: however, these results must be considered less significant because not confirmed for all the dyes used as a substrate for enzyme activity determination. The initial hypothesis of the present experimental work considered the possibility to enhance the degradation of the selected OMPs by rising the activity of specific enzymes through the application of specific DO perturbation strategies. The results herewith obtained seem to indicate that the longest and the shortest frequencies tested were capable of enhancing OMPs removal, and this was correlated with the higher Lip activity.

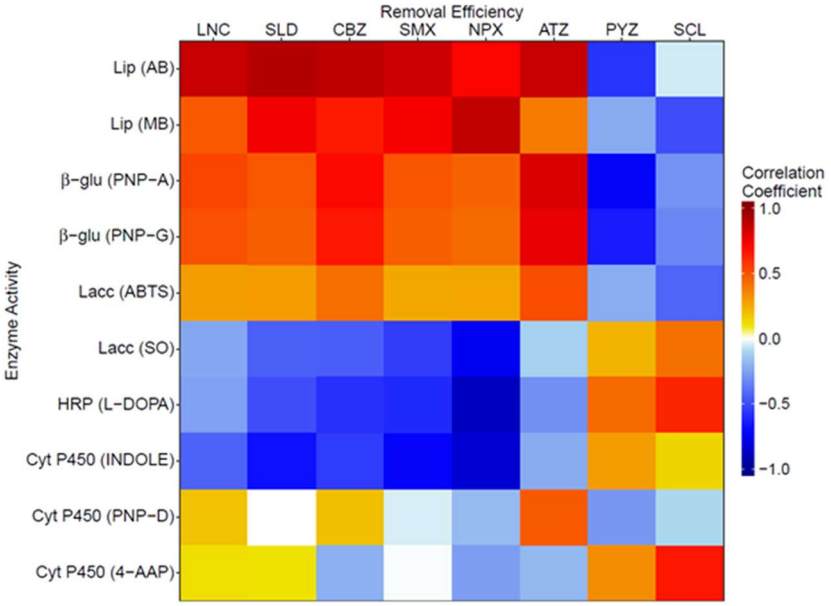

Figure 28 Correlation coefficient matrix between the removal efficiency of each OMP and the activity of the target enzymes measured at t=48 h

1.6.2.3 Microbial speciation

During the same tests, the microbial speciation was also determined, in order to evaluate if it could be modified as a consequence of the DO perturbation strategies. A total of 432 operational taxonomic units (97% OTUs) were identified in biomass samples at the end of each test (t=48 h), of which 425 were represented by bacteria and 7 by archaea. In general, the microbial speciation, as reported in Figure 29, showed the presence of the bacterial families dominant in wastewaters (Xu et al., 2018; Zhang et al., 2018, 2017). Particularly, bacteria families and relative abundance (%) were comparable in C, E1 and E3 tests; the most relevant families were present in the following order:

Rhodocyclaceae>Comamonadaceae>Xanthomonadaceae>Saprospiraceae>Chitinophagaceae>Flavobacteriaceae>Cthophagaceae.

This finding is in agreement with other works reporting that these bacterial families are the main responsible for the efficient degradation of some OMPs (such as ibuprofen and carbamazepine) (Fischer and Majewsky, 2014; Shchegolkova et al., 2016).

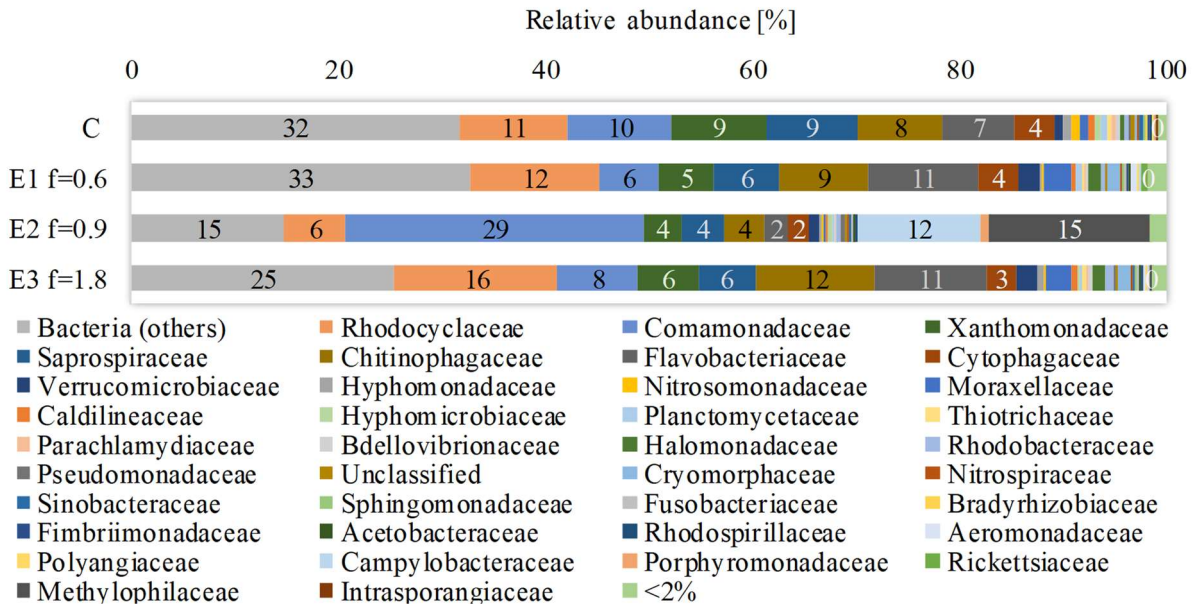

Figure 29 Bacterial communities structure measured at t=48 h for each DO perturbation (averaged values of two replicates)

A slightly different distribution from the other tests was observed in the bacteria families found after the E2 test. Particularly, a relevant increase of *Comamonadaceae* was detected at the expenses of the other families; in addition, *Campylobacteraceae* and *Methylophilaceae* were also identified at 12% and 15%, respectively. Therefore, selection of these species was favoured by the intermediate frequency perturbation. It is worth of note that OMPs removal efficiency measured in the E2 test was the lowest one with respect to the values recorded in the other tests: this suggests that the bacterial families selected under this DO perturbed condition were not relevant to the goal of the OMPs degradation enhancement. It is important to highlight that the group named as Bacteria (others) in Figure 29 includes bacteria which were not classified at the family level, and therefore grouped as "others". This group was found to be the most abundant in the E1 and E3 tests where the removals were higher; therefore, this group should include those species with higher capacity of synthesising oxidoreductases which carries OMPs degradation.

With respect to the study by Bains et al. (2019), the bacteria composition was affected in a different extent. Particularly, the activated sludge from the domestic sewage WWTP used in the present study showed to be less sensitive to DO concentration changes. Indeed, the bacteria composition between the DO perturbed and non-perturbed conditions did not change significantly, and the prevalence of Bacteria (Others) and *Rhodocyclaceae* was observed in both cases. By contrast, *Comamonadaceae* was found to be the most abundant family in the dairy farm sludge used in the study by Bains et al. (2019), in both the control test (constant DO level) and at frequency f=0.5 1/h and f=0.25 1/h.

It is noteworthy that the domestic sludge was collected from the recycle loop of the aerobic oxidation tank. Therefore, the bacteria population was already subjected to aerobic conditions: this might explain the low difference observed between the perturbed and non-perturbed conditions also in term of OMPs removal as compared to the value observed in the previous study.

1.6.2.4 Acetate and nitrogen time-profiles

Figure 30 shows nitrite and nitrate concentrations (expressed in terms of mg/L N) measured during the tests conducted at the different DO perturbations.

Acetate and ammonia concentrations are not here shown since the values were always below the limits of detection of the analytical method (LOD=0.1 mg/L), as also observed in the control test. This indicates that, due to the continuous mode of feeding, rate of ammonium and carbon supply to the reactors likely corresponded to the oxidation rate carried out by the microorganisms.

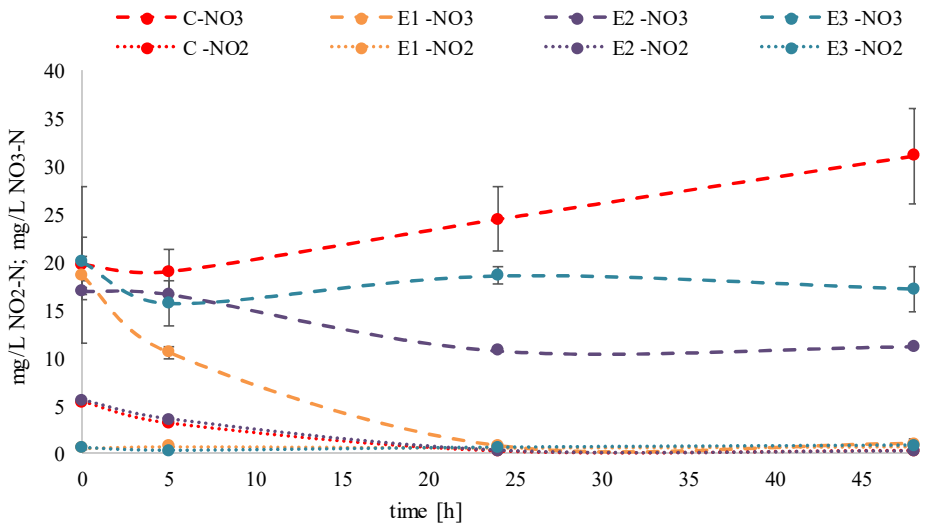

Figure 30 Concentrations of nitrate and nitrite nitrogen for each DO perturbation (error bars indicate the standard deviation of two replicates)

The high concentration of nitrate measured at the beginning of tests was due to the steady state nitrification reached at the end of the acclimatization period which occurred before the start of the experiments. Continuous nitrate production, without an appreciable formation of nitrite, was observed throughout the control test: the nitrogen mass balance confirmed that complete nitrification occurred without any inhibition of the nitrifying bacteria. Therefore, the relatively high load of OMPs did not negatively affect the ammonia oxidation process. Application of the DO perturbations modified the nitrate patterns with respect to that observed in the control tests, with different effects depending on the specific frequency. For instance, in the E3 (f=1.8 1/h) test, nitrate remained almost constant, whereas in the E2 and even more in the E1, nitrate concentrations decreased with time. Comparing these patterns with that measured in the control tests, it can be deemed that by increasing the duration of the OFF phase

(aeration switched off), i.e. from E3 to E1, anoxic conditions were likely to be progressively established within the reactors. These conditions favoured denitrification, with reduction of nitrate into nitrogen gas. Therefore, by reducing the perturbation frequency, simultaneous nitrification-denitrification was achieved within the same reactor.

As a confirmation of the remarks reported above, a specific nitrogen removal rate (SNRR, g N/g MLVSS·d) was calculated, which considered the combined effect of nitrification-denitrification processes under the different conditions. The SNRR was calculated at t=24 h, which was considered the time corresponding to the maximum reaction rate, and at t=48 h to obtain the average value along the test. The results obtained are reported in Table 13.

A decreasing trend of the SNRR values can be observed at increasing frequencies, i.e. the duration of the aeration phase. The lowest value (below zero) of SNRR was calculated in the control test (C), indicating an accumulation of nitrate-nitrogen in the system due to the continuous oxidation of ammonium (provided through the feeding). In the test conducted at the highest frequency (f=1.8 1/h), the SNRR was still very low and remained pretty constant between t=24 h and t= 48 h, showing that the nitrification and denitrification rates were similar.

Table 13 Specific nitrogen removal rate (SNRR) calculated at t=24 h and t=48 h in the experimental tests at the different DO perturbations and in the control test

Test	**SNRR (24 h)**	**SNRR (48 h)**
	[g N/g MLVSS d]	
E1 f=0.6	0.0058	0.0029
E2 f=0.9	0.0038	0.0019
E3 f=1.8	0.0004	0.0004
C	-0.0001	-0.0011

In the other two tests, the SNRR value increased as the frequency decreased, thus validating the hypothesis that optimal conditions for simultaneous nitrification-denitrification were established. Therefore, the DO perturbation strategies did not negatively affect the carbon removal process nor the ammonia nitrogen oxidation; instead it allowed to establish the complete nitrogen removal process within the same biological reactor.

1.7 Removal processes at real scale

1.7.1 Wastewater treatment plants

1.7.1.1 OMPs occurrence

Figure 31 shows the average concentration of target OMPs measured in the influent and effluent of each WWTP over the entire monitoring period. In the plot, each bar represents the cumulated concentration of all the target OMPs in one WWTP. Although total OMPs concentration varied among the plants, a reduction from the influent to the effluent can be observed in most of the plants.

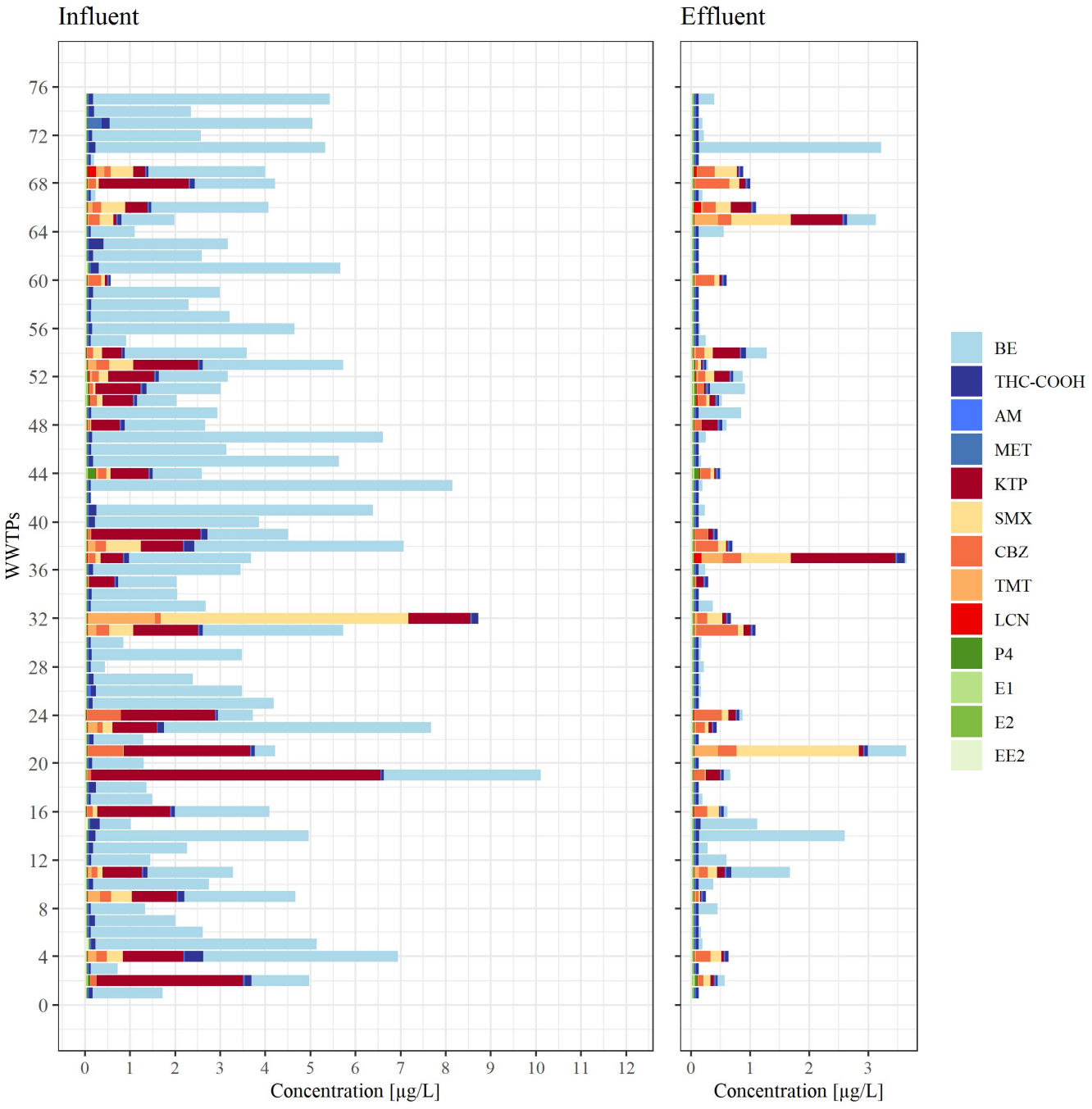

Figure 31 Average concentrations in the influent and effluent of each WWTP measured over the entire monitoring period (each bar represents one WWTP)

BE was the most abundant compound found in the influent, followed by KTP and the other pharmaceuticals. Concentration of steroids and others illicit drugs (AM, MET and THC-COOH) were not relevant in most of the influent and effluent samples. The difference in the concentration profiles has to be ascribed to the different characteristics of the plants such as the uses of the population served by the plant and the treatment lay-outs, as well as to the sampling season during the year and the environmental conditions which can affect stability of the OMPs in the sewage network (Castiglioni et al., 2013; Couto et al., 2019).

Statistical data of the 13 OMPs detected are summarised in Table 14 in terms of minimum, maximum and average concentration in the influent (IN) and effluent (OUT) samples. The minimum value corresponds to the MRL, which represents the minimum concentration that can be reported as a quantitated value for the analysed sample (U.S. Environmental protection Agency, EPA, 2009). The same table also lists the frequency of detection, F_D, which indicates the percentage of measurements that provided a value above the Minimum Reporting Level (MRL).

Table 14 Minimum, maximum and average concentrations in the influent (IN) and effluent (OUT) of the 76 WWTPs monitored. FD=frequency of detection

Compound	Minimum		Maximum		Average		F_D	
	IN [µg/L]	OUT [µg/L]	IN [µg/L]	OUT [µg/L]	IN [µg/L]	OUT [µg/L]	IN [%]	OUT [%]
BE	0.01	0.01	8.02	3.08	2.36	0.17	96	56
THC-COOH	0.03	0.03	0.41	0.28	0.08	0.03	58	6
AM	0.02	0.02	0.11	0.02	0.02	0.02	1	0
MET	0.01	0.01	0.30	0.01	0.02	0.01	16	0
KTP	0.05	0.05	6.41	1.77	1.19	0.18	88	48
SMX	0.01	0.01	5.49	2.07	0.30	0.19	64	69
CBZ	0.01	0.01	0.78	0.89	0.17	0.20	95	95
TMT	0.01	0.01	1.49	0.40	0.10	0.05	38	40
LCN	0.01	0.01	0.19	0.13	0.02	0.02	19	17
P4	0.01	0.01	1.15	0.39	0.02	0.01	15	1
E1	0.01	0.01	0.05	0.01	0.01	0.01	11	0
E2	0.01	0.01	0.01	0.01	0.01	0.01	0	0
EE2	0.02	0.02	0.08	0.02	0.02	0.02	4	0

The contaminants found with the highest frequency of detection in the influent were: BE (96%), CBZ (95%), KTP (88%) and SMX (64%). The same compounds were also found most frequently in the effluent samples: BE (56%), CBZ (95%), KTP (48%) and SMX (69%).

Similar frequencies of detection were reported by Loos et al. (2013) for CBZ and KTP in the effluents of 90 WWTPs in Europe. Bijlsma et al. (2012) found for BE, F_D values equal to 100% and 75% in the

influent and effluent of Dutch WWTPs, respectively. On the other hand, the contaminants found with the lowest F_D were steroids, AM and MET.

It is noteworthy that regarding the class of steroids, the limits of detection assumed in the present study to be equal to the corresponding MLR, were above the values suggested by the 2015/495/UE decision as the maximum acceptable detection limits of the analytical methods used for their monitoring (which were 0.035 ng/L for EE2 and 0.4 ng/L for E1 and E2) (Barbosa et al., 2016; European Commission, 2015). In order to be able to lower the MLR, samples complex pre-treatment would be necessary. However, since the aim of the present investigation was to conduct a monitoring campaign with a routine-based approach, a higher number of samples was preferred to the more expensive pre-treatment to provide reliable data. As a consequence, the low frequency of detection highlighted for the class of steroids in the present study might result higher by adopting a different analytical method.

Figure 32 depicts the same data shown in Figure 31 and Table 14, expressed in terms of influent and effluent concentrations measured in the 76 WWTPs monitored in the study.

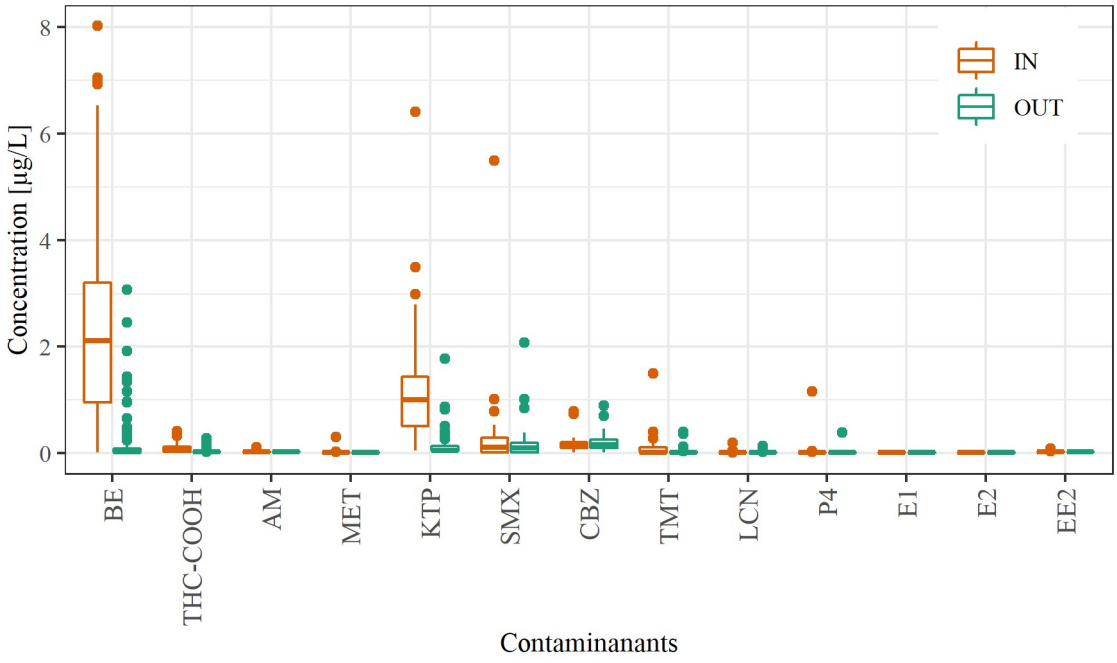

Figure 32 Influent (IN) and effluent (OUT) concentrations measured in the 76 WWTPs monitored

As shown by Figure 32, the highest influent concentration was 8.02 µg/L of BE, which is the major metabolite of cocaine; this contaminant was also that one showing the widest variability among the WWTPs. The two second highest influent concentrations were 6.41 µg/L of KTP and 5.49 µg/L of SMX, both belonging to the class of pharmaceuticals. Particularly, KTP is a nonsteroidal anti-inflammatory drug with analgesic and antipyretic effects, whereas SMX is a sulphonamide bacteriostatic antibiotic that is most commonly used in the Bactrim drug. Among the investigated compounds, E1, E2, EE2 and

AM were found at the lowest concentrations (similar to the MRL). In general, illicit drugs and pharmaceuticals showed higher concentrations than steroids.

As seen in Figure 32, similarly to the findings from the influent, the highest OMP concentrations in the effluent samples were of BE, KTP and SMX, with 3.08 µg/L, 1.77 µg/L and 2.07 µg/L concentrations, respectively. It is noteworthy that SMX, CBZ, TMT and LCN showed very similar influent and effluent F_D values: for instance, SMX with 64% influent and 69% effluent.

Table 2 (see page 25) provides an overview of the main data reported by the specialized literature regarding the influent and effluent concentrations of the target OMPs measured in WWTPs.

In general, the values found in the present study for influent and effluent concentrations fall within the ranges reported by the specialized literature; however, it is worth noting that these ranges are quite broad because of the differences among the investigated plants. Some specific comment can be made about the different OMPs. Particularly, with respect to the specialized literature data, the present study measured higher inlet concentrations for BE: for instance, the maximum influent concentration was 8.02 µg/L while Table 2 lists a value of 4.75 µg/L as the top of the range. About the BE in effluent, the concentrations measured in the present study fall within the range reported by the literature. Influent concentrations of THC-COOH fall within the reported range, although the highest value was higher than the top level of the range. Similar observations can be done for the effluent values.

Differently, the highest values of the illicit drugs AM and MET were below the top limits of the reported range; however, the concentrations measured in the WWTPs of the present study still fall within the literature range. Similar findings were obtained the for the effluent. About KTP, the upper value of the influent range was significantly higher than that of this study, i.e. 11.24 µg/L compared to 6.41 µg/L. Conversely, the highest effluent concentration was lower than the maximum value found in the present study.

For SMX concentrations, the influent concentrations were similar, whereas the effluent values exceeded the highest level of the reported range. TMT showed higher values than those listed in Table 2. Both influent and effluent concentrations of LCN and CBZ measured in the present study were far below the upper level of the ranges indicated by others scientific studies. Ranges of all steroid concentrations found in the existing literature are of similar low magnitude as the those measured in the present study.

1.7.1.2 Seasonal variations of concentration profiles

It is likely that warmer seasons favour more social human activities played outside, while lower temperatures may cause more illness and restrict the time used for socialising. Since illicit drugs and pharmaceuticals concentrations in the sewage networks are linked to human consumption and behaviour and to environmental conditions, there might be a correlation between seasonal changes and the discharged contaminant loads (Couto et al., 2019). Table 15 shows the average influent concentrations for each OMP measured over the two years-period of monitoring, and the percentage difference with the average season concentration.

Each season was considered three months-long and defined as: Winter (December, January and February), Spring (March, April and May), Summer (June, July and August) and Autumn (September, October and November). The grey coloured cells indicate the highest percentage difference per OMP. The star highlights the cases when the average concentration was equal to the MRL: in such a case, the seasonal variation was considered not relevant.

Table 15 Seasonal variations of the influent concentration of the investigated OMPs

		MET	TMT	SMX	THC-COOH	P4	BE	LCN	CBZ	KTP	AM	EE2	E2	E1
Average	[µg/L]	0.02	0.10	0.31	0.08	0.02	2.38	0.02	0.17	1.21	0.02*	0.01*	0.01*	0.02*
Winter	[%]	57	-90	-76	12	-10	-11	-16	-27	18	-4	38	0	3
Spring	[%]	-34	100	88	16	-59	15	12	15	-3	-4	-30	0	-6
Summer	[%]	-16	-18	-24	9	412	42	23	-23	-68	-4	-30	0	-6
Autumn	[%]	-31	-90	-97	-58	-59	-31	-44	326	72	4	-30	0	-6

The highest percentage increase with season change was found for P4 (412%) in summer. However, such a relevant increase cannot be considered significant since the extremely low value of the average influent concentration (measured over the entire monitoring period) leads to obtain higher percentage increase. Therefore, looking at the OMPs found at the highest average concentrations, i.e. BE and KTP, their variations accounted for 42% and 72%, in summer (average temperature 25°C) and autumn (average temperature 20°C), respectively. KTP is an anti-inflammatory drug used for its analgesic and antipyretic effects. It is likely that autumnal conditions favour illness, giving rise to higher drug consumption. CBZ, SMX and TMT also showed differences due to season changes. Generally, spring (average temperature 14°C) and summer were the seasons more affecting the contaminant presence in the influent, by increasing the concentrations with respect to the averages. The observed changes might be also due to the effects of the environmental temperatures on the chemical stability of the contaminants in water. Furthermore, reactions of OMP with other substances or their molecule breakdown might be affected by the local temperature (Castiglioni et al., 2013).

1.7.1.3 Removal efficiencies

Figure 33 illustrates the removal efficiencies (R) calculated using Eq. 41, for each contaminant and for each class of WWTP as listed in Table 3. The legend of the plot shows the classes of WWTPs and in brackets the number of plants belonging to each class. On the right side of the plot are reported the number of measurements used to build each box and in brackets the total number of measurements. The orange boxes were built considering all the WWTPs monitored (All WWTPs).

As mentioned above, when the influent and effluent concentrations were both equal to the MRL, the removal was not calculated. This occurred for E1 and E2 in all the 110 and 123 analysed samples, respectively. The removal percentages were only calculated for P4 and EE2 within the steroid family, because their influent concentrations were above the MRL. P4 and EE2 removal percentages ranged between 50% and 75% (see Figure 33).

As illustrated by Figure 33, TMT, LCN, CBZ and SMX exhibited removal efficiency below 50%; both CBZ and SMX provided significant F_D values, thus giving to these data a statistical relevancy. Furthermore, these removals are also confirmed by other studies, as outlined in Table 2.

For all other OMPs' the values were found equal or greater than 50%. Particularly, the best removals were observed for BE (R > 95%) and KTP (R > 75%), with a homogeneous distribution of the data as highlighted by the dimensions of the boxes in Figure 3 (a "small" box indicates the values of removal are similar). THC-COOH was also similarly removed by all classes of WWTPs, with an average removal efficiency of 60%. TMT was removed between 35% and 90% for the majority of samples. The removal of MET was higher than 50% in all the WWTPs, whereas AM was most detected under MRL (the removal was calculated in one sample one, resulting to be 82%).

Aside from the low removal of LCN, CBZ and SMX, the other OMPS were removed for more than 50%; given the small concentrations, these values can be considered representative of good removals.

Looking at the data reported in Figure 33 with respect to the different type of treatment, it is difficult to find a clear correlation with the removal efficiency. In most of the cases, the different classes of WWTPs are responsible of similar performance. Furthermore, most of the contaminants showed a difference between the treatments which can be considered comparable to the variability of the data, which in turn depends on the specific conditions and characteristics of the plants.

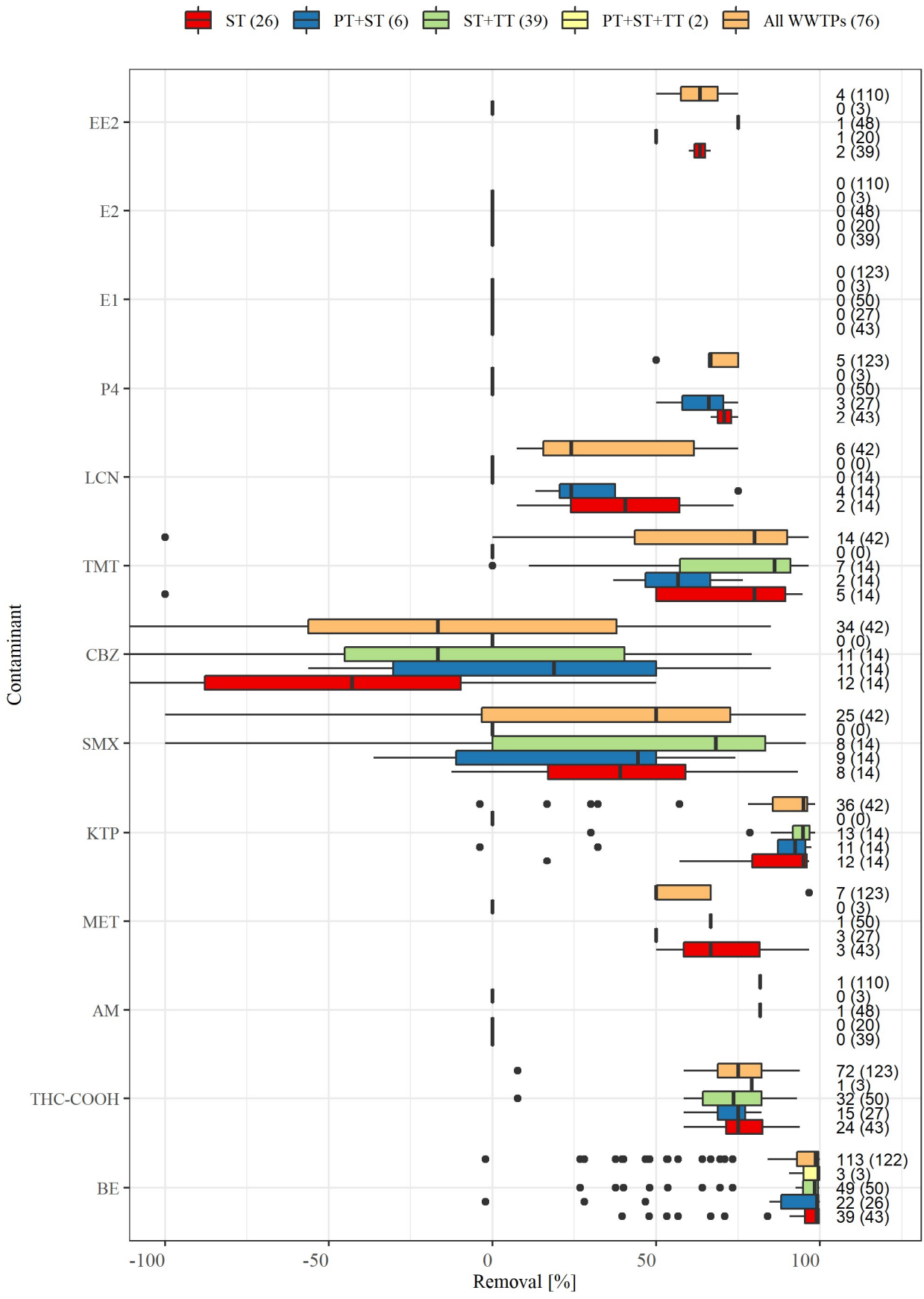

Figure 33 Removal efficiency of each OMP for the different classes of WWTPs

1.7.1.4 Standardised removal efficiencies

For a better evaluation of the influence of the different classes of treatment plants on removal efficiencies, the Standardized Removal Efficiency (SRE) was calculated for each contaminant by following Eq. 42. The SRE weighs the removal efficiencies per treatment class taking into account the overall average and the standard deviation of R per OMP and the number of measurements available per treatment class. Figure 34 shows the SRE distribution for all the OMPs by class of wastewater treatment. On the right side of the plot are reported the number of measurements used to build each box and in brackets the total number of measurements available. In the plot, the red circles indicate the average values of SREs. The position of this symbol compared to the 0 value of SRE indicates the overall removal achieved by a class of WWTPs with respect to the average removal of the entire dataset: the right side of the graph indicates a better removal, while the left side lower removal.

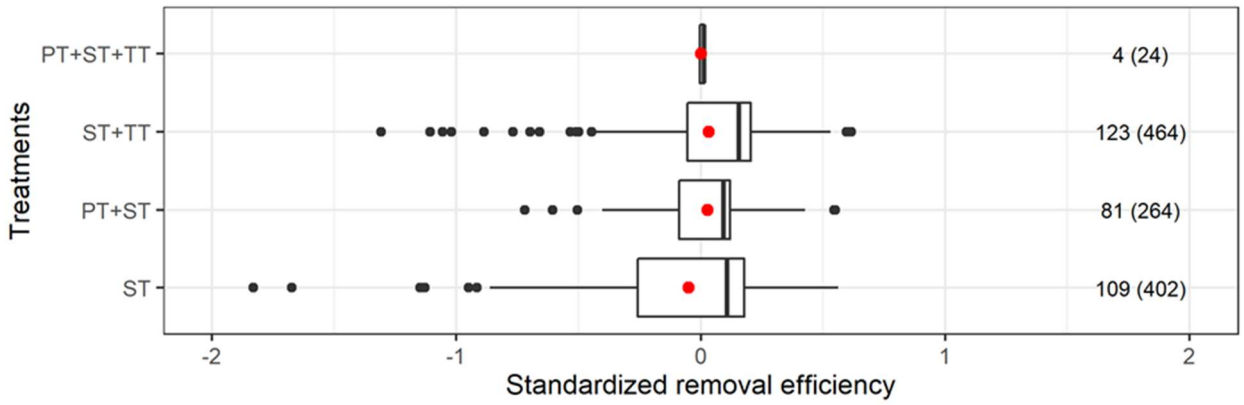

Figure 34 Standardized removal efficiency of the different classes of WWTPs, related to all the contaminants together

Looking at the average values of SRE, it can be assessed that there were not significant differences between the first three classes of treatments, i.e. (PT+ST+TT), (ST+TT) and (PT+ST). The plants with the sole secondary treatments showed the lowest removal and more widely dispersed results.

Based on the most probable SRE values (which are those one falling within 25^{th}-75^{th} percentile and graphically represented by the box) and the median value (50^{th} percentile), the (ST+TT) showed to be capable of the best removal. The (PT+ST+TT) class also provided good results: however, the available data were too low (4) to consider them representative since the removal were weighted also by the number of measurement available for the considered condition (as described in Eq. 42). Indeed, this treatment lay-out was the less commonly found among the investigated WWTPs.

Based on these results, it seems that the tertiary treatment which is included in the (ST+TT) lay-out, has a good impact on the overall removal of the investigated OMPs and this is in accordance with several scientific studies (Morlay et al., 2018; Rizzo et al., 2019; Yadav et al., 2019).

1.7.2 Drinking water treatment plant

1.7.2.1 Workflow

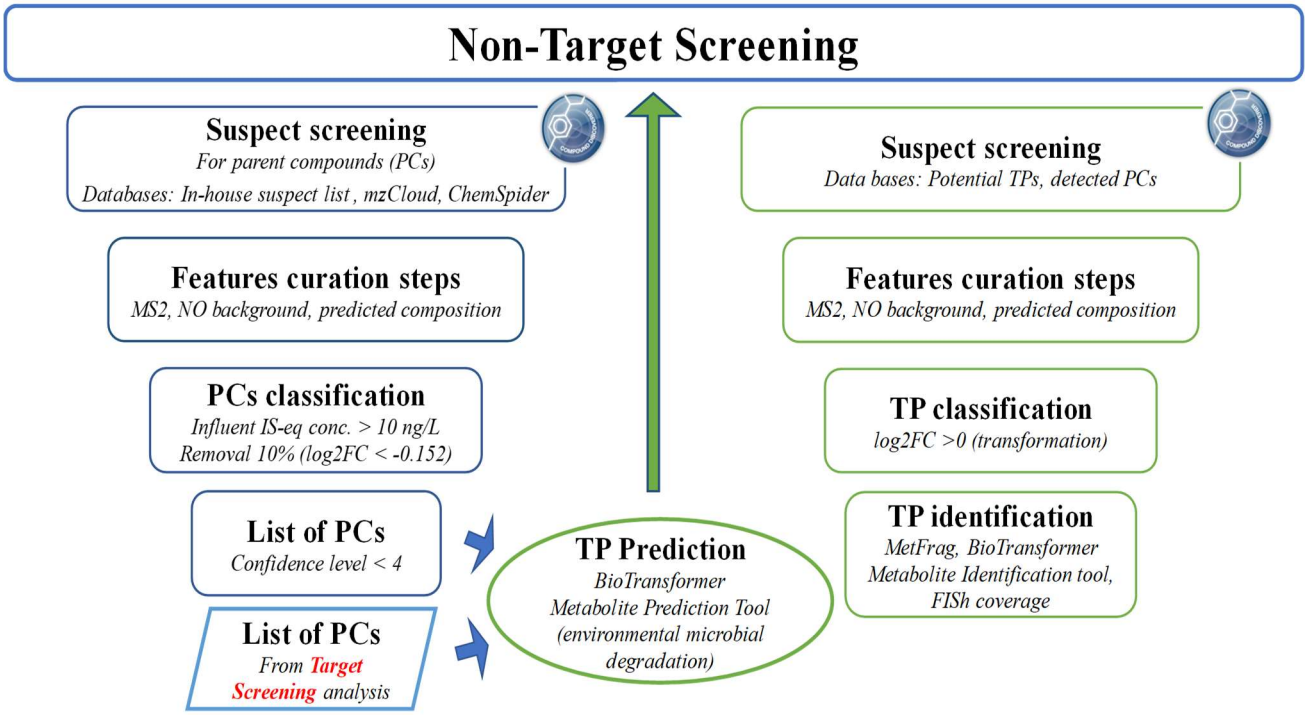

Figure 35 Workflow for TP identification from NTS data

A data-driven workflow was developed for the identification of TPs based on feature treatment profiles and TP prediction followed by suspect screening. Features were classified as PC or TP based on the trend of the feature intensity between influent and effluent samples (treatment profile). TP prediction was performed for a list of detected OMPs, referred to as PCs, using the prediction software BioTransformer (http://biotransformer.ca/).

The workflow consisted of three main phases: 1) Parents compound identification, 2) TP prediction, 3) TP identification. More details are reported below, and a schematic description of the workflow is shown in Figure 35. To evaluate the advantage in using NTS instead of target screening data for the selection of PCs, lists of PCs detected with the respective screening were both used to predict TPs (as highlighted in Figure 2 by the light blue box).

Parents compound identification

Classification of features into PCs was performed based on the Internal Standard equivalent concentration (IS-eq Conc.) and the reduction (removal) of the intensity of the between influent and effluent samples. This reduction can also be expressed as fold change (log2FC). Since Compound

Discoverer provides the values log2FC for pairs of samples, it was chosen as parameter for the PC classification.

Features were classified as PCs if they met the following criteria:

a) Influent IS eq conc. > 10 ng/L in at least one location;

b) minimum removal of 10% which corresponds to a log2FC < -0.152, at least in one location.

We chose this strategy to account for the complexity and low OMP concentrations of the real scale samples. As RSF are not the first treatment step of a drinking water treatment plant, the concentration of OMPs detected in the samples were already low in the influent samples. Moreover, there is not necessarily a one-to-one relationship between parent compound decrease and TP formation, but one PC can form multiple TPs and also the same TP can be formed from multiple PCs. Additionally, also partial PC removal can cause an increase of TP to a low, but toxicologically relevant concentration.

For all features classified as PCs, feature identification based on MS1 and MS2 information was attempted and the resulting confidence level of identification determined according to Schymanski et al. (2014). The confidence level was assigned through visual inspection of fragmentation spectra of the candidates and FISh coverage calculation in Compound Discoverer.

If the highest level of confidence was reached by more than one suspect candidate, all candidates were used in the TP prediction step. For PC features for which a corresponding TP was detected, further steps to confirm the identification were performed, following the same procedure described in section *Transformation product identification*.

Transformation product prediction

The OMPs defined as PCs were used to predict their possible environmental microbial degradation TPs, as described in section *Transformation product prediction*, using the metabolite prediction module of BioTransformer (BMPT). The resulting suspect list of predicted TPs consisted of an elemental formula, monoisotopic mass and InChI as structural identifier. The name used to identify the molecules was defined merging the CAS of the PC and the metabolite ID proposed by BioTransformer (e.g. 116459-29-1-BTM00004). This list was used for a second suspect screening of the NTS data in addition to the lists of detected PCs.

Subsequently, the features that matched a suspect were filtered for positive log2FC (increasing intensity from influent to effluent) indicating that they were being formed, in at least one location, and structurally elucidated. Furthermore, the BioTransformer module BMIT was also used to confirm tentative identifications (as described in section *Spectral similarity*).

Transformation product identification

To confirm the tentatively identified TPs, and to assign a confidence level to the assignment the tentative candidates were matched against an in-house suspect list based on mass and retention time (RT); if both

criteria matched, a confidence level of 1 was assigned. For all other tentatively identified TPs as well as their respective PC features, the experimental MS2 spectra were compared with the *in silico* predicted spectra of the possible candidates using MetFrag and FISh in Compound Discoverer.

1.7.2.2 Application to real scale drinking water treatment plants

The developed workflow was applied to NTS data from influent and effluent samples collected in spring 2018 from 7 RSF in the Netherlands (1., 6., 4., 3., 5., 7. and WPC 2.). The RSF were from different drinking water treatment plants, with varied treatment configurations and water sources. As a consequence, the initial OMP levels, the bacterial communities present in the filters, and the resulting OMP removal rates as did vary significantly.

NTS data and principal component analysis

The total number of NTS features detected across all samples was 534. The feature identifier (feature ID) was defined by molecular weight (M.W.) and RT, i.e. M.W. / RT.

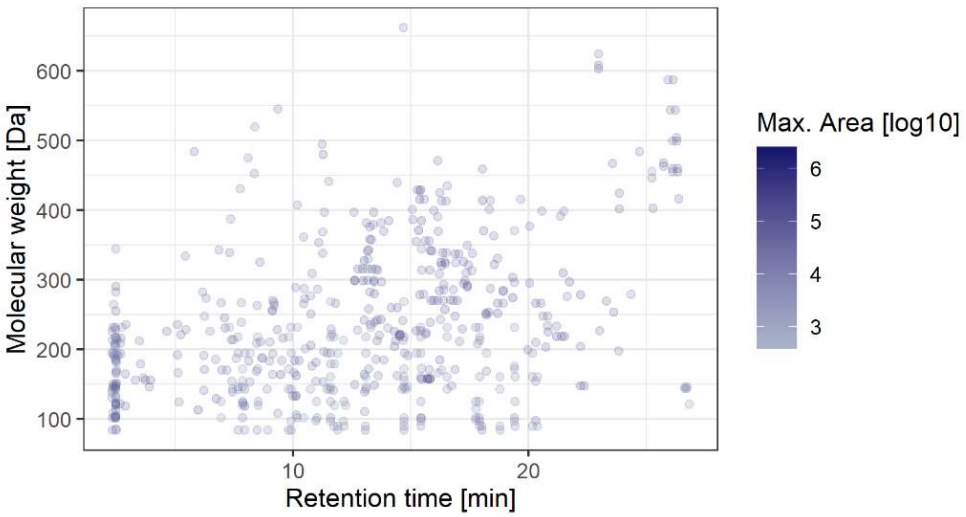

Figure 36 Molecular weight and intensity distribution of features in relation to retention time

Overall, features were characterized by low signal intensities, highlighting the low contamination level of the samples as referred to as IS-eq conc. (see Figure 36).

To explore relationship between water sources, RSF and/or treatment steps, principal component analysis (PCA) was performed. Figure 37 shows the PCA results. The samples were coloured according to their location and shaped according to the sample type.

The first two of the principal components (Dim1 and Dim2) explained approximately 21% and 11% of the variance in the data set, respectively. Influent and effluent samples from the same location roughly clustered in the same area of the plot, indicating that water quality is the more relevant difference between samples than the effect of treatment.

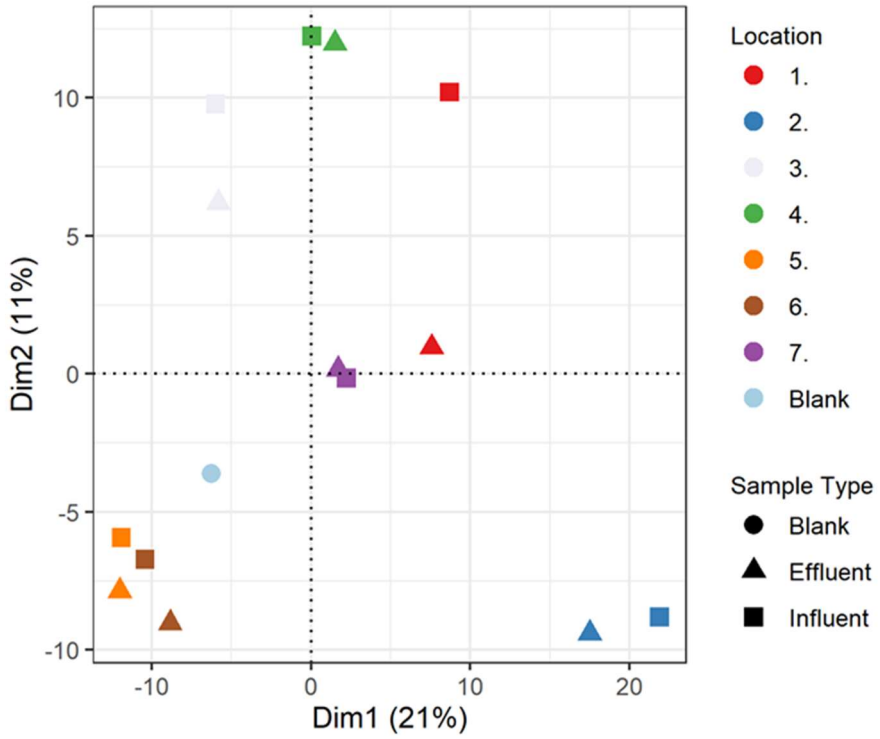

Figure 37 Score plot of the two main PCA dimensions. Samples are coloured according to their location and shaped according to the sample type

Figure 38 shows a qualitative description of the dataset, as intensity of features detected per location in the influent and effluent samples. The shape of the violins indicates the distribution of the features by intensity. The width of the violin is proportional to the number of features with a given intensity.
In the locations 1. and 6. the highest feature intensities (around 10^5) were detected, but also the overall lowest intensities with most of the values below 100. In contrast, the locations 4. and 5. showed many features in the upper part of the distribution. In most of the locations the distribution of the feature intensity between influent and effluent remain roughly the same. However, there is an increase of the number of features at low intensity in the effluent, graphically represented by a downward shift of the effluent distribution. This behaviour is more evident in 1. and 6., where there is an increase in the number of features at low intensity in the effluent at the expense of the features with highest intensity in the influent. 3. and WPC 2., on the other hand, displayed similar distribution of the intensities before and after the treatments, suggesting a weak effect of RSF treatment.

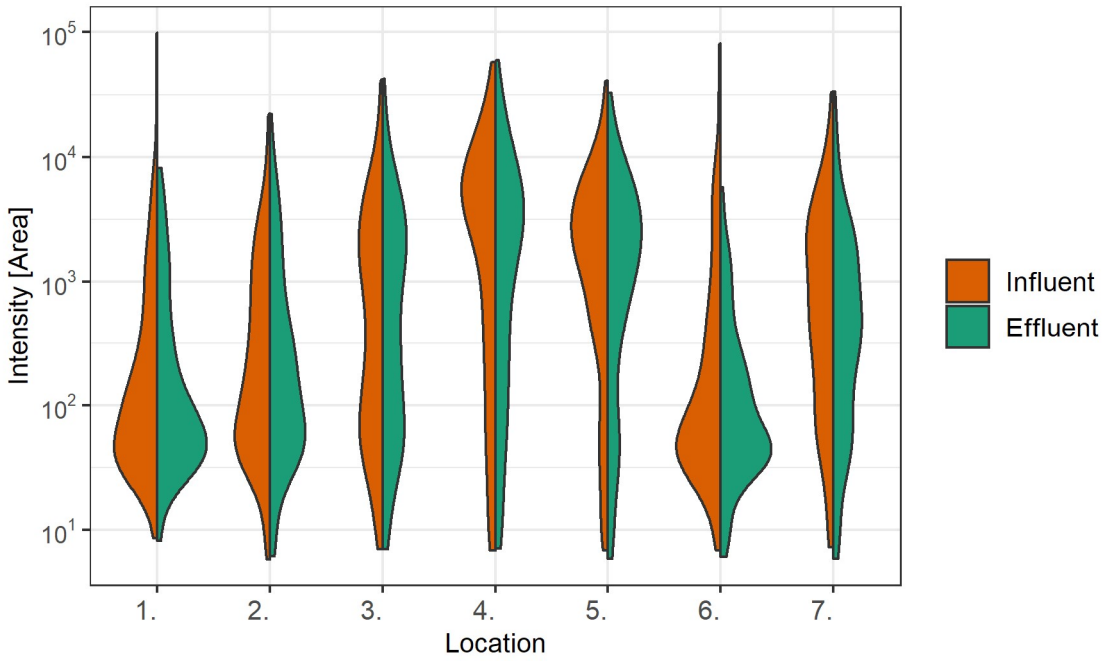

Figure 38 Distribution of feature intensities detected in influent and effluent samples per location (RSF)

Detection of parent compounds and transformation products

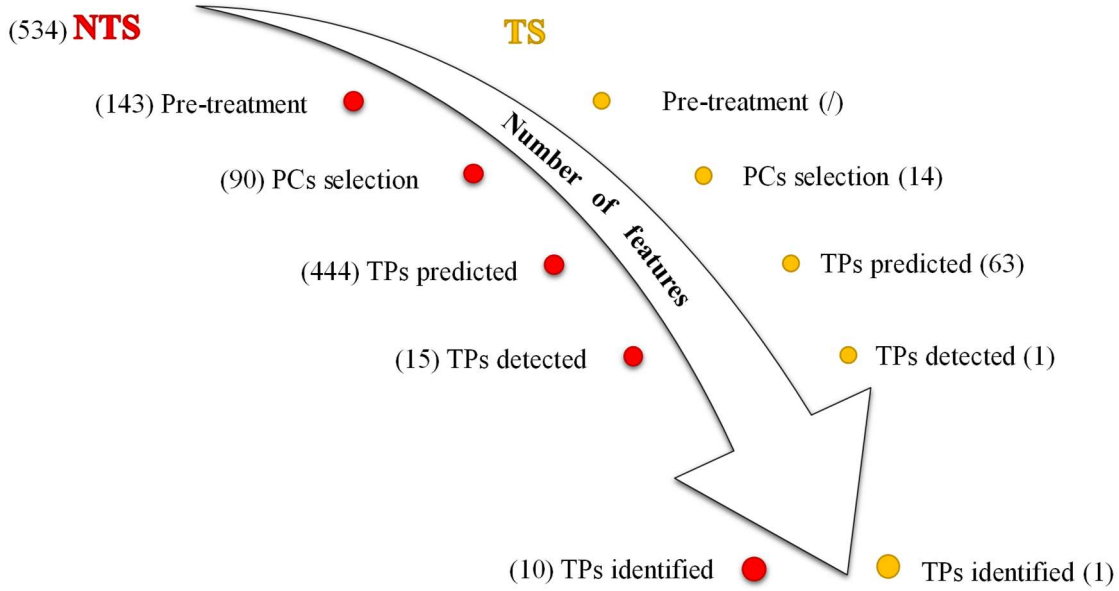

Figure 39 Application of the proposed workflow to the experimental dataset obtained in NTS and TS, reported in the left and right side of the figure respectively. The number of features obtained from each step are reported in brackets

From the total features detected in NTS (534), 90 exceeded an IS-eq conc. of 10 ng/L in the influent and 10% removal (log2FC < -0.152) and were thus classified as PC (as showed in Figure 39). 444 potential TPs were predicted for these PC using BMPT. Among the 534 total features, 140 showed an increasing intensity from influent to effluent at least in one location 15 of these matched the TP suspect list based

on accurate mass and formula. For the identified TPs, retrieval of the respective parent compounds was attempted.

The same criteria for the selection of PCs, applied to NTS data, were also applied to TS data: within the 127 target compounds 14 were classified as PC because their influent concentration was above 10 ng/L and the removal was higher than 10% at least in one location. For this list of PCs 63 tentative TPs were predicted by BMPT. Subsequently only one of the NTS features matched this TP suspect list, emphasizing the importance of NTS to monitor TPs.

Figure 39 shows the main steps of the applied workflow and the number of features obtained in each step. Furthermore, it compares the number of compounds detected by NTS and target screening.

The list of detected TP features is reported in Table 16. The first row of the table contains the feature which matched TP suspect lists from both target and non-target screening (feature ID: 267.18335 / 9.2). Where available, PC information is also included.

Structural identification of transformation products and their parent compounds

Through the identification step of the developed workflow, a confidence level (CL), a structure and a name were assigned to both TPs and PCs. As highlighted in Table 16, 10 features were identified with a confidence level range from 1 to 3, and then considered successfully identified: 2 features were identified with CL equal to 1, 5 with CL 2 and 3 with CL 3.

8 of these features were known compounds; their structures were listed in one of the used databases, i.e. mzCloud, EAWAG Biocatalysis/Biodegradation Database, EPA DSSTox, EPA Toxcast and/or PubChem). For the remaining two features, named 2372-82-9-BTM00001 and 120013-45-8-BTM00001, the experimental spectra matched the *in silico* predicted structures proposed by BMPT (CL=2). However, they were missing from all databases and no information on these compounds could be found in the literature.

Details on the identification parameters for confidence level determination for TPs and PCs are provided in Table 17 and Table 18, respectively. In the two tables, spectral similarity parameters are reported: FISh coverage (the values can range from 0 to 100), spectral similarity score calculated through MetFrag, number of fragment/ions matched between the experimental spectrum and the *in silico* fragmented spectrum of the candidate's structure carried out through MetFrag. In addition, chemicals identifiers are listed, i.e. SMILE, InChI and CAS.

5 out of the 10 identified TPs could be linked to their PCs. Moreover, most of the TPs were also selected as PCs. While this may seem like a paradox, it could be due to the varied water sources and water pre-treatments applied.

Therefore, there is a change in term of behaviour of the same substance between the studied RSF. It can be related to the interactions with different mix of contaminant and bacteria community as well.

Lastly as further elucidation, the spectral similarity between supposed PCs and respective TPs was assessed for the 5 features where a link was found. The results can be found in the Figure S.M. 7) as

similarity score and the Head-to-tail plot. The best similarities between the spectra were obtained for the pair Dehydrodeoxy donepezil - 120013-45-8-BTM00001 (reported in Figure 40), Phe-Ala – (S)-2-amino-N-ethyl-3-phenylpropionamide, Laurylamine dipropylenediamine - 2372-82-9-BTM00001 corresponding to a similarity score equal to 0.89, 0.48, 0.26, respectively.

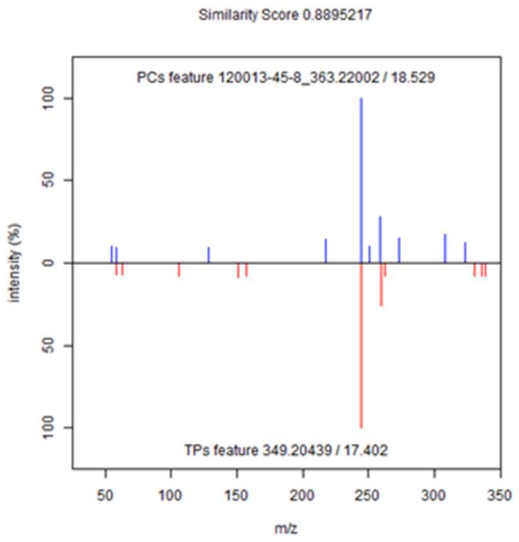

Figure 40 Spectra similarity plots of Dehydrodeoxy donepezil (PC, upper spectrum) and 120013-45-8-BTM00001 (TP, lower spectrum)

1.7.2.3 Evaluation of the proposed workflow

The feature intensity profiles between influent and effluent samples from real scale RSFs show that for some features, the intensity decreases and increases depending on the location, which causes an overlap between the PC and TP sets (Figure 41). The same compound can thus behave in opposite ways in different RSFs. PCs are expected to be removed and in their place TPs should form through a specific process, nevertheless this study showed that the same compound can behave as PC (decreasing intensity during the treatment) or TP (increasing intensity) depending on the location.

It is essential to notice that the intensities of the features were overall very low as well as the difference between influent and effluent (log2FC), as showed in Supplementary materials (Figure S.M. 8).

This complicated the identification and the interpretation of the reactions involved in the transformation process. A toxicological risk assessment of the identified TPs is needed to evaluate whether the low concentration levels could potentially pose a risk to human or environmental health.

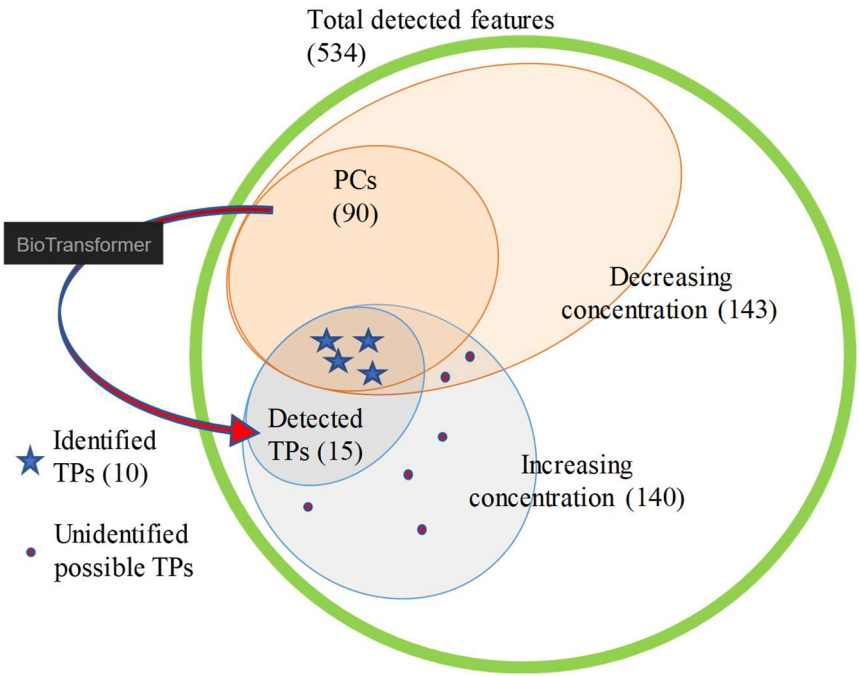

Figure 41 Venn diagram: logical relations between the steps of the proposed workflow. The number of features or compounds selected in each step are given in brackets

In order to validate the proposed workflow, we applied it to the well-studied biotic TP Gabapentin-lactam (Henning et al. (2018)). Gapapentin-lactam is a derivative of the anti-convulsant agent Gabapentin which was also present in the PC list. In the NTS data, Gabapentin-Lactam was classified as PC because it was detected in 4. influent sample and removed around 46% in the same location. In contrast, in the locations 3. and WPC 2., the intensity of Gabapentin-lactam increased in the effluent samples (as showed in Supplementary materials, Figure S.M. 9). However, the compound was not identified as a TP with the developed workflow as it was not predicted by BMPT as a TP of Gabapentin. This example proves that while BioTransformer is a useful tool, as 10 of the TPs it predicted could be identified in the RSF samples, it cannot be considered comprehensive. In Figure 41 possible unidentified TPs are represented by red dots.

Table 16 Detected TPs proposed structures. The asterisk indicates the feature belonged to TPs suspect list from both TS and NTS. When it was possible the PC was also reported

FeatureID	Transformation Products				FeatureID	Parent Compounds			
M.W / RT	Formula	CL	Structure	Proposed name	M.W / RT	Formula	CL	Structure	Proposed Name
267.18335 / 9.2*	$C_{15}H_{25}NO_3$	1	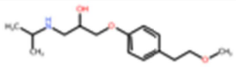	Metoprolol	/	/	/	/	/
245.11631 / 7.09	$C_{13}H_{15}N_3O_2$	1	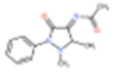	N-Acetylaminoantipyrine	/	/	/	/	/
298.29815 / 12.61	$C_{18}H_{38}N_2O$	2	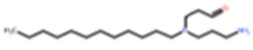	2372-82-9-BTM00001	299.33003 / 12.619	$C_{18}H_{41}N_3$	2		Laurylamine dipropylenediamine
139.09953 / 13.041	$C_8H_{13}NO$	2	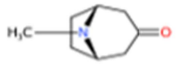	Tropinone	141.11517 / 11.724	$C_8H_{15}NO$	2	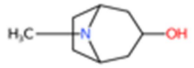	Tropine
236.116 / 5.091	$C_{12}H_{16}N_2O_3$	2	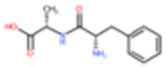	Phe-Ala	/	/	/	/	/
349.20439 / 17.402	$C_{23}H_{27}NO_2$	2	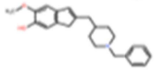	120013-45-8-BTM00001	363.22002 / 18.529	$C_{24}H_{29}NO_2$	2	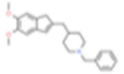	Dehydrodeoxy donepezil
169.11015 / 8.457	$C_9H_{15}NO_2$	2	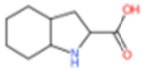	(2S,3aR,7aS)-Octahydro-1H-indole-2-carboxylic acid|3	/	/	/	/	/
267.147 / 6.96	$C_{14}H_{21}NO_4$	3	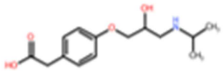	Atenolol acid or Metoprolol acid	/	/	/	/	/
192.12621 / 5.094	$C_{11}H_{16}N_2O$	3	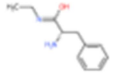	(S)-2-amino-N-ethyl-3-phenylpropionamide	236.116 / 5.091	$C_{12}H_{16}N_2O_3$	2	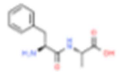	Phe-Ala
141.11517 / 11.724	$C_8H_{15}NO$	3	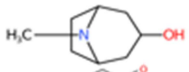	Tropine	289.16775 / 10.108	$C_{17}H_{23}NO_3$	2	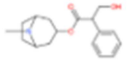	Atropine
139.09953 / 7.441	$C_8H_{13}NO$	4	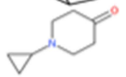	1-cyclopropyl-4-piperidone	/	/	/		/
662.19414 / 14.693	$C_{34}H_{34}N_2O_{10}S$	4	/	/	/	/	/	/	/
201.1729 / 10.52	$C_{11}H_{23}NO_2$	4	/	/	/	/	/	/	/
187.15703 / 7.586	$C_{10}H_{21}NO_2$	4	/	/	/	/	/	/	/
265.18892 / 10.44	$C_{14}H_{21}NO_4$	4	/	/	/	/	/	/	/

Table 17 Identification parameters of the Transformation products with confidence level (CL) < 4

FeatureID M.W / RT	FISh coverage	MetFrag Spectral similarity Score	n. Ions matched	SMILE	InChI	Proposed CAS
267.18335 / 9.2*	100	3.24	6	COCCc1ccc(OCC(O)CNC(C)C)cc1	InChI=1S/C15H25NO3/c1-12(2)16-10-14(17)11-19-15-6-4-13(5-7-15)8-9-18-3/h4-7,12,14,16-17H,8-11H2,1-3H3	37350-58-6
245.11631 / 7.09	71.43	3.93	6	CC1N(C)N(C(=O)C1=NC(C)=O)C1=CC=CC=C1	InChI=1S/C13H15N3O2/c1-9-12(14-10(2)17)13(18)16(15(9)3)11-7-5-4-6-8-11/h4-8H,1-3H3,(H,14,17)	83-15-8
298.29815 / 12.61	60	0.89	3	CCCCCCCCCCCCCN(CCCN)CCC=O	InChI=1S/C18H38N2O/c1-2-3-4-5-6-7-8-9-10-11-15-20(16-12-14-19)17-13-18-21/h18H,2-17,19H2,1H3	/
139.09953 / 13.041	75.86	3.11	10	CN1C2CCC1CC(=O)C2	InChI=1S/C8H13NO/c1-9-6-2-3-7(9)5-8(10)4-6/h6-7H,2-5H2,1H3	532-24-1
236.116 / 5.091	100	1.82	1	C[C@@H](C(=O)O)NC(=O)[C@H](CC1=CC=CC=C1)N	InChI=1S/C12H16N2O3/c1-8(12(16)17)14-11(15)10(13)7-9-5-3-2-4-6-9/h2-6,8,10H,7,13H2,1H3,(H,14,15)(H,16,17)/t8-,10-/m0/s1	3918-87-4
349.20439 / 17.402	66.67	0.07	2	COc1cc2C=C(CC3CCN(CC3)Cc4ccccc4)Cc2cc1O	InChI=1S/C23H27NO2/c1-26-23-15-21-13-19(12-20(21)14-22(23)25)11-17-7-9-24(10-8-17)16-18-5-3-2-4-6-18/h2-6,13-15,17,25H,7-12,16H2,1H3	/
169.11015 / 8.457	42.86	3.92	4	C1CCC2C(C1)CC(N2)C(=O)O	InChI=1S/C9H15NO2/c11-9(12)8-5-6-3-1-2-4-7(6)10-8/h6-8,10H,1-5H2,(H,11,12)/t6-,7+,8+/m1/s1	145438-94-4
267.147 / 6.96	60	2.96	3	CC(C)NCC(COC1=CC=C(C=C1)CC(=O)O)O	InChI=1S/C14H21NO4/c1-10(2)15-8-12(16)9-19-13-5-3-11(4-6-13)7-14(17)18/h3-6,10,12,15-16H,7-9H2,1-2H3,(H,17,18)	56392-14-4
192.12621 / 5.094	66.67	1.54	1	CCN=C(O)[C@@H](N)Cc1ccccc1	InChI=1S/C12H16N2O3/c1-8(12(16)17)14-11(15)10(13)7-9-5-3-2-4-6-9/h2-6,8,10H,7,13H2,1H3,(H,14,15)(H,16,17)/t8-,10-/m0/s1	35373-93-4
141.11517 / 11.724	75	1.09	2	CN1C2CCC1CC(C2)O	InChI=1S/C8H15NO/c1-9-6-2-3-7(9)5-8(10)4-6/h6-8,10H,2-5H2,1H3	120-29-6

Table 18 Identification parameters of the Parent compound of the identified TPs

FeatureID M.W / RT	FISh coverage	MetFrag Spectral similarity Score	n. Ions matched	SMILE	InChI	Proposed CAS
299.33003 / 12.619	78.5	0.8881	3	CCCCCCCCCCCCCN(CCCN)CCCN	InChI=1S/C18H41N3/c1-2-3-4-5-6-7-8-9-10-11-16-21(17-12-14-19)18-13-15-20/h2-20H2,1H3	2372-82-9
141.11517 / 11.724	75	1.0928	2	CN1C2CCC1CC(C2)O	InChI=1S/C8H15NO/c1-9-6-2-3-7(9)5-8(10)4-6/h6-8,10H,2-5H2,1H3	120-29-6
363.22002 / 18.529	83.3	0.2479	4	COC1=C(C=C2C=C(CC2=C1)CC3CCN(CC3)CC4=CC=CC=C4)OC	InChI=1S/C24H29NO2/c1-26-23-15-21-13-20(14-22(21)16-24(23)27-2)12-18-8-10-25(11-9-18)17-19-6-4-3-5-7-19/h3-7,13,15-16,18H,8-12,14,17H2,1-2H3	120013-45-8
236.116 / 5.091	100	2.3977	1	CC(C(=O)O)NC(=O)C(CC1=CC=CC=C1)N	InChI=1S/C12H16N2O3/c1-8(12(16)17)14-11(15)10(13)7-9-5-3-2-4-6-9/h2-6,8,10H,7,13H2,1H3,(H,14,15)(H,16,17)/t8-,10-/m0/s1	3918-87-4
289.16775 / 10.108	33	0.5998	1	CN1C2CCC1CC(C2)OC(=O)C(CO)C3=CC=CC=C3	InChI=1S/C17H23NO3/c1-18-13-7-8-14(18)10-15(9-13)21-17(20)16(11-19)12-5-3-2-4-6-12/h2-6,13-16,19H,7-11H2,1H3	51-55-8

Conclusions

1.8 Removal processes at laboratory scale

1.8.1 Batch tests

Methanphetamine

Aim of the present part of the study was to provide a better knowledge of the fate of MET in the WWTPs for domestic sewage. Furthermore, in order to make detection of MET in the complex matrices of wastewater and sludge more reliable, a detailed study was conducted by investigating the effects of the macro-components of wastewater on the analytical determination. Matrix effect tests highlighted that main components of wastewater affect detection of MET for about 9-23%, which is comparable with the uncertainties of the analytical method (about ±28%). Therefore, the adopted method can be considered reliable and can be used on routine basis for MET determinations in wastewater.

Batch tests highlighted that MET concentrations in the range 50-200 ng/L can be completely removed in the oxidation reactor, with the process to be mainly ascribed to the biological activity of both heterotrophic and autotrophic bacteria. Furthermore, the respirometric tests showed that MET does not induce any inhibition; by contrast, being a nitrogenous compound, it might favour the nitrifying bacteria activity. Adsorption of MET onto activated sludge solids was always very low: therefore, from a MET contamination point of view, reuse of excess sludge, as usually adopted in the WWTPs for final disposal, does not represent a source of negative impact on the environment.

11-nor-9carboxy-Δ9-THC and benzoylecgonine

The UPLC-MS/MS method developed for measuring BE and THC-COOH in wastewater demonstrated to be relatively rapid and with repeatability<10% and bias uncertainty<10%. Furthermore, it did not require any pre-treatment of the liquid sample. The study also showed the suitability and reliability of the USE method to extract BE and THC-COOH in the sludge flocs (recovery>75%). Therefore, the proposed analytical method is suitable to be applied for a rapid detection of BE and THC-COOH in wastewater and sludge samples in the treatment plants.

Batch tests highlighted that BE and THC-COOH in the range 500-4000 ng/L and 50-2000 ng/L concentrations, respectively, can be efficiently removed in the biological reactor of a WWTP in less than 24 h. The respirometric tests showed that both BE and THC-COOH do induce inhibition of the biological activity in the reactor only when they are present at the higher concentrations among those tested; this inhibition determines a decrease of the nitrification and COD removal efficiency. It must be pointed out that 2000 ng/L THC-COOH represents an unusual level of contamination, which is found only in rare recreational events (Carmona et al., 2014).

About the removal processes, in the case of BE the efficiency was measured to be in the range 91-95% and was due to biodegradation by heterotrophic bacteria; THC-COOH removal accounted from 75% to

100% depending on the initial concentration, and was due to a combination of biodegradation and adsorption onto activated sludge flocs. Therefore, the biological reactor of a WWTP can be used to get rid of these contaminants from both wastewater and sludge, even at high concentrations.

Perfluorooctane sulfonic acid and perfluorooctanoic acid

The present study allowed to obtain a better understanding of the fate and processes occurring to PFOA and PFOS in the activated sludge reactor of a WWTP. Results of the experimental activity highlighted that PFOA and PFOS are removed from the liquid phase with efficiency ranging from 59% to 68% and from 66% to 96%, respectively, for initial concentrations from 200 ng/L to 4000 ng/L, respectively; this gives rise to a residual mass left over in the liquid phase ranging from 41% to 32% and from 34% to 4%, respectively, for the same concentrations. The mass removed from the liquid phase is partly found adsorbed onto the sludge and partly lost from the system due to processes other than adsorption and biodegradation, which are likely mediated by the microbial activity. The adsorbed mass on the activated sludge was measured to be 43-48% and approximately 60% for PFOA and PFOS, respectively, at concentrations from 200 ng/L to 4000 ng/L. PFOS showed a sorption potential on the sludge higher than PFOA.

The presence of PFOA and PFOS even at the highest concentration (4000 ng/L) does not exert a significant effect on the microbial activity and the nitrification and carbon removal in the biological reactor.

These results have been obtained under laboratory-controlled conditions, and therefore need to be confirmed under real operating conditions. However, they still represent the first step to assess the best strategies to adopt for the management of these pollutants in the WWTP. Particularly, since PFOA has been demonstrated to remain distributed between the liquid and the sludge phases at the end of the secondary treatment, the risk assessment on the final effluent should be carried out to evaluate the potential adverse effects on the environment and the human health when it is discharged or reused. Based on this evaluation, it can be deemed the need to add an additional treatment in the WWTP for a more advanced removal. About the PFOS, it was demonstrated that it remains mainly concentrated in the sludge phase, from which it can be released to a very low extent. Therefore, adsorbed compounds on the sludge should not represent a source of risk; however, specific studies on this issue are also required.

1.8.2 Continuous feeding tests

The present experimental work confirmed that the DO perturbation in the activated sludge reactor, which consists in the sudden change of the oxygen concentration, can affect the OMPs removal efficiency. Particularly, under the conditions of the study, the lowest and highest frequencies (E1, f=0.6 1/h, with aeration ON=11 min and OFF=83 min), and (E3, f= 1.8 1/h, with aeration ON=11 min and OFF=23 min) were capable of improving the removal of some of the selected OMPs, with an average increase of

30% with respect to the control tests conducted under non perturbed continuous aeration. An increase was also observed at the same frequencies in the activity of Lignin Peroxidase equal to 42% and 37% at E1 and E3, respectively, as compared to the control. The enhancement of the removal efficiency and of the target enzyme was well statistically correlated. By contrast, the effect of the DO perturbations on the microbial speciation was found to be negligible.

The lowest aeration frequency provided additional advantages: energy consumption was saved, and complete nitrogen removal was established within the same biological reactor.

It can be concluded that a proper control of the aeration/non-aeration frequency in the biological reactor of a WWTP can produce an improvement of the biological removal process of some OMPs and of nitrogen, without negatively affecting carbon biodegradation.

With respect to the previous study, it was confirmed the positive effect of the DO perturbed conditions, particularly at the lowest frequency, on the OMPs removal; however, the specific enhancement depends on the source of sludge and the type of micropollutant. Further investigations are needed to better understand the oxygen perturbation strategy to adopt at full-scale.

1.9 Removal processes at real scale

1.9.1 Wastewater treatment plants

The present part of the study aimed at investigating the occurrence, seasonal variation and removal of 13 OMPs in 76 WWTPs located in the central Italy.

Although the heterogeneous characteristics of the investigated plants (e.g. treatment lay-out, catchment area, treatment capacity), some general conclusions can be drawn:

- the contaminants belonging to the class of steroids were mostly present at concentrations under the MRL;
- within the class of illicit drugs, AM and MET were detected at concentrations close to MRL, BE was the contaminant found at the highest concentration (average influent concentration equal to 2.3 µg/L) and also that one being removed at the higher extent (the median removal value was 100%), whereas THC-COOH showed an average concentration slightly above the MRL (0.08 versus 0.03 µg/L) and removal above 60% in most of the investigated WWTPs;
- in the class of pharmaceuticals, the most relevant concentration was found for KTP with an average influent value equal to 1.2 µg/L and removal between 75% and 99% in most of the plants; CBZ showed the most heterogeneous distribution of the removal efficiency, also with negative values; TMT and SMX were detected in the influent at average concentrations of 0.1 µg/L and 0.3 µg/L, respectively, and removed in the range 45%-80% and 7%-75%, respectively;
- the WWTPs with the tertiary treatment showed the best efficiency (expressed as SRE);
- the most relevant increases of the influent concentration due to season change was observed for TMT and SMX in Spring, BE in Summer, for CBZ and KTP in Autumn.

1.9.2 Drinking water treatment plants

The data-driven workflow presented here, based on the combination of feature intensity profiles between influent and effluent samples and the prediction of biotic TPs, allowed to identify TPs in LC-HRMS based NTS data from real scale drinking water treatment samples.

15 TPs were detected with a suspect screening using a suspect list generated with the BioTransformer metabolite prediction tool. The structure of 10 of these was elucidated with confidence levels ranging from 1 to 3. Among them, 8 TPs were identified as known compounds based on the match of several databases (mzCloud, ChemSpider, Norman network SusDat, PubChem); only two of them were not found. Even if the TPs concentration measured in the samples was low, an (eco)toxicological assessment is necessary to verify if these compounds can represent a concrete risk at those contamination levels.

Moreover, our study shows that the behaviour of a certain molecule can change depending on specific conditions: all compounds appeared to behave as TPs (transformed) or as PCs (removed) according to the location.

The general approach was effective for our complex and varied dataset (samples from 7 different RSF at real scale), but an improvement is required to reduce the manual work necessary to assign the

confidence level and to verify the structure similarity. Besides, BioTransformer proved to be useful but not comprehensive for the prediction of all the possible TPs resulting from a list of PCs.

General conclusions and further prospective

The main results obtained through the present Ph.D. thesis highlight that in the activated sludge process MET and BE removals are mainly ascribed to biological activity, while THC-COOH is removed through a combination of biodegradation and adsorption onto activated sludge flocs. Values of removals measured at laboratory scale were comparable to those observed in the monitored full-scale WWTPs. Therefore, biological treatments represent an effective system for the removal of some OMPs.

PFOA and PFOS confirmed to be persistent and not biodegradable compounds and can be removed from the liquid phase mainly through adsorption onto sludge flocs; however, processes other than adsorption and biodegradation are also involved which are responsible of a loss from the system. All these processes were likely mediated by the microbial activity.

The continuous feeding tests proved that is possible to stimulate enzyme biocatalytic processes in activated sludge treatment by varying the dissolved oxygen concentration inside the reactor, obtaining an enhancement on the removal of not easily biodegradable compounds, such as CBZ, ATZ, SMX. This strategy provides also advantages in term of nitrogen removals and energy consumption.

Confirmation was obtained in the full-scale WWTPs observations where, at constant oxygen concentration in the biological reactor, the same compounds and also LNZ showed lower removal.

The full-scale study about wastewater treatments proved also that the application of tertiary treatments provides an improvement in the removals of most target OMPs; furthermore, it showed that some illicit drugs (BE and THC-COOH) and KTP are the pollutants detected at highest concentrations and most frequently, but they were well removed. The concentration of steroids in real samples was usually under the detection limits (MRL).

The proposed method for the identification of transformation products formed during biological drinking water treatments in Rapid Sand Filters showed to be reliable, despite the difficulties encountered in the validation of the proposed workflow. Moreover, it was highlighted the need of a better understanding of the effective consequences of OMPs presence and their transformation products in aquatic environment.

Further developments of the present study should aim at addressing the knowledge of the fate of OMPs in the entire water cycle; particularly, it would be interesting to look for a link between WWTPs effluents and the quality of the receiving waters, together with the evaluation of the risk for both humans and aquatics organisms related to the presence of OMPs and their transformation products.

Additionally, since some OMPs were proved to be partially transferred into wasted sludge, the knowledge will be accomplished if also information about the effects of the sludge line of WWTPs on OMPs distribution and the final consequences due to sludge reuse (e.g. in agriculture) would be assessed.

References

Ahmed, M.B., Zhou, J.L., Ngo, H.H., Guo, W., Thomaidis, N.S., Xu, J., 2017. Progress in the biological and chemical treatment technologies for emerging contaminant removal from wastewater: A critical review. J. Hazard. Mater. 323, 274–298. https://doi.org/10.1016/j.jhazmat.2016.04.045

Ahrens, L., Yeung, L.W.Y., Taniyasu, S., Lam, P.K.S., Yamashita, N., 2011. Partitioning of perfluorooctanoate (PFOA), perfluorooctane sulfonate (PFOS) and perfluorooctane sulfonamide (PFOSA) between water and sediment. Chemosphere 85, 731–737. https://doi.org/10.1016/j.chemosphere.2011.06.046

Alneyadi, A.H., Rauf, M.A., Ashraf, S.S., 2018a. Oxidoreductases for the remediation of organic pollutants in water – a critical review. Crit. Rev. Biotechnol. 0, 1–18. https://doi.org/10.1080/07388551.2017.1423275

Alneyadi, A.H., Rauf, M.A., Ashraf, S.S., 2018b. Oxidoreductases for the remediation of organic pollutants in water–a critical review. Crit. Rev. Biotechnol. 38, 971–988. https://doi.org/10.1080/07388551.2017.1423275

Álvarez-Ruiz, R., Andrés-Costa, M.J., Andreu, V., Picó, Y., 2015. Simultaneous determination of traditional and emerging illicit drugs in sediments, sludges and particulate matter. J. Chromatogr. A 1405, 103–115. https://doi.org/10.1016/j.chroma.2015.05.062

Andrés-Costa, M.J., Andreu, V., Picó, Y., 2017. Liquid chromatography–mass spectrometry as a tool for wastewater-based epidemiology: Assessing new psychoactive substances and other human biomarkers. TrAC - Trends Anal. Chem. 94, 21–38. https://doi.org/10.1016/j.trac.2017.06.012

Arvaniti, O.S., Andersen, H.R., Thomaidis, N.S., Stasinakis, A.S., 2014. Sorption of Perfluorinated Compounds onto different types of sewage sludge and assessment of its importance during wastewater treatment. Chemosphere 111, 405–411. https://doi.org/10.1016/j.chemosphere.2014.03.087

Arvaniti, O.S., Stasinakis, A.S., 2015. Review on the occurrence, fate and removal of perfluorinated compounds during wastewater treatment. Sci. Total Environ. 524–525, 81–92. https://doi.org/10.1016/j.scitotenv.2015.04.023

Asif, M.B., Hai, F.I., Dhar, B.R., Ngo, H.H., Guo, W., Jegatheesan, V., Price, W.E., Nghiem, L.D., Yamamoto, K., 2018. Impact of simultaneous retention of micropollutants and laccase on micropollutant degradation in enzymatic membrane bioreactor. Bioresour. Technol. 267, 473–480. https://doi.org/10.1016/j.biortech.2018.07.066

Avendaño, S.M., Zhong, G., Liu, J., 2015. Comment on ‘‘Biodegradation of perfluorooctanesulfonate (PFOS) as an emerging contaminant.’ Chemosphere 138, 1037–1038. https://doi.org/http://dx.doi.org/10.1016/j.chemosphere.2015.03.022

Bagnall, J., Malia, L., Lubben, A., Kasprzyk-Hordern, B., 2013. Stereoselective biodegradation of

amphetamine and methamphetamine in river microcosms. Water Res. 47, 5708–18. https://doi.org/10.1016/j.watres.2013.06.057

Bains, A., Perez-Garcia, O., Lear, G., Greenwood, D.R., Swift, S., Middleditch, M.J., Kolodziej, E.P., Singhal, N., 2019. Induction of microbial oxidative stress as a new strategy to enhance the enzymatic degradation of organic micropollutants in synthetic wastewater. Environ. Sci. Technol. https://doi.org/10.1021/acs.est.9b02219

Baker, D.R., Kasprzyk-Hordern, B., 2013. Spatial and temporal occurrence of pharmaceuticals and illicit drugs in the aqueous environment and during wastewater treatment: New developments. Sci. Total Environ. 454–455, 442–456. https://doi.org/10.1016/j.scitotenv.2013.03.043

Baker, D.R., Kasprzyk-Hordern, B., 2011. Multi-residue analysis of drugs of abuse in wastewater and surface water by solid-phase extraction and liquid chromatography-positive electrospray ionisation tandem mass spectrometry. J. Chromatogr. A 1218, 1620–1631. https://doi.org/10.1016/j.chroma.2011.01.060

Barbosa, M.O., Moreira, N.F.F., Ribeiro, A.R., Pereira, M.F.R., Silva, A.M.T., 2016. Occurrence and removal of organic micropollutants: An overview of the watch list of EU Decision 2015/495. Water Res. 94, 257–279. https://doi.org/10.1016/j.watres.2016.02.047

Bassin, J.P., Pronk, M., Kraan, R., Kleerebezem, R., Van Loosdrecht, M.C.M., 2011. Ammonium adsorption in aerobic granular sludge, activated sludge and anammox granules. Water Res. 45, 5257–5265. https://doi.org/10.1016/j.watres.2011.07.034

Becker, A.M., Suchan, M., Gerstmann, S., Frank, H., 2010. Perfluorooctanoic acid and perfluorooctane sulfonate released from a waste water treatment plant in Bavaria, Germany. Environ. Sci. Pollut. Res. 17, 1502–1507. https://doi.org/10.1007/s11356-010-0335-x

Ben, W., Zhu, B., Yuan, X., Zhang, Y., Yang, M., Qiang, Z., 2018. Occurrence, removal and risk of organic micropollutants in wastewater treatment plants across China: Comparison of wastewater treatment processes. Water Res. 130, 38–46. https://doi.org/10.1016/j.watres.2017.11.057

Benner, J., Helbling, D.E., Kohler, H.P.E., Wittebol, J., Kaiser, E., Prasse, C., Ternes, T.A., Albers, C.N., Aamand, J., Horemans, B., Springael, D., Walravens, E., Boon, N., 2013. Is biological treatment a viable alternative for micropollutant removal in drinking water treatment processes? Water Res. 47, 5955–5976. https://doi.org/10.1016/j.watres.2013.07.015

Bertelkamp, C., Reungoat, J., Cornelissen, E.R., Singhal, N., Reynisson, J., Cabo, A.J., van der Hoek, J.P., Verliefde, A.R.D., 2014. Sorption and biodegradation of organic micropollutants during river bank filtration: A laboratory column study. Water Res. 52, 231–241. https://doi.org/10.1016/j.watres.2013.10.068

Bettencourt Da Silva, R.J.N., Camões, M.F.G.F.C., Seabra E Barros, J., 1999. Validation and quality control schemes based on the expression of results with uncertainty. Anal. Chim. Acta 393, 167–175. https://doi.org/10.1016/S0003-2670(99)00337-2

Bijlsma, L., Emke, E., Hernández, F., De Voogt, P., 2012. Investigation of drugs of abuse and relevant metabolites in Dutch sewage water by liquid chromatography coupled to high resolution mass

spectrometry. Chemosphere 89, 1399–1406. https://doi.org/10.1016/j.chemosphere.2012.05.110

Bijlsma, L., Serrano, R., Ferrer, C., Tormos, I., Hernández, F., 2014. Occurrence and behavior of illicit drugs and metabolites in sewage water from the Spanish Mediterranean coast (Valencia region). Sci. Total Environ. 487, 703–709. https://doi.org/10.1016/j.scitotenv.2013.11.131

Binelli, A., Marisa, I., Fedorova, M., Hoffmann, R., Riva, C., 2013. First evidence of protein profile alteration due to the main cocaine metabolite (benzoylecgonine) in a freshwater biological model. Aquat. Toxicol. 140–141, 268–278. https://doi.org/10.1016/j.aquatox.2013.06.013

Binelli, A., Pedriali, A., Riva, C., Parolini, M., 2012. Illicit drugs as new environmental pollutants: Cyto-genotoxic effects of cocaine on the biological model Dreissena polymorpha. Chemosphere 86, 906–911. https://doi.org/10.1016/j.chemosphere.2011.10.056

Bletsou, A.A., Jeon, J., Hollender, J., Archontaki, E., Thomaidis, N.S., 2015. Targeted and non-targeted liquid chromatography-mass spectrometric workflows for identification of transformation products of emerging pollutants in the aquatic environment. TrAC - Trends Anal. Chem. 66, 32–44. https://doi.org/10.1016/j.trac.2014.11.009

Boix, C., Ibáñeez, M., Fabregat-Safont, D., Morales, E., Pastor, L., Sancho, J. V., S??nchez-Ram??rez, J.E., Hern??ndez, F., 2016. Analytical methodologies based on LC-MS/MS for monitoring selected emerging compounds in liquid and solid phases of the sewage sludge. MethodsX 3, 333–342. https://doi.org/10.1016/j.mex.2016.04.010

Boni, M.R., Chiavola, A., Di Marcantonio, C., Sbaffoni, S., Biagioli, S., Cecchini, G., Frugis, A., 2018. A study through batch tests on the analytical determination and the fate and removal of methamphetamine in the biological treatment of domestic wastewater. Environ. Sci. Pollut. Res. https://doi.org/10.1007/s11356-018-1321-y

Brack, W., Dulio, V., Ågerstrand, M., Allan, I., Altenburger, R., Brinkmann, M., Bunke, D., Burgess, R.M., Cousins, I., Escher, B.I., Hernández, F.J., Hewitt, L.M., Hilscherová, K., Hollender, J., Hollert, H., Kase, R., Klauer, B., Lindim, C., Herráez, D.L., Miège, C., Munthe, J., O'Toole, S., Posthuma, L., Rüdel, H., Schäfer, R.B., Sengl, M., Smedes, F., van de Meent, D., van den Brink, P.J., van Gils, J., van Wezel, A.P., Vethaak, A.D., Vermeirssen, E., von der Ohe, P.C., Vrana, B., 2017. Towards the review of the European Union Water Framework management of chemical contamination in European surface water resources. Sci. Total Environ. 576, 720–737. https://doi.org/10.1016/j.scitotenv.2016.10.104

Brunner, A.M., Vughs, D., Siegers, W., Bertelkamp, C., Hofman-Caris, R., Kolkman, A., ter Laak, T., 2019. Monitoring transformation product formation in the drinking water treatments rapid sand filtration and ozonation. Chemosphere 214, 801–811. https://doi.org/10.1016/j.chemosphere.2018.09.140

Buck, R.C., Franklin, J., Berger, U., Conder, J.M., Cousins, I.T., de Voogt, P., Jensen, A.A., Kannan, K., Mabury, S.A., van Leeuwen, S.P., 2011. Perfluoroalkyl and polyfluoroalkyl substances in the environment: Terminology, classification, and origins. Integr. Environ. Assess. Manag. 7, 513–541. https://doi.org/10.1002/ieam.258

Carmona, E., Andreu, V., Picó, Y., 2014. Occurrence of acidic pharmaceuticals and personal care products in Turia River Basin: From waste to drinking water. Sci. Total Environ. 484, 53–63. https://doi.org/10.1016/j.scitotenv.2014.02.085

Castiglioni, S., Bijlsma, L., Covaci, A., Emke, E., Harman, C., Hernández, F., Kasprzyk-Hordern, B., Ort, C., van Nuijs, A.L.N., de Voogt, P., Zuccato, E., 2016. Estimating community drug use through wastewater-based epidemiology, Assessing illicit drugs in wastewater: advances in wastewater-based drug epidemiology, EMCDDA Insights 22. https://doi.org/10.2810/017397

Castiglioni, S., Bijlsma, L., Covaci, A., Emke, E., Hernández, F., Reid, M., Ort, C., Thomas, K. V., Van Nuijs, A.L.N., De Voogt, P., Zuccato, E., 2013. Evaluation of uncertainties associated with the determination of community drug use through the measurement of sewage drug biomarkers. Environ. Sci. Technol. 47, 1452–1460. https://doi.org/10.1021/es302722f

Castiglioni, S., Thomas, K. V., Kasprzyk-Hordern, B., Vandam, L., Griffiths, P., 2014. Testing wastewater to detect illicit drugs: State of the art, potential and research needs. Sci. Total Environ. 487, 613–620. https://doi.org/10.1016/j.scitotenv.2013.10.034

Castiglioni, S., Valsecchi, S., Polesello, S., Rusconi, M., Melis, M., Palmiotto, M., Manenti, A., Davoli, E., Zuccato, E., 2015. Sources and fate of perfluorinated compounds in the aqueous environment and in drinking water of a highly urbanized and industrialized area in Italy. J. Hazard. Mater. 282, 51–60. https://doi.org/10.1016/j.jhazmat.2014.06.007

Castiglioni, S., Zuccato, E., Crisci, E., Chiabrando, C., Fanelli, R., Bagnati, R., 2006. Identification and measurement of illicit drugs and their metabolites in urban wastewater by liquid chromatography-tandem mass spectrometry. Anal .Chem. 78, 8421–8429. https://doi.org/10.1021/ac061095b

Causanilles, A., Baz-Lomba, J.A., Burgard, D.A., Emke, E., González-Mariño, I., Krizman-Matasic, I., Li, A., Löve, A.S.C., McCall, A.K., Montes, R., van Nuijs, A.L.N., Ort, C., Quintana, J.B., Senta, I., Terzic, S., Hernandez, F., de Voogt, P., Bijlsma, L., 2017. Improving wastewater-based epidemiology to estimate cannabis use: focus on the initial aspects of the analytical procedure. Anal. Chim. Acta 988, 27–33. https://doi.org/10.1016/j.aca.2017.08.011

Chiavola, A., Boni, M.R., Di Marcantonio, C., Cecchini, G., Biagioli, S., Frugis, A., 2019. A laboratory-study on the analytical determination and removal processes of THC-COOH and bezoylecgonine in the activated sludge reactor. Chemosphere 222, 83–90. https://doi.org/10.1016/j.chemosphere.2019.01.117

Chiavola, A., Di Marcantonio, C., Boni, M.R., Biagioli, S., Frugis, A., Cecchini, G., 2020. Experimental investigation on the perfluorooctanoic and perfluorooctane sulfonic acids fate and behaviour in the activated sludge reactor. Process Saf. Environ. Prot. 134, 406–415. https://doi.org/10.1016/j.psep.2019.11.003

Chiavola, A., Romano, R., Bongirolami, S., Giulioli, S., 2017. Optimization of Energy Consumption in the Biological Reactor of a Wastewater Treatment Plant by Means of Oxy Fuzzy and ORP Control. Water. Air. Soil Pollut. 228, 11270. https://doi.org/10.1007/s11270-017-3462-x

Chiavola, Agostina, Tedesco, P., Boni, M.R., 2017. Fate of selected drugs in the wastewater treatment plants (WWTPs) for domestic sewage. Environ. Sci. Pollut. Res. 1–11. https://doi.org/10.1007/s11356-017-9313-x

Chiavola, A., Tedesco, P., Boni, M.R., 2016. Fate of some endocrine disruptors in batch experiments using activated and inactivated sludge. Water. Air. Soil Pollut. 227. https://doi.org/10.1007/s11270-016-3126-2

Clarke, B.O., Smith, S.R., 2011. Review of "emerging" organic contaminants in biosolids and assessment of international research priorities for the agricultural use of biosolids. Environ. Int. 37, 226–247. https://doi.org/10.1016/j.envint.2010.06.004

Couto, C.F., Lange, L.C., Amaral, M.C.S., 2019. Occurrence, fate and removal of pharmaceutically active compounds (PhACs) in water and wastewater treatment plants—A review. J. Water Process Eng. 32, 100927. https://doi.org/10.1016/j.jwpe.2019.100927

Dalahmeh, S.S., Alziq, N., Ahrens, L., 2019. Potential of biochar filters for onsite wastewater treatment: Effects of active and inactive biofilms on adsorption of per- and polyfluoroalkyl substances in laboratory column experiments. Environ. Pollut. 247, 155–164. https://doi.org/10.1016/j.envpol.2019.01.032

Dauchy, X., Boiteux, V., Bach, C., Colin, A., Hemard, J., Rosin, C., Munoz, J.F., 2017. Mass flows and fate of per- and polyfluoroalkyl substances (PFASs) in the wastewater treatment plant of a fluorochemical manufacturing facility. Sci. Total Environ. 576, 549–558. https://doi.org/10.1016/j.scitotenv.2016.10.130

Daughton, C.G., Ternes, T.A., 1999. Pharmaceuticals and personal care products in the environment: agents of subtle change? Environ. Health Perspect. 107, 907–938. https://doi.org/10.1289/ehp.99107s6907

Daylight Chemical Information Systems, I., 2008. Daylight Theory Manual [WWW Document]. URL https://www.daylight.com/dayhtml/doc/theory/ (accessed 9.17.19).

Decision, C., 2002. 2002/657/EC: Commission Decision of 12 August 2002 implementing Council Directive 96/23/EC concerning the performance of analytical methods and the interpretation of results (Text with EEA relevance) (notified under document number C(2002) 3044). Off. J. Eur. Communities 8–36. https://doi.org/10.1017/CBO9781107415324.004

Díaz-Cruz, M.S., García-Galán, M.J., Guerra, P., Jelic, A., Postigo, C., Eljarrat, E., Farré, M., López de Alda, M.J., Petrovic, M., Barceló, D., Petrovic, M., Barceló, D., 2009. Analysis of selected emerging contaminants in sewage sludge. TrAC - Trends Anal. Chem. 28, 1263–1275. https://doi.org/10.1016/j.trac.2009.09.003

Directive 2000/60/EC of the European parliament and of the council of 23 October 2000 establishing a framework for Community action in the field of water policy, 2000. . Off. J. Eur. Communities.

Djoumbou-Feunang, Y., Fiamoncini, J., Gil-de-la-Fuente, A., Greiner, R., Manach, C., Wishart, D.S., 2019. BioTransformer: A comprehensive computational tool for small molecule metabolism prediction and metabolite identification. J. Cheminform. 11, 1–25.

https://doi.org/10.1186/s13321-018-0324-5

Djoumbou Feunang, Y., Eisner, R., Knox, C., Chepelev, L., Hastings, J., Owen, G., Fahy, E., Steinbeck, C., Subramanian, S., Bolton, E., Greiner, R., Wishart, D.S., 2016. ClassyFire: automated chemical classification with a comprehensive, computable taxonomy. J. Cheminform. 8, 1–20. https://doi.org/10.1186/s13321-016-0174-y

Eaton, A.D., Clesceri, L.S., Rice, E.W., Greenberg, A.E., 2005. Standard Methods for the Examination of Water and Wastewater, Centennial Edition.

Edgar, R.C., 2013. UPARSE: highly accurate OTU sequences from microbial amplicon reads. Nat. Methods 10, 996–8. https://doi.org/10.1038/nmeth.2604

Ellis, L.B.M., Gao, J., Fenner, K., Wackett, L.P., 2008. The University of Minnesota pathway prediction system: predicting metabolic logic. Nucleic Acids Res. 36, 427–432. https://doi.org/10.1093/nar/gkn315

EMCDDA, 2017. European Drug Report 2017: Trends and Developments. https://doi.org/10.2810/88175

Erhayem, M., Al-tohami, F., Mohamed, R., Ahmida, K., 2015. Isotherm , Kinetic and Thermodynamic Studies for the Sorption of Mercury (II) onto Activated Carbon from Rosmarinus officinalis Leaves. Am. J. Anal. Chem. 6, 1–10. https://doi.org/10.4236/ajac.2015.61001

Eskandarpour, A., Onyango, M.S., Ochieng, A., Asai, S., 2008. Removal of fluoride ions from aqueous solution at low pH using schwertmannite. J. Hazard. Mater. 152, 571–579. https://doi.org/10.1016/j.jhazmat.2007.07.020

European Commission, 2018. COMMISSION IMPLEMENTING DECISION (EU) 2018/840 of 5 June 2018. Off. J. Eur. Union 141, 9–12.

European Commission, 2015. Commission Implementing Regulation (EU) 2015/495 of 20 March 2015 establishing a watch list of substances for Union-wide monitoring in the field of water policy pursuant to Directive 2008/105/EC of the European Parliament and of the Council. Off. J. Eur. Union L78/40, 20–30. https://doi.org/http://eur-lex.europa.eu/pri/en/oj/dat/2003/l_285/l_28520031101en00330037.pdf

Fischer, K., Majewsky, M., 2014. Cometabolic degradation of organic wastewater micropollutants by activated sludge and sludge-inherent microorganisms. Appl. Microbiol. Biotechnol. 98, 6583–6597. https://doi.org/10.1007/s00253-014-5826-0

Foo, K.Y., Hameed, B.H., 2010. Insights into the modeling of adsorption isotherm systems. Chem. Eng. J. 156, 2–10. https://doi.org/10.1016/j.cej.2009.09.013

Gago-Ferrero, P., Borova, V., Dasenaki, M.E., Thomaidis, N.S., 2015. Simultaneous determination of 148 pharmaceuticals and illicit drugs in sewage sludge based on ultrasound-assisted extraction and liquid chromatography-tandem mass spectrometry. Anal. Bioanal. Chem. 407, 4287–4297. https://doi.org/10.1007/s00216-015-8540-6

Gambino, M., Cappitelli, F., 2016. Mini-review: Biofilm responses to oxidative stress. Biofouling 32, 167–178. https://doi.org/10.1080/08927014.2015.1134515

Garcia-Rodríguez, A., Matamoros, V., Fontàs, C., Salvadó, V., 2014. The ability of biologically based wastewater treatment systems to remove emerging organic contaminants--a review. Environ. Sci. Pollut. Res. Int. 21, 11708–11728. https://doi.org/10.1007/s11356-013-2448-5

Gerrity, D., Trenholm, R.A., Snyder, S.A., 2011. Temporal variability of pharmaceuticals and illicit drugs in wastewater and the effects of a major sporting event. Water Res. 45, 5399–5411. https://doi.org/10.1016/j.watres.2011.07.020

Global Water Research Coalition, 2008. Development of an International armaceuticals Priority Lis Relevant forfhe Water Cycle Development of an International Priority List of Pharmaceuticals Relevant for the Water Cycle.

Gogoi, A., Mazumder, P., Tyagi, V.K., Tushara Chaminda, G.G., An, A.K., Kumar, M., 2018. Occurrence and fate of emerging contaminants in water environment: A review. Groundw. Sustain. Dev. 6, 169–180. https://doi.org/10.1016/j.gsd.2017.12.009

Gómez, M.J., Herrera, S., Solé, D., García-Calvo, E., Fernández-Alba, A.R., 2012. Spatio-temporal evaluation of organic contaminants and their transformation products along a river basin affected by urban, agricultural and industrial pollution. Sci. Total Environ. 420, 134–145. https://doi.org/10.1016/j.scitotenv.2012.01.029

Gonzalez-Gil, L., Krah, D., Ghattas, A.-K., Carballa, M., Wick, A., Helmholz, L., Lema, J.M., Ternes, T.A., 2019. Biotransformation of organic micropollutants by anaerobic sludge enzymes. Water Res. 152, 202–214. https://doi.org/10.1016/j.watres.2018.12.064

Grassi, M., Rizzo, L., Farina, A., 2013. Endocrine disruptors compounds, pharmaceuticals and personal care products in urban wastewater: Implications for agricultural reuse and their removal by adsorption process. Environ. Sci. Pollut. Res. 20, 3616–3628. https://doi.org/10.1007/s11356-013-1636-7

Han, B.C., Jiang, W.L., Zhang, Y., Wei, W., Chen, J., 2018. Profile of organic carbon and nitrogen removal by a continuous flowing conventional activated sludge reactor with pulse aeration. Process Saf. Environ. Prot. 117, 439–445. https://doi.org/10.1016/j.psep.2018.05.022

He, Q., Chen, L., Zhang, S., Wang, L., Liang, J., Xia, W., Wang, H., Zhou, J., 2018. Simultaneous nitrification, denitrification and phosphorus removal in aerobic granular sequencing batch reactors with high aeration intensity: Impact of aeration time. Bioresour. Technol. 263, 214–222. https://doi.org/10.1016/j.biortech.2018.05.007

Hedegaard, M.J., Albrechtsen, H.J., 2014. Microbial pesticide removal in rapid sand filters for drinking water treatment - Potential and kinetics. Water Res. 48, 71–81. https://doi.org/10.1016/j.watres.2013.09.024

Hedegaard, M.J., Arvin, E., Corfitzen, C.B., Albrechtsen, H.J., 2014. Mecoprop (MCPP) removal in full-scale rapid sand filters at a groundwater-based waterworks. Sci. Total Environ. 499, 257–264. https://doi.org/10.1016/j.scitotenv.2014.08.052

Helbling, D.E., Hollender, J., Kohler, H.-P.E., Singer, H., Fenner, K., 2010. High-throughput identification of microbial transformation products of organic micropollutants. Environ. Sci.

Technol. 44, 6621–6627. https://doi.org/10.1021/es100970m

Henning, N., Kunkel, U., Wick, A., Ternes, T.A., 2018. Biotransformation of gabapentin in surface water matrices under different redox conditions and the occurrence of one major TP in the aquatic environment. Water Res. 137, 290–300. https://doi.org/10.1016/j.watres.2018.01.027

Hernández, F., Castiglioni, S., Covaci, A., Voogt, P. de, Emke, E., Kasprzyk-Hordern, B., Ort, C., Reid, M., Sancho, J. V., Thomas, K. V., Nuijs, A.L.N. van, Zuccato, E., Bijlsma, Lubertus, 2016. Mass spectrometric strategies for the investigation of biomarkers of illicit drug use in wastewater. Mass Spectrom Rev. Wiley Onli. https://doi.org/10.1002/mas.21525

Hollender, J., Schymanski, E.L., Singer, H.P., Ferguson, P.L., 2017. Nontarget Screening with High Resolution Mass Spectrometry in the Environment: Ready to Go? Environ. Sci. Technol. 51, 11505–11512. https://doi.org/10.1021/acs.est.7b02184

Hu, Z., Song, X., Wei, C., Liu, J., 2017. Behavior and mechanisms for sorptive removal of per fl uorooctane sulfonate by layered double hydroxides. Chemosphere 187, 196–205. https://doi.org/10.1016/j.chemosphere.2017.08.082

Imma Ferrer, E.M.T., 2008. EPA Method 1694 : Agilent' s 6410A LC/MS/MS Solution for Pharmaceuticals and Personal Care Products in Water, Soil, Sediment, and Biosolids by HPLC/MS/MS Application Note. Group 12.

Jelic, A., Cruz-Morató, C., Marco-Urrea, E., Sarrà, M., Perez, S., Vicent, T., Petrović, M., Barcelo, D., 2012. Degradation of carbamazepine by Trametes versicolor in an air pulsed fluidized bed bioreactor and identification of intermediates. Water Res. 46, 955–964. https://doi.org/10.1016/j.watres.2011.11.063

Jelic, A., Gros, M., Ginebreda, A., Cespedes-Sánchez, R., Ventura, F., Petrovic, M., Barcelò, D., 2011. Occurrence, partition and removal of pharmaceuticals in sewage water and sludge during wastewater treatment. Water Res. 45, 1165–1176. https://doi.org/10.1016/j.watres.2010.11.010

Johansson, J.H., Yan, H., Berger, U., Cousins, I.T., 2017. Water-to-air transfer of branched and linear PFOA: Influence of pH, concentration and water type. Emerg. Contam. 3, 46–53. https://doi.org/10.1016/j.emcon.2017.03.001

Kaiser, E., Prasse, C., Wagner, M., Bröder, K., Ternes, T.A., 2014. Transformation of oxcarbazepine and human metabolites of carbamazepine and oxcarbazepine in wastewater treatment and sand filters. Environ. Sci. Technol. 48, 10208–10216. https://doi.org/10.1021/es5024493

Karigar, C.S., Rao, S.S., 2011. Role of Microbial Enzymes in the Bioremediation of Pollutants: A Review. Enzyme Res. 2011, 1–11. https://doi.org/10.4061/2011/805187

Kolekar, P.D., Phugare, S.S., Jadhav, J.P., 2014. Biodegradation of atrazine by Rhodococcus sp. BCH2 to N-isopropylammelide with subsequent assessment of toxicity of biodegraded metabolites. Environ. Sci. Pollut. Res. 21, 2334–2345. https://doi.org/10.1007/s11356-013-2151-6

Kwon, B.G., Lim, H.J., Na, S.H., Choi, B.I., Shin, D.S., Chung, S.Y., 2015. Reply to comment on '"Biodegradation of perfluorooctanesulfonate (PFOS) as an emerging contaminant."'

Chemosphere 138, 1039–1044. https://doi.org/http://dx.doi.org/10.1016/j.chemosphere.2015.03.021

Kwon, B.G., Lim, H.J., Na, S.H., Choi, B.I., Shin, D.S., Chung, S.Y., 2014. Biodegradation of perfluorooctanesulfonate (PFOS) as an emerging contaminant. Chemosphere 109, 221–225. https://doi.org/10.1016/j.chemosphere.2014.01.072

Li, Z., Kaserzon, S.L., Plassmann, M.M., Sobek, A., Gómez Ramos, M.J., Radke, M., 2017. A strategic screening approach to identify transformation products of organic micropollutants formed in natural waters. Environ. Sci. Process. Impacts 19, 488–498. https://doi.org/10.1039/c6em00635c

Liou, J.S.C., Szostek, B., DeRito, C.M., Madsen, E.L., 2010. Investigating the biodegradability of perfluorooctanoic acid. Chemosphere 80, 176–183. https://doi.org/10.1016/j.chemosphere.2010.03.009

Little, J.L., Williams, A.J., Pshenichnov, A., Tkachenko, V., 2012. Identification of "known unknowns" utilizing accurate mass data and chemspider. J. Am. Soc. Mass Spectrom. 23, 179–185. https://doi.org/10.1007/s13361-011-0265-y

Liu, S., 2015. Cooperative adsorption on solid surfaces. J. Colloid Interface Sci. 450, 224–238. https://doi.org/10.1016/j.jcis.2015.03.013

Loganathan, B.G., Sajwan, K.S., Sinclair, E., Senthil Kumar, K., Kannan, K., 2007. Perfluoroalkyl sulfonates and perfluorocarboxylates in two wastewater treatment facilities in Kentucky and Georgia. Water Res. 41, 4611–4620. https://doi.org/10.1016/j.watres.2007.06.045

Loos, R., Carvalho, R., António, D.C., Comero, S., Locoro, G., Tavazzi, S., Paracchini, B., Ghiani, M., Lettieri, T., Blaha, L., Jarosova, B., Voorspoels, S., Servaes, K., Haglund, P., Fick, J., Lindberg, R.H., Schwesig, D., Gawlik, B.M., 2013. EU-wide monitoring survey on emerging polar organic contaminants in wastewater treatment plant effluents. Water Res. 47, 6475–6487. https://doi.org/10.1016/j.watres.2013.08.024

Loos, R., Gawlik, B.M., Boettcher, K., Locoro, G., Contini, S., Bidoglio, G., 2009. Sucralose screening in European surface waters using a solid-phase extraction-liquid chromatography-triple quadrupole mass spectrometry method. J. Chromatogr. A 1216, 1126–1131. https://doi.org/10.1016/j.chroma.2008.12.048

Mackuľak, T., Bodík, I., Hasan, J., Grabic, R., Golovko, O., Vojs-Staňová, A., Gál, M., Naumowicz, M., Tichý, J., Brandeburová, P., Híveš, J., 2016. Dominant psychoactive drugs in the Central European region: A wastewater study. Forensic Sci. Int. 267, 42–51. https://doi.org/10.1016/j.forsciint.2016.08.016

Mark L. Ferrey, John T. Wilson, Cherri Adair, Chunming Su, Dennis D. Fine, X.L., Washington, J.W., 2012. Behavior and Fate of PFOA and PFOS in Sandy Aquifer Sediment. Ground Water Monit. Remediat. 32, 42–52. https://doi.org/10.1111/j1745–6592.2012.01395.x

Martin, Jonathan W Kannan, K., Berger, U., De Voogt, P., Field, J., Franklin, J., Giesy, J.P., Harner, T., Muir, D.C.G., Scott, B., Kaiser, M., Järnberg, U., Jones, K.C., Mabury, S.A., Schroeder, H.,

Simcik, M., Sottani, C., Van Bavel, B., Karrman, A., Lindstrom, G., Van Leeuwen, S., 2004. Peer reviewed: analytical challenges hamper perfluoroalkyl research. Env. Sci Technol 248A-255A.

Metcalf & Eddy, 2015. Wastewater Engineering Treatment and Resource Recovery, Fifth edit. ed, McGraw-Hill Education. https://doi.org/10.1007/978-1-349-06927-9_4

Metcalf, Eddy, 2013. Wastewater Engineering: Treatment and Reuse, 5th edition, McGraw-Hill Education.

Miller, T.H., Bury, N.R., Owen, S.F., MacRae, J.I., Barron, L.P., 2018. A review of the pharmaceutical exposome in aquatic fauna. Environ. Pollut. 239, 129–146. https://doi.org/10.1016/j.envpol.2018.04.012

Mishra, S., Noronha, S.B., Suraishkumar, G.K., 2005. Increase in enzyme productivity by induced oxidative stress in Bacillus subtilis cultures and analysis of its mechanism using microarray data. Process Biochem. 40, 1863–1870. https://doi.org/10.1016/j.procbio.2004.06.055

Morlay, C., Gasperi, J., Guillossou, R., Mailler, R., Le Roux, J., Rocher, V., Vulliet, E., Nauleau, F., 2018. Organic micropollutants in a large wastewater treatment plant: What are the benefits of an advanced treatment by activated carbon adsorption in comparison to conventional treatment? Chemosphere 218, 1050–1060. https://doi.org/10.1016/j.chemosphere.2018.11.182

Mu, Y., Liu, X., Wang, L., 2018. A Pearson's correlation coefficient based decision tree and its parallel implementation. Inf. Sci. (Ny). 435, 40–58. https://doi.org/10.1016/j.ins.2017.12.059

Naghdi, M., Taheran, M., Brar, S.K., Kermanshahi-pour, A., Verma, M., Surampalli, R.Y., 2018. Removal of pharmaceutical compounds in water and wastewater using fungal oxidoreductase enzymes. Environ. Pollut. 234, 190–213. https://doi.org/10.1016/j.envpol.2017.11.060

Naidu, R., Arias Espana, V.A., Liu, Y., Jit, J., 2016. Emerging contaminants in the environment: Risk-based analysis for better management. Chemosphere 154, 350–357. https://doi.org/10.1016/j.chemosphere.2016.03.068

Nefau, T., Karolak, S., Castillo, L., Boireau, V., Levi, Y., 2013. Presence of illicit drugs and metabolites in influents and effluents of 25 sewage water treatment plants and map of drug consumption in France. Sci. Total Environ. 461–462, 712–722. https://doi.org/10.1016/j.scitotenv.2013.05.038

Noguera-Oviedo, K., Aga, D.S., 2016. Lessons learned from more than two decades of research on emerging contaminants in the environment. J. Hazard. Mater. 316, 242–251. https://doi.org/10.1016/j.jhazmat.2016.04.058

Oecd, 2010. Test No. 209: Activated Sludge, Respiration Inhibition Test. OECD Guidel. Test. Chem. Sect. 2 Eff. Biot. Syst. 209, 1–18. https://doi.org/10.1787/9789264070080-en

Pal, R., Megharaj, M., Kirkbride, K.P., Naidu, R., 2015. Adsorption and desorption characteristics of methamphetamine, 3,4-methylenedioxymethamphetamine, and pseudoephedrine in soils. Environ. Sci. Pollut. Res. 22, 8855–8865. https://doi.org/10.1007/s11356-014-2940-6

Pal, R., Megharaj, M., Kirkbride, K.P., Naidu, R., 2013. Illicit drugs and the environment - A review.

Sci. Total Environ. 463–464, 1079–1092. https://doi.org/10.1016/j.scitotenv.2012.05.086

Pan, C.-G., Liu, Y.-S., Ying, G.-G., 2016. Perfluoroalkyl substances (PFASs) in wastewater treatment plants and drinking water treatment plants: Removal efficiency and exposure risk. Water Res. 106, 562–570. https://doi.org/10.1016/j.watres.2016.10.045

Parolini, M., Binelli, A., 2014. Oxidative and genetic responses induced by Δ-9-tetrahydrocannabinol (Δ-9-THC) to Dreissena polymorpha. Sci. Total Environ. 468–469, 68–76. https://doi.org/10.1016/j.scitotenv.2013.08.024

Parsons, J.R., Sáez, M., Dolfing, J., Voogt, P. De, 2008. Reviews of Environmental Contamination and Toxicology Vol 196. Rev. Environ. Contam. Toxicol. 196. https://doi.org/10.1007/978-0-387-78444-1

Patrolecco, L., Capri, S., Ademollo, N., 2015. Occurrence of selected pharmaceuticals in the principal sewage treatment plants in Rome (Italy) and in the receiving surface waters. Environ. Sci. Pollut. Res. 22, 5864–5876. https://doi.org/10.1007/s11356-014-3765-z

Persistent Organic Pollutants Review Committee Twelfth Meeting, 2016. Risk profile on pentadecafluorooctanoic acid (CAS No: 335-67-1, PFOA, perfluorooctanooic acid), its is salts and PPFOA-related compoounds. UNITED NATIONS.

Plazinski, W., Dziuba, J., Rudzinski, W., 2013. Modeling of sorption kinetics: The pseudo-second order equation and the sorbate intraparticle diffusivity. Adsorption 19, 1055–1064. https://doi.org/10.1007/s10450-013-9529-0

Postigo, C., López de Alda, M.J., Barceló, D., 2010. Drugs of abuse and their metabolites in the Ebro River basin: Occurrence in sewage and surface water, sewage treatment plants removal efficiency, and collective drug usage estimation. Environ. Int. 36, 75–84. https://doi.org/10.1016/j.envint.2009.10.004

Quirantes, M., Nogales, R., Romero, E., 2017. Sorption potential of different biomass fly ashes for the removal of diuron and 3,4-dichloroaniline from water. J. Hazard. Mater. 331, 300–308. https://doi.org/10.1016/j.jhazmat.2017.02.047

Racamonde, I., Villaverde-de-Sáa, E., Rodil, R., Quintana, J.B., Cela, R., 2012. Determination of Δ9-tetrahydrocannabinol and 11-nor-9-carboxy-Δ9-tetrahydrocannabinol in water samples by solid-phase microextraction with on-fiber derivatization and gas chromatography-mass spectrometry. J. Chromatogr. A 1245, 167–174. https://doi.org/10.1016/j.chroma.2012.05.017

Ramirez, K.S., Leff, J.W., Barberán, A., Bates, T.S., Betley, J., Crowther, T.W., Kelly, F.E., Oldfield, E.E., Shaw, E.A., Steenbock, C., Bradford, M.A., Wall, D.H., Fierer, N., 2014. Biogeographic patterns in below-ground diversity in New York City's Central Park are similar to those observed globally. Proc. R. Soc. B Biol. Sci. 281, 20141988. https://doi.org/10.1098/rspb.2014.1988

Rizzo, L., Malato, S., Antakyali, D., Beretsou, V.G., Đolić, M.B., Gernjak, W., Heath, E., Ivancev-Tumbas, I., Karaolia, P., Lado Ribeiro, A.R., Mascolo, G., McArdell, C.S., Schaar, H., Silva, A.M.T., Fatta-Kassinos, D., 2019. Consolidated vs new advanced treatment methods for the removal of contaminants of emerging concern from urban wastewater. Sci. Total Environ. 655,

986–1008. https://doi.org/10.1016/j.scitotenv.2018.11.265

Rodriguez-Narvaez, O.M., Peralta-Hernandez, J.M., Goonetilleke, A., Bandala, E.R., 2017. Treatment technologies for emerging contaminants in water: A review. Chem. Eng. J. 323, 361–380. https://doi.org/10.1016/j.cej.2017.04.106

Rosi-Marshall, E.J., Snow, D., Bartelt-Hunt, S.L., Paspalof, A., Tank, J.L., 2015. A review of ecological effects and environmental fate of illicit drugs in aquatic ecosystems. J. Hazard. Mater. 282, 18–25. https://doi.org/10.1016/j.jhazmat.2014.06.062

Ruttkies, C., Schymanski, E.L., Wolf, S., Hollender, J., Neumann, S., 2016. MetFrag relaunched: Incorporating strategies beyond in silico fragmentation. J. Cheminform. 8, 1–16. https://doi.org/10.1186/s13321-016-0115-9

Saad, M., Tahir, H., Khan, J., Hameed, U., Saud, A., 2017. Synthesis of polyaniline nanoparticles and their application for the removal of Crystal Violet dye by ultrasonicated adsorption process based on Response Surface Methodology. Ultrason. Sonochem. 34, 600–608. https://doi.org/10.1016/j.ultsonch.2016.06.022

Schollée, J.E., Bourgin, M., von Gunten, U., McArdell, C.S., Hollender, J., 2018. Non-target screening to trace ozonation transformation products in a wastewater treatment train including different post-treatments. Water Res. 142, 267–278. https://doi.org/10.1016/j.watres.2018.05.045

Schollée, J.E., Schymanski, E.L., Hollender, J., 2016. Statistical Approaches for LC-HRMS Data to Characterize, Prioritize, and Identify Transformation Products from Water Treatment Processes, in: ACS Symposium Series. pp. 45–65. https://doi.org/10.1021/bk-2016-1241.ch004

Schollée, J.E., Schymanski, E.L., Stravs, M.A., Gulde, R., Thomaidis, N.S., Hollender, J., 2017. Similarity of High-Resolution Tandem Mass Spectrometry Spectra of Structurally Related Micropollutants and Transformation Products. J. Am. Soc. Mass Spectrom. Soc. Mass Spectrom. 28, 2692–2704. https://doi.org/10.1007/s13361-017-1797-6

Schymanski, E.L., Avak, S.E., Loos, M., Hollender, J., 2015. Prioritizing Unknown Transformation Products from Biologically- Treated Wastewater Using High-Resolution Mass Spectrometry, Multivariate Statistics, and Metabolic Logic. Anal. Chem. 87, 12121–12129. https://doi.org/10.1021/acs.analchem.5b02905

Schymanski, E.L., Jeon, J., Gulde, R., Fenner, K., Ruff, M., Singer, H.P., Hollender, J., 2014. Identifying small molecules via high resolution mass spectrometry: Communicating confidence. Environ. Sci. Technol. 48, 2097–2098. https://doi.org/10.1021/es5002105

Senta, I., Krizman, I., Ahel, M., Terzic, S., 2013. Integrated procedure for multiresidue analysis of dissolved and particulate drugs in municipal wastewater by liquid chromatography-tandem mass spectrometry. Anal. Bioanal. Chem. 405, 3255–3268. https://doi.org/10.1007/s00216-013-6720-9

Shanavas, S., Salahuddin Kunju, A., Varghese, H.T., Yohannan Panicker, C., 2011. Comparison of Langmuir and Harkins-Jura Adsorption Isotherms for the Determination of Surface Area of Solids. Orient. J. Chem. 27, 245–252.

Shchegolkova, N.M., Krasnov, G.S., Belova, A.A., Dmitriev, A.A., Kharitonov, S.L., Klimina, K.M.,

Melnikova, N. V., Kudryavtseva, A. V., 2016. Microbial community structure of activated sludge in treatment plants with different wastewater compositions. Front. Microbiol. 7, 1–15. https://doi.org/10.3389/fmicb.2016.00090

Singhal, N., Perez-Garcia, O., 2016. Degrading Organic Micropollutants: The Next Challenge in the Evolution of Biological Wastewater Treatment Processes. Front. Environ. Sci. 4, 1–5. https://doi.org/10.3389/fenvs.2016.00036

Skolnik, M.I., 2009. Introduction To Second Edition. New York 1081, 1–590. https://doi.org/10.1017/CBO9780511608117.001

Smith, J.W.N., Beuthe, B., Dunk, M., Demeure, S., Carmona, J.M.M., Medve, A., Spence, M.J., Pancras, T., Schrauwen, G., Held, T., Baker, K., Ross, I., Slenders, H., 2016. Environmental fate and effects of polyand perfluoroalkyl substances (PFAS). CONCAWE Reports 1–107.

Sousa, J.C.G., Ribeiro, A.R., Barbosa, M.O., Pereira, M.F.R., Silva, A.M.T., 2017. A review on environmental monitoring of water organic pollutants identified by EU guidelines. J. Hazard. Mater. 344, 146–162. https://doi.org/10.1016/j.jhazmat.2017.09.058

Spataro, F., Ademollo, N., Pescatore, T., Rauseo, J., Patrolecco, L., 2019. Antibiotic residues and endocrine disrupting compounds in municipal wastewater treatment plants in Rome, Italy. Microchem. J. 148, 634–642. https://doi.org/10.1016/j.microc.2019.05.053

Stadler, L.B., Love, N.G., 2019. Oxygen Half-Saturation Constants for Pharmaceuticals in Activated Sludge and Microbial Community Activity under Varied Oxygen Levels. Environ. Sci. Technol. 53, 1918–1927. https://doi.org/10.1021/acs.est.8b06051

Stasinakis, A.S., Thomaidis, N.S., Arvaniti, O.S., Asimakopoulos, A.G., Samaras, V.G., Ajibola, A., Mamais, D., Lekkas, T.D., 2013. Contribution of primary and secondary treatment on the removal of benzothiazoles, benzotriazoles, endocrine disruptors, pharmaceuticals and perfluorinated compounds in a sewage treatment plant. Sci. Total Environ. 463–464, 1067–1075. https://doi.org/10.1016/j.scitotenv.2013.06.087

Stevens-Garmon, J., Drewes, J.E., Khan, S.J., McDonald, J.A., Dickenson, E.R. V, 2011. Sorption of emerging trace organic compounds onto wastewater sludge solids. Water Res. 45, 3417–3426. https://doi.org/10.1016/j.watres.2011.03.056

Stoll, V.S., Blanchard, J.S., 1990. [4] Buffers: principles and practice. Methods Enzymol. 182, 24–38. https://doi.org/10.1016/0076-6879(90)82006-N

Subedi, B., Kannan, K., 2014. Mass loading and removal of select illicit drugs in two wastewater treatment plants in New York State and estimation of illicit drug usage in communities through wastewater analysis. Environ. Sci. Technol. 48, 6661–6670. https://doi.org/10.1021/es501709a

Teodosiu, C., Gilca, A.F., Barjoveanu, G., Fiore, S., 2018. Emerging pollutants removal through advanced drinking water treatment: A review on processes and environmental performances assessment. J. Clean. Prod. 197, 1210–1221. https://doi.org/10.1016/j.jclepro.2018.06.247

The European Parlament and the Council of the European Union, 2018a. Proposal for regulation of the the european parliament and of the councilon minimum requirements for water reuse. Eur.

Comm. 0169.

The European Parlament and the Council of the European Union, 2018b. Proposal for a DIRECTIVE OF THE EUROPEAN PARLIAMENT AND OF THE COUNCIL on the quality of water intended for human consumption (recast) 0332.

The European Parlament and the Council of the European Union, 2013. Directives 2013/39/EU as regards priority substances in the field of water policy. Off. J. Eur. Union 2013, 1–17. https://doi.org/http://eur-lex.europa.eu/legal-content/EN/TXT/?uri=celex:32013L0039

The European Parliament, 2008. Directive 2008/105/Ce. Off. J. Eur. Union 84–97.

Thomaidi, V.S., Stasinakis, A.S., Borova, V.L., Thomaidis, N.S., 2016. Assessing the risk associated with the presence of emerging organic contaminants in sludge-amended soil: A country-level analysis. Sci. Total Environ. 548–549, 280–288. https://doi.org/10.1016/j.scitotenv.2016.01.043

Tiwari, B., Sellamuthu, B., Ouarda, Y., Drogui, P., Tyagi, R.D., Buelna, G., 2017. Review on fate and mechanism of removal of pharmaceutical pollutants from wastewater using biological approach. Bioresour. Technol. 224, 1–12. https://doi.org/10.1016/j.biortech.2016.11.042

Tjanowiczro, M., Bojanowska-Czajka, A., Bartosiewicz, I., Kulisa, K., 2018. Advanced Oxidation/Reduction Processes treatment for aqueous perfluorooctanoate (PFOA) and perfluorooctanesulfonate (PFOS) – A review of recent advances. Chem. Eng. J. 336, 170–199. https://doi.org/10.1016/j.cej.2017.10.153

Tran, N.H., Gin, K.Y.H., 2017. Occurrence and removal of pharmaceuticals, hormones, personal care products, and endocrine disrupters in a full-scale water reclamation plant. Sci. Total Environ. 599–600, 1503–1516. https://doi.org/10.1016/j.scitotenv.2017.05.097

Tran, N.H., Reinhard, M., Gin, K.Y.H., 2018. Occurrence and fate of emerging contaminants in municipal wastewater treatment plants from different geographical regions-a review. Water Res. 133, 182–207. https://doi.org/10.1016/j.watres.2017.12.029

Tran, N.H., Urase, T., Ngo, H.H., Hu, J., Ong, S.L., 2013. Insight into metabolic and cometabolic activities of autotrophic and heterotrophic microorganisms in the biodegradation of emerging trace organic contaminants. Bioresour. Technol. 146, 721–731. https://doi.org/10.1016/j.biortech.2013.07.083

Trapido, M., Epold, I., Bolobajev, J., Dulova, N., 2014. Emerging micropollutants in water/wastewater: growing demand on removal technologies. Environ. Sci. Pollut. Res. 12217–12222. https://doi.org/10.1007/s11356-014-3020-7

U.S. Environmental Protection Agency, 2009. U.S. EPA. “Method 538: Determination of Selected Organic Contaminants in Drinking Water by Direct Aqueous Injection-Liquid Chromatography/Tandem Mass Spectrometry (DAI-LC/MS/MS),” Revision 1.0.

United Nations, 2006. Risk Profile of Perfluorooctane sulfonate. Rev. Lit. Arts Am. 34.

van der Hoek, C., Bannink, A., Tineke, S., 2015. An update of the lists with compounds that are relevant for the drinking water production from the river Meuse - 2015 1–63.

Vanderford, B.J., Pearson, R.A., Rexing, D.J., Snyder, S.A., 2003. Analysis of Endocrine Disruptors,

Pharmaceuticals, and Personal Care Products in Water Using Liquid Chromatography/Tandem Mass Spectrometry. Anal. Chem. 75, 6265–6274. https://doi.org/10.1021/ac034210g

Vilardi, G., Di Palma, L., Verdone, N., 2017. Heavy metals adsorption by banana peels micro-powder. Equilibrium modeling by non-linear models. Chinese J. Chem. Eng. https://doi.org/10.1016/j.cjche.2017.06.026

Wei, C., Song, X., Wang, Q., Hu, Z., 2017. Sorption kinetics, isotherms and mechanisms of PFOS on soils with different physicochemical properties. Ecotoxicol. Environ. Saf. 142, 40–50. https://doi.org/10.1016/j.ecoenv.2017.03.040

White, S.S., Fenton, S.E., Hines, E.P., 2011. Endocrine disrupting properties of perfluorooctanoic acid. J. Steroid Biochem. Mol. Biol. 127, 16–26. https://doi.org/10.1016/j.jsbmb.2011.03.011

Wickham, H., 2016. ggplot2: Elegant Graphics for Data Analysis. Springer-Verlag New York.

Williams, A.J., Grulke, C.M., Edwards, J., McEachran, A.D., Mansouri, K., Baker, N.C., Patlewicz, G., Shah, I., Wambaugh, J.F., Judson, R.S., Richard, A.M., 2017. The CompTox Chemistry Dashboard: A community data resource for environmental chemistry. J. Cheminform. 9, 1–27. https://doi.org/10.1186/s13321-017-0247-6

Xiao, F., 2017. Emerging poly- and perfluoroalkyl substances in the aquatic environment: A review of current literature. Water Res. 124, 482–495. https://doi.org/10.1016/j.watres.2017.07.024

Xu, S., Yao, J., Ainiwaer, M., Hong, Y., Zhang, Y., 2018. Analysis of Bacterial Community Structure of Activated Sludge from Wastewater Treatment Plants in Winter. Biomed Res. Int. 2018, 1–8. https://doi.org/10.1155/2018/8278970

Yadav, M.K., Short, M.D., Gerber, C., Awad, J., van den Akker, B., Saint, C.P., 2019. Removal of emerging drugs of addiction by wastewater treatment and water recycling processes and impacts on effluent-associated environmental risk. Sci. Total Environ. 680, 13–22. https://doi.org/10.1016/j.scitotenv.2019.05.068

Ying, Z., Droste, R.L., 2015. Sorption of microconstituents onto primary sludge. Water Sci. Technol. 72, 779–784. https://doi.org/10.2166/wst.2015.270

Yu, J., Hu, J., Tanaka, S., Fujii, S., 2009. Perfluorooctane sulfonate (PFOS) and perfluorooctanoic acid (PFOA) in sewage treatment plants. Water Res. 43, 2399–2408. https://doi.org/10.1016/j.watres.2009.03.009

Zareitalabad, P., Siemens, J., Hamer, M., Amelung, W., 2013. Perfluorooctanoic acid (PFOA) and perfluorooctanesulfonic acid (PFOS) in surface waters, sediments, soils and wastewater - A review on concentrations and distribution coefficients. Chemosphere 91, 725–732. https://doi.org/10.1016/j.chemosphere.2013.02.024

Zearley, T.L., Summers, R.S., 2012. Removal of trace organic micropollutants by drinking water biological filters. Environ. Sci. Technol. 46, 9412–9419. https://doi.org/10.1021/es301428e

Zhang, B., Xu, X., Zhu, L., 2018. Activated sludge bacterial communities of typical wastewater treatment plants: distinct genera identification and metabolic potential differential analysis. AMB Express 8. https://doi.org/10.1186/s13568-018-0714-0

Zhang, B., Xu, X., Zhu, L., 2017. Structure and function of the microbial consortia of activated sludge in typical municipal wastewater treatment plants in winter. Sci. Rep. 7, 1–11. https://doi.org/10.1038/s41598-017-17743-x

Zhang, C., Yan, H., Li, F., Hu, X., Zhou, Q., 2013. Sorption of short- and long-chain perfluoroalkyl surfactants on sewage sludges. J. Hazard. Mater. 260, 689–699. https://doi.org/10.1016/j.jhazmat.2013.06.022

Zhang, W., Zhang, Y., Taniyasu, S., Yeung, L.W.Y., Lam, P.K.S., Wang, J., Li, X., Yamashita, N., Dai, J., 2013. Distribution and fate of perfluoroalkyl substances in municipal wastewater treatment plants in economically developed areas of China. Environ. Pollut. 176, 10–17. https://doi.org/10.1016/j.envpol.2012.12.019

Zhou, Q., Deng, S., Zhang, Q., Fan, Q., Huang, J., Yu, G., 2010. Sorption of perfluorooctane sulfonate and perfluorooctanoate on activated sludge. Chemosphere 81, 453–458. https://doi.org/10.1016/j.chemosphere.2010.08.009

Zuccato, E., Castiglioni, S., 2009. Illicit drugs in the environment. Philos. Trans. R. Soc. A Math. Phys. Eng. Sci. 367, 3965–3978. https://doi.org/10.1098/rsta.2009.0107

Zuccato, E., Castiglioni, S., Fanelli, R., 2005. Identification of the pharmaceuticals for human use contaminating the Italian aquatic environment. J. Hazard. Mater. 122, 205–209. https://doi.org/10.1016/j.jhazmat.2005.03.001

Supplementary materials

1.10 Removal processes at laboratory scale - Batch tests

1.10.1 Methamphetamine

Figure S.M. 1 Batch tests at blank condition (MET concentration equal to 0 ng/L). Time-profiles of (a) COD removal efficiency and (b) ammonia, nitrate and nitrite concentrations (error bar indicate the standard deviation)

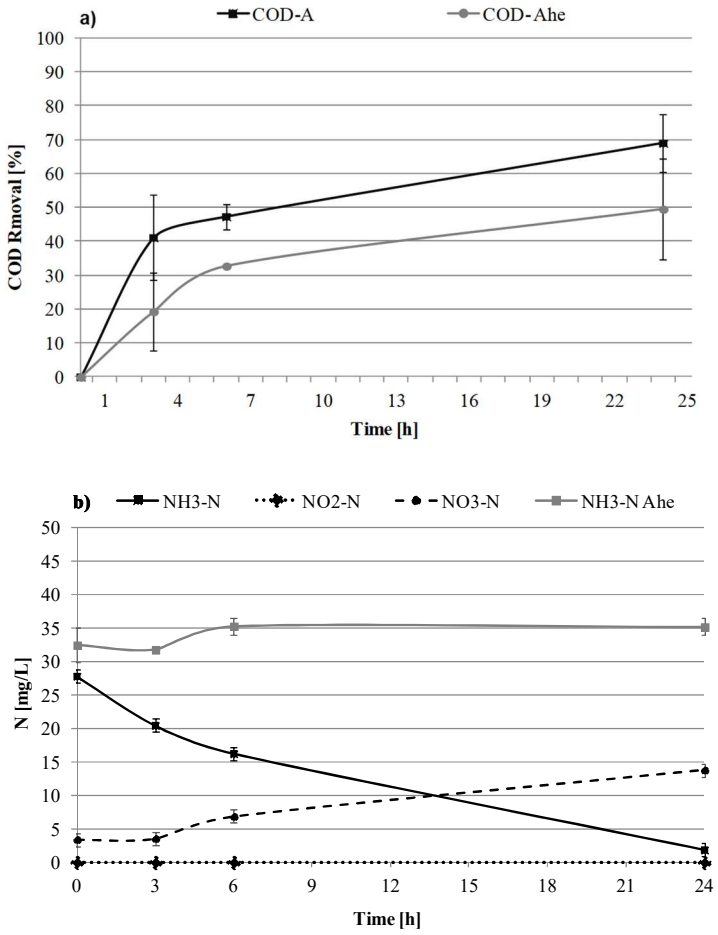

1.10.2 11-nor-9carboxy-Δ9-THC and benzoylecgonine

Table S.M. 1 UPLC-MS/MS applied parameters: DP= declustering potential; EP= entrance potential; CE= collision energy; CXP= collision cell exit potential

Compound	Q1 mass dalton	Q3 mass dalton	RT min	DP volts	EP volts	CE volts	CXP volts
benzoylecgonine-1	290.1	168.2	4.5	30	10	25	12
benzoylecgonine-2	290.1	105	4.5	30	10	41	12
11nor9carboxydelta9 THC-1	343.2	299.2	6.2	-30	-10	-29	-12
11nor9carboxydelta9 THC-2	343.2	245.1	6.2	-30	-10	-37	-12

Figure S.M. 2 Chromatograms of the standard solutions injected to create the calibration curve of THC-COOH: in grey the area of the second ion transition

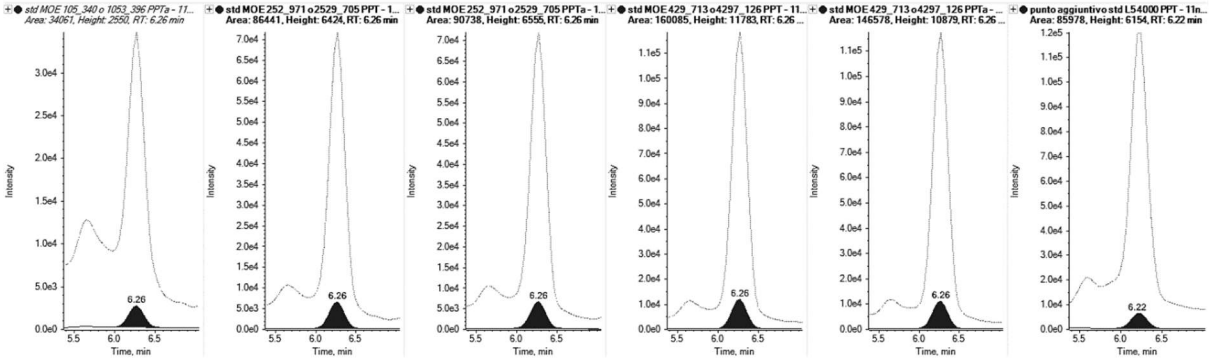

Figure S.M. 3 Time-profiles of BE removal efficiency in the liquid phase during the Heterotrophic biological tests (error bars indicate the SDR%)

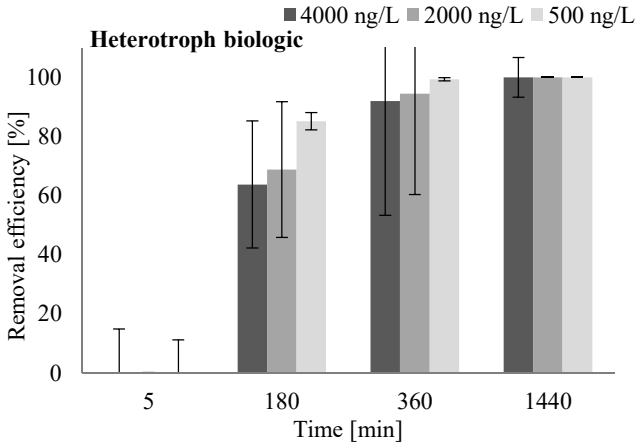

Figure S.M. 4 Time-profiles of THC-COOH removal efficiency in the liquid phase during the Heterotrophic biological tests (error bars indicate the SDR%)

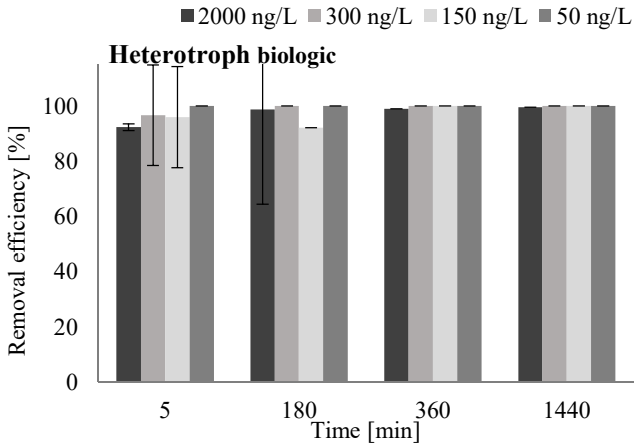

.

1.10.3 Perfluorooctane sulfonic acid and perfluorooctanoic acid

Table S.M. 2 HPLC-MS/MS applied parameters: DP= declustering potential; EP= entrance potential; CE= collision energy; CXP= collision cell exit potential

Compound	Q1 mass	Q3 mass	RT	DP	EP	CE	CXP
	dalton	dalton	min	volts	volts	volts	volts
perfluorooctane sulfonic acid-1	498.8	98.9	11	-60	-4.5	-122	-10
perfluorooctane sulfonic acid-2	498.8	79.8	11	-60	-4.5	-98	-10
perfluorooctanoic acid-1	412.8	368.9	9.5	-5	-4.5	-14	-10
perfluorooctanoic acid-2	412.8	168.7	9.5	-5	-4.5	-24	-10
perfluorooctane sulfonic acid (13C8)-1	507	79.9	7.20	-40	-10	-100	-4
perfluorooctane sulfonic acid (13C8)-2	507	98.9	7.20	-40	-10	-100	-4

Table S.M. 3 Results of the application of the kinetics models to the Activated sludge tests of PFOA and PFOS

		Unit	PFOA				PFOS				
	C_o	ng/L	200	500	1000	4000	200	500	1000	4000	
	q_{e-exp}	ng/g	49.04	143.33	265.41	1150.86	54.76	181.50	384.27	1636.88	
	k_d	L/kg	344.71	465.72	401.82	431.02	946.64	1946.23	3143.71	4681.54	
Zero	R^2		0.81	0.63	0.75	0.81	0.39	0.74	0.92	0.82	
	k_0	ng/L·h	2.78	5.04	13.97	47.98	0.12	1.20	1.57	6.81	
First	R^2		0.86	0.73	0.85	0.90	0.40	0.77	0.95	0.91	
	k_1	1/h	0.03	0.02	0.03	0.03	0.00	0.01	0.01	0.03	
Second	R^2		0.91	0.82	0.93	0.96	0.41	0.77	0.97	0.97	
	k_2	L/ng·h	0.00	0.00	0.00	0.00	0.00	0.00	0.00	0.00	
Saturation	R^2		1.00	1.00	1.00	1.00	1.00	1.00	1.00	1.00	
	k_s	ng/L·h	-1.85	-11.19	-16.92	-68.06	0.33	-5.05	-6.97	-82.13	
	K_a	ng/L	-176.43	-407.72	-896.47	-3257.53	-123.1	-254.83	-433.11	-1487.73	
Pseudo-first	R^2		0.88	0.59	0.92	0.95	0.32	0.32	0.88	0.84	
	k_1'	1/h	0.08	0.07	0.08	0.08	-0.06	0.02	0.18	0.18	
	$q_{e, calc}$	ng/g	4.63	5.71	9.55	16.90	0.86	2.87	6.59	12.17	
Pseudo-second	R^2		0.98	1.00	0.99	1.00	1.00	1.00	1.00	1.00	
	k_2'	g/ng·h	0.01	0.01	0.003	0.001	0.23	0.03	0.03	0.01	
	$q_{e, calc}$	ng/g	52.04	145.91	275.43	1215.52	54.89	182.28	385.34	1640.86	
IDM	R^2		0.91	0.84	0.91	0.92	0.18	0.76	0.64	0.62	
	k_{id}	$ng/g \cdot h^{0.5}$	6.69	13.57	39.99	146.41	0.18	2.85	18.74	80.69	
	C	ng/g	17.32	82.49	85.72	521.76	53.44	166.81	310.79	1323.10	
Elovich	R^2		0.73	0.96	0.98	0.97	0.00	0.63	0.96	0.96	
	a	ng/g·h	5872.58	450025.77	7515.33	212987.8	0.00	1.56E+42	3.98E+10	1.08E+11	
	b	g/ng	0.24	0.10	0.03	0.01	-8067	0.56	0.06	0.01	

Table S.M. 4 Results of the application of the adsorption isotherm models to the Sterilized sludge tests of PFOA and PFOS

		Unit	PFOA	PFOS
Freundlich	R^2		0.73	0.99
	1/n		1.63	1.02
	K_F	ng/g	0.01	5.66
Langmuir	R^2		0.64	0.99
	K_L	L/ng	-1586.82	-74507.30
	Qo	ng/g	-704.73	-470814.24
BET	R^2		0.01	0.83
	C_{BET}	L/ng	1.00	1.00
	q_s	ng/g	338.45	6364.29
DRK	R^2		0.62	0.96
	q_s	ng/g	2481.72	2788.87
	K_{ad}	mol^2/kJ^2	0.40	0.06
Tempkin	R^2		0.63	0.96
	b_T		0.40	0.44
	A_T	L/g	0.00	0.02
Harkins-Jura	R^2		0.66	0.95
	A	ng^2/g^2	18616.52	191197.02
	B		2.91	2.44

1.11 Removal processes at laboratory scale - Continuous feeding tests

Table S.M. 5 Validation parameters of the analytical method for OMPs detection

Compound	R^2	REC Deionized water [%]	REC SyWW [%]	LOD [mg/L]	LOQ [%]	Repeatability [%]
CBZ	0.9969	130	123	0.0007	0.0015	1.1
LNC	0.9835	84	69	0.0002	0.0004	3.2
SLD	0.9745	23	23	0.0041	0.0083	20.6
SMX	0.9970	85	90	0.0019	0.0038	6.3
NPX	0.9940	54	60	0.0143	0.0285	13.2
SCL	0.9798	34	30	0.0183	0.0366	14.2
ATZ	0.9626	174	173	0.0003	0.0005	1.7
PYZ	0.9863	11	12	0.0015	0.0030	35.8

Table S.M. 6 Target oxidoreductases and dyes used to detect their activity in respective buffers

Target enzyme	Enzyme substrate (Dye)	Solution buffer
Lignin peroxidase (LiP)	Methylene Blue	acetate buffer
	Azure B	acetate buffer
Horseradish peroxidase (HRP)	L-DOPA	acetate buffer
	ABTS	acetate buffer
Laccase (Lac)	Sudan Orange	acetate buffer
	ABTS	acetate buffer
β-glucosidase (β-glu)	pNP-A	acetate buffer
	pNP-G	acetate buffer
Cytochrome P450 (Cyp450)	pNP-12	phosphate buffer
	Indole	phosphate buffer
	4-AAP	phosphate buffer

Figure S.M. 5 Time profiles of OMPs concentration in each test (error bars indicate the standard deviation of two replicates). (■ Constant, ■ f = 0.6, ■ f = 0.9, ■ f = 1.8)

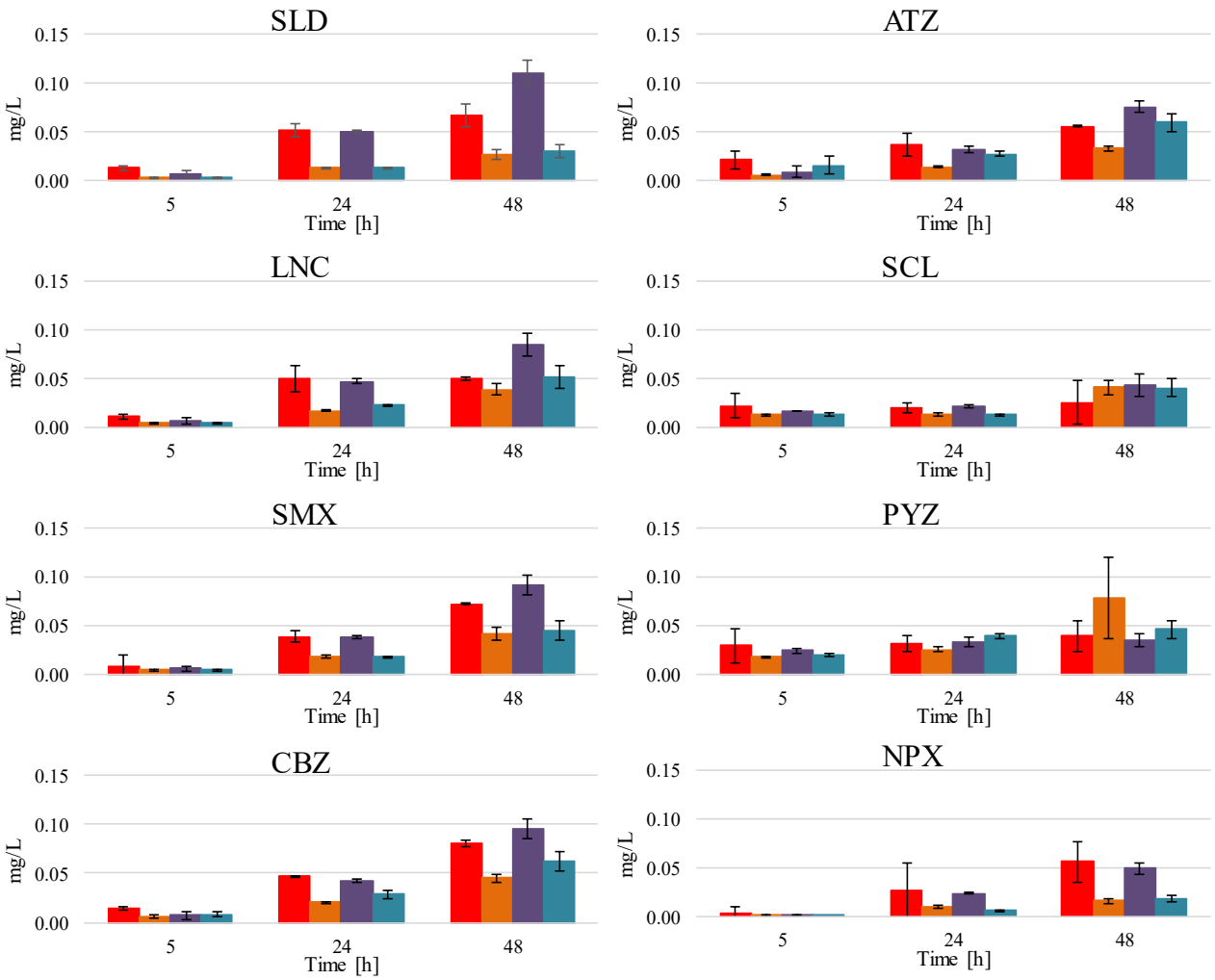

Figure S.M. 6 Time profiles of the target enzymes activity in each test (C, E1, E2, E3) (error bars indicate the standard deviation of two replicates)

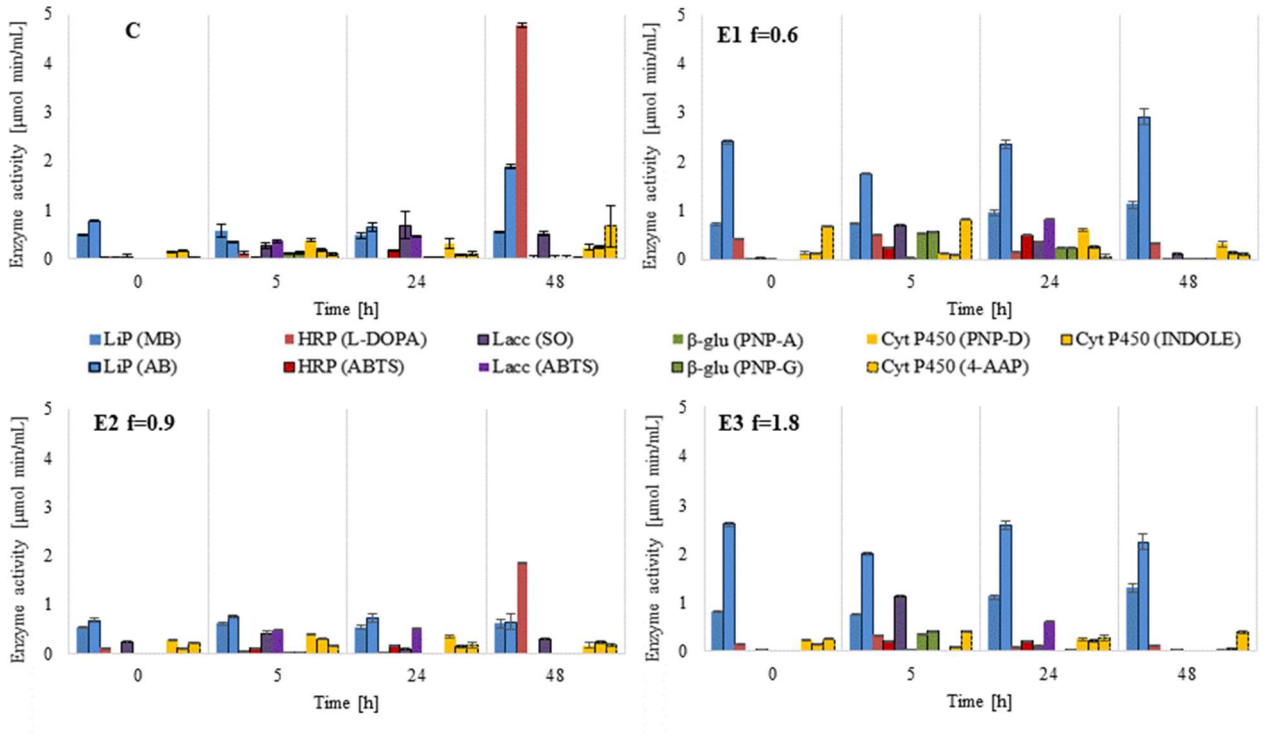

1.13 Removal processes at real scale – WWTPs

Table S.M. 7 UPLC-MS/MS applied parameters: MRL= minimum reporting level; RT= retention time; DP= declustering potential; EP= entrance potential; CE= collision energy; CXP= collision cell exit potential

Compound	MRL µg/L	Q1 mass dalton	Q3 mass dalton	RT min	DP volts	EP volts	CE volts	CXP volts
11nor9carboxydelta9 THC-1	0.025	343.2	299.2	6.2	-30	-10	-29	-12
11nor9carboxydelta9 THC-2		343.2	245.1	6.2	-30	-10	-37	-12
amphetamine-2	0.02	136.2	119.1	3.5	20	9	10	30
benzoylecgonine-1	0.01	290.1	168.2	4.5	30	10	25	12
benzoylecgonine-2	0.01	290.1	105	4.5	30	10	41	12
methamphetamine-1	0.01	150.3	91.2	3.8	30	10	24	12
methamphetamine-2	0.01	150.3	119.1	3.8	30	10	11	12
17a ethynylestradiol-1	0.02	297.2	107.1	5.6	30	10	22	12
17a ethynylestradiol-2	0.02	297.2	159.1	5.6	30	10	22	12
17b estradiol-1	0.01	273.2	107	5.6	30	10	29	12
17b estradiol-2	0.01	273.2	159.2	5.6	30	10	20	12
estrone-1	0.01	271.2	133.1	5.9	120	10	47	13
estrone-2	0.01	271.2	157	5.9	120	10	47	13
carbamazepine-1	0.01	237.1	194.2	5.4	80	10	20	4
carbamazepine-2	0.01	237.1	193.1	5.4	80	10	50	4
progesterone-1	0.01	315.2	109.1	6.6	80	10	35	4
progesterone-2	0.01	315.2	97.1	6.6	80	10	35	4
ketoprofen-1	0.05	255.1	105.1	5.6	86	7	35	8
ketoprofen-2	0.05	255.1	209.2	5.6	86	7	22	5
lincomycin hydrochloride-1	0.01	407.4	126.1	3.7	32	10	29	4
lincomycin hydrochloride-2	0.01	407.4	359.2	3.7	93	10	27	4
sulfamethoxazole-1	0.01	254.1	156.1	4.5	85	8	23	7
sulfamethoxazole-2	0.01	254.1	92.1	4.5	85	8	40	7
trimethoprim-1	0.01	291.1	230.2	4.1	80	10	35	4
trimethoprim-2	0.01	291.1	261.2	4.1	120	10	47	13

Table S.M. 8 Main lay-out and sampling days of each WWTP

Abbreviations:

ST Secondary treatment	SP Primary settler	UV Ultraviolet disinfection
	OS Oxidation tank	FG Filtration
PT Primary treatment	DE Denitrification tank	MF Microfiltration
TT Tertiary treatment	SS Secondary settler	UF Ultrafiltration
	MBBR Moving Bed Biological Reactor	FA Filter oxidation tank
	MBR Membrane Biological Reactor	PF Chemical phosphorous removal
	DC Chlorination	MIX Combined disinfection systems
	DP Peracetic acid disinfection	

Code	Treatment class	Treatments	N. Sampling days
1	ST+TT	OS+DE+SS+MF+DC	1
2	ST+TT	MBBR+DE+SS+FG+MF	3
3	ST+TT	OS+SS+MF+DC	1
4	ST	OS+DE+SS+DC	1
5	ST+TT	OS+DE+SS+FG+MF+DP	1
6	ST+TT	OS+DE+SS+FG+MF+DC	1
7	ST+TT	OS+SS+DE+DC+FA	1
8	PT+ST+TT	SP+OS+SS+DE+FGDC	1
9	ST+TT	MBR+UF	1
10	PT+ST+TT	SP+OS+DE+SS+FG+DC	2
11	ST	OS+DE+SS+DC	2
12	ST+TT	OS+DE+SS+MF+DC	1
13	ST+TT	OS+DE+SS+MF+UV	1
14	PT+ST	PT+OS+SS+DC	1
15	ST	OS+DE+SS+DP	1
16	ST+TT	OS+DE+SS+FG+MIX	2
17	ST+TT	OS+DE+SS+MF+UV	1
18	ST+TT	OS+DE+SS+FG+DC	1
19	ST	OS+SS+DC	3
20	ST+TT	OS+DE+SS+MF+DC	1
21	ST+TT	OS+DE+SS+FG+DP	1
22	ST	OS+SS+DC	1
23	ST+TT	OS+DE+SS+FG+FG+DP	1
24	ST+TT	OS+SS+FA+DP	2
25	PT+ST	SP+OS+DE+SS+DP	4
26	ST+TT	OS+DE+SS+FG+DC	2
27	ST+TT	OS+DE+SS+FG+MIX	2
28	ST	OS+DE+SS+DP	1
29	ST	OS+SS	2
30	ST+TT	OS+DE+SS+FG+MIX	1
31	ST	OS+DE+SS+DP	1
32	ST+TT	OS+DE+SS+DC+MF	1
33	ST+TT	OS+DE+SS+FG+FA	1

34	ST	OS+DE+SS+DC	1
35	ST	OS+SS+DC	1
36	ST+TT	OS+DE+SS+FG+MIX	1
37	ST	OS+SS+DE+DP	3
38	ST+TT	OS+DE+SS+FG+FG+MIX	3
39	ST+TT	OS+DE+SS+FA+DC	1
40	ST+TT	OS+DE+SS+FG+DC	1
41	ST+TT	OS+DE+SS+FG+FG+DP	1
42	ST	OS+SS+DP	1
43	ST	OS+SS+DC	1
44	PT+ST	SP+OS+DE+SS+DP	8
45	ST+TT	OS+SS+MF+DP	1
46	ST	OS+DE+SS+DC	1
47	ST+TT	OS+DE+SS+FG+FG+DP	2
48	ST+TT	OS+SS+FT+DP	1
49	ST	OS+SS+DE+DP	2
50	ST	OS+DE+SS+DC	5
51	ST	OS+DE+SS+DC	2
52	PT+ST	SP+OS+SS+DC	7
53	PT+ST	SP+OS+DE+SS+DP	4
54	PT+ST	SP+BIOFILTRI+SS	3
55	ST+TT	OS+DE+SS+MF+DP	1
56	ST	MBBR+DE+SS+DC	1
57	ST+TT	OS+SS+FT+DC	1
58	ST+TT	OS+SS+FG+MF+DC	1
59	ST+TT	OS+SS+DE+MF+DP	1
60	ST	OS+DE+SS+DC	1
61	ST	OS+SS+DE+DP	1
62	ST+TT	OS+DE+SS+MF+UV	1
63	ST	OS+DE+SS+DC	1
64	ST	OS+DE+SS+DC	1
65	ST+TT	OS+DE+SS+MF+DP	3
66	ST+TT	OS+DE+SS+FG+DP	1
67	ST+TT	OS+SS+MF+DP	1
68	ST	OS+SS+DC	3
69	ST+TT	OS+DE+SS+FG+DC	1
70	ST	OS+DE+SS+DC	1
71	ST	OS+SS	1
72	ST+TT	OS+DE+SS+FG+MF+DC	1
73	ST	OS+SS+DC	1
74	ST	OS+SS+DC	1
75	ST	OS+DE+SS+DC	1
76	ST+TT	OS+SS+MF+DC	1

1.15 Removal processes at real scale – DWTPs

Table S.M. 9 Characteristics of the selected RSFs

Name	Source water	Treatment plant configuration
1.	Bethune polder + Amsterdam Rhine Canal	$FeCl_3$, ***RSF***, O_3, SOF, GAC, SSF
2.	Lateraalkanaal (river Meuse)	RBF, CA, ***RSF***, GAC, UVDES
3.	Lievekanaal	Reservoir, NITFI, FLOT, ***RSF***, O_3, GAC
4.	Lake IJssel	DS, FS, ***RSF***, partial stream GAC
5.	Lek river	FFS ($FeCl_3$) – ***RSF*** – DINF – CA –RSF – O_3 – SOF – GAC - SSF
6.	Meuse river	$FeSO_4$ dosing, $FeCl_3$ dosing, ***RSF***, DINF, SOF, PAC, CA, SSF, RSF
7.	Meuse river	Reservoirs, chlorination/H_2SO_4, $FeCl_3$ dosing, $FeCl_3$/NaOH dosing, **RSF**, UV-GAC

FFS = Floc Formation and Sedimentation, RSF = rapid sand filtration (or dual media filtration), DINF = Dune Infiltration, CA = cascade aeration, O3 = ozone, SOF = softening, GAC = Granular Activated Carbon, SSF = Slow Sand Filtration, PAC = Powdered Activated Carbon, DS = Drum Sieves, FS = Flocculation/Sedimentation, NF = Nano Filtration, UF = Ultra Filtration, RBF = River Bank Filtration, UVDES = UV desinfection, NITFI = Nitrification, FLOT = Flotation

Table S.M. 10 Summary of data processing parameters and Compound Discoverer 3.0

Select Spectra

1. General Settings:

- Precursor Selection: Use MS (n - 1) Precursor
- Use Isotope Pattern in Precursor Reevaluation: True
- Provide Profile Spectra: Automatic
- Store Chromatograms: False

2. Spectrum Properties Filter:

- Lower RT Limit: 2.3
- Upper RT Limit: 27
- First Scan: 0
- Last Scan: 0
- Ignore Specified Scans: (not Specified)
- Lowest Charge State: 0
- Highest Charge State: 0
- Min. Precursor Mass: 100 Da
- Max. Precursor Mass: 5000 Da
- Total Intensity Threshold: 0
- Minimum Peak Count: 1

3. Scan Event Filters:

- Mass Analyzer: (not Specified)
- MS Order: Any
- Activation Type: (not Specified)
- Min. Collision Energy: 0
- Max. Collision Energy: 1000
- Scan Type: Any
- Polarity Mode: (not Specified)

4. Peak Filters:

- S/N Threshold (FT-only): 1.5

5. Replacements for Unrecognized Properties:

- Unrecognized Charge Replacements: 1
- Unrecognized Mass Analyzer Replacements: ITMS
- Unrecognized MS Order Replacements: MS2
- Unrecognized Activation Type Replacements: CID
- Unrecognized Polarity Replacements: +
- Unrecognized MS Resolution@200 Replacements: 60000
- Unrecognized MSn Resolution@200 Replacements: 30000

Detect Compounds

1. General Settings:

- Mass Tolerance [ppm]: 5 ppm
- Intensity Tolerance [%]: 30
- S/N Threshold: 3
- Min. Peak Intensity: 50000
- Ions:

[M+2H]+2

[M+ACN+H]+1

[M+Cl]-1

[M+H]+1

[M+H+MeOH]+1

[M+H-H2O]+1

[M+K]+1

[M+Na]+1

[M+NH4]+1

[M-H]-1

- Base Ions: [M+H]+1; [M-H]-1
- Min. Element Counts: C H
- Max. Element Counts: C90 H190 BR3 CL4 F6 K2 N10 NA2 O18 P3 S5

2. Peak Detection:

- Filter Peaks: True
- Max. Peak Width [min]: 0.8
- Remove Singlets: False
- Min. # Scans per Peak: 3
- Min. # Isotopes: 1

Group Compounds

1. Compound Consolidation:

- Mass Tolerance: 5 ppm
- RT Tolerance [min]: 0.1

2. Fragment Data Selection:

- Preferred Ions: [M+H]+1; [M-H]-1

Search mzCloud

1. Search Settings:

- compound Classes: all
- Match Ion Activation Type: True
- Match Ion Activation Energy: Match with Tolerance
- Ion Activation Energy Tolerance: 20

- Apply Intensity Threshold: True
- Precursor Mass Tolerance: 10 ppm
- FT Fragment Mass Tolerance: 10 ppm
- IT Fragment Mass Tolerance: 0.4 Da
- Identity Search: HighChem DP
- Similarity Search: Similarity Forward
- Library: Reference
- Post Processing: Recalibrated
- Match Factor Threshold: 50
- Max. # Results: 20

Assign Compound Annotations

1. General Settings:

- Mass Tolerance: 3 ppm

2. Data Sources:

- Data Source #1: MassList Search
- Data Source #2: mzCloud Search
- Data Source #3: ChemSpider Search
- Data Source #4: Predicted Compositions
- Data Source #5: (not specified)

Search ChemSpider

1. Search Settings:

- Database(s):

EAWAG Biocatalysis/Biodegradation Database

EPA DSSTox

EPA Toxcast

- Search Mode: By Formula or Mass
- Mass Tolerance: 3 ppm
- Max. # of results per compound: 20
- Max. # of Predicted Compositions to be searched per Compound: 3
- Result Order (for Max. # of results per compound): Order By Reference Count (DESC)

2. Predicted Composition Annotation:

- Check All Predicted Compositions: True

Apply mzLogic

1. Search Settings:

- FT Fragment Mass Tolerance: 10 ppm
- IT Fragment Mass Tolerance: 0.4 Da
- Max. # Compounds: 0
- Max. # mzCloud Similarity Results to consider per Compound: 10

- Match Factor Threshold: 30

Predict Compositions

1. Prediction Settings:

- Mass Tolerance: 3 ppm
- Min. Element Counts: C H
- Max. Element Counts: C90 H190 BR3 CL8 F18 N10 O18 P3 S5
- Min. RDBE: 0
- Max. RDBE: 40
- Min. H/C: 0.1
- Max. H/C: 3.5
- Max. # Candidates: 10
- Max. # Internal Candidates: 500

2. Pattern Matching:

- Intensity Tolerance [%]: 30
- Intensity Threshold [%]: 0.1
- S/N Threshold: 3
- Min. Spectral Fit [%]: 30
- Min. Pattern Cov. [%]: 80
- Use Dynamic Recalibration: True

3. Fragments Matching:

- Use Fragments Matching: True
- Mass Tolerance: 5 ppm
- S/N Threshold: 3

Search Mass Lists

1. Search Settings:

- Mass Lists:

suspectlist.massList

TPs_list_RSF_NTS_Spring.massList

PCs_list_RSF_NTS_Spring.massList

TPs_list_RSF_TS_Spring.massList

- Mass Tolerance: 3 ppm
- Use Retention Time: False
- RT Tolerance [min]: 0.5

Fill Gaps

1. General Settings:

- Mass Tolerance: 5 ppm
- S/N Threshold: 1.5
- Use Real Peak Detection: True

Mark Background Compounds

1. General Settings:

- Max. Sample/Blank: 10
- Max. Blank/Sample: 0
- Hide Background: False

Merge Features

1. Peak Consolidation:

- Mass Tolerance: 3 ppm
- RT Tolerance [min]: 0.1

Differential Analysis

1. General Settings:

- Log10 Transform Values: True

Table S.M. 11 Suspect List used for the Suspect screening of PCs

DTXSID	PREFERRED_NAME	MOLECULAR_FORMULA	MONOISOTOPIC_MASS	MS_READY_SMILES
DTXSID4024195	MCPA	C9H9ClO3	200.0240218	CC1=C(OCC(O)=O)C=CC(Cl)=C1
DTXSID2041468	3,4-Dichlorophenylurea	C7H6Cl2N2O	203.9857182	NC(=O)NC1=CC=C(Cl)C(Cl)=C1
DTXSID3042180	N-(3,4-Dichlorophenyl)-N'-methylurea	C8H8Cl2N2O	218.0013683	CNC(=O)NC1=CC(Cl)=C(Cl)C=C1
DTXSID30891504	10,11-Dihydro-10,11-dihydroxycarbamazepine	C15H14N2O3	270.1004423	NC(=O)N1C2=CC=CC=C2C(O)C(O)C2=C1C=CC=C2
DTXSID6020147	1,2,3-Benzotriazole	C6H5N3	119.0483472	N1N=NC2=C1C=CC=C2
DTXSID70274236	2-(Methylthio)benzothiazole	C8H7NS2	181.0019916	CSC1=NC2=CC=CC=C2S1
DTXSID5021386	2,4,6-Trichlorophenol	C6H3Cl3O	195.9249478	OC1=C(Cl)C=C(Cl)C=C1Cl
DTXSID1020439	2,4-Dichlorophenol	C6H4Cl2O	161.9639201	OC1=C(Cl)C=C(Cl)C=C1
DTXSID0020442	2,4-Dichlorophenoxyacetic acid	C8H6Cl2O3	219.9693995	OC(=O)COC1=C(Cl)C=C(Cl)C=C1
DTXSID1024966	2,4-Dichloroaniline	C6H5Cl2N	160.9799046	NC1=CC=C(Cl)C=C1Cl
DTXSID0020523	2,4-Dinitrophenol	C6H4N2O5	184.0120212	OC1=C(C=C(C=C1)[N+]([O-])=O)[N+]([O-])=O
DTXSID7022170	2,6-Dichlorobenzamide	C7H5Cl2NO	188.9748192	NC(=O)C1=C(Cl)C=CC=C1Cl
DTXSID4052213	2'-Aminoacetophenone	C8H9NO	135.0684139	CC(=O)C1=CC=CC=C1N
DTXSID1024467	2-Aminobenzothiazole	C7H6N2S	150.0251694	NC1=NC2=C(S1)C=CC=C2
DTXSID6061315	Benzothiazolone	C7H5NOS	151.009185	OC1=NC2=CC=CC=C2S1
DTXSID1022053	2-Methyl-4,6-dinitrophenol	C7H6N2O5	198.0276713	CC1=C(O)C(=CC(=C1)[N+]([O-])=O)[N+]([O-])=O
DTXSID50274037	4-Methyl-1,2,3-benzotriazole	C7H7N3	133.0639972	CC1=C2NN=NC2=CC=C1
DTXSID70881186	5,6-Dimethyl-1H-benzotriazole	C8H9N3	147.0796473	CC1=CC2=NNN=C2C=C1C
DTXSID0047450	5-Chlorobenzotriazole	C6H4ClN3	153.0093748	ClC1=CC2=C(NN=N2)C=C1
DTXSID1038743	5-Methyl-1H-benzotriazole	C7H7N3	133.0639972	CC1=CC2=C(NN=N2)C=C1
DTXSID1030606	Acesulfame potassium	C4H4KNO4S	200.9498103	CC1=CC(=O)NS(=O)(=O)O1
DTXSID2020006	Acetaminophen	C8H9NO2	151.0633285	CC(=O)NC1=CC=C(O)C=C1
DTXSID0044521	Diatrizoic acid	C11H9I3N2O4	613.76964	CC(=O)NC1=C(I)C(C(O)=O)=C(I)C(NC(C)=O)=C1I
DTXSID2022628	Atenolol	C14H22N2O3	266.1630426	CC(C)NCC(O)COC1=CC=C(CC(N)=O)C=C1
DTXSID9020112	Atrazine	C8H14ClN5	215.0937732	CCNC1=NC(NC(C)C)=NC(Cl)=N1
DTXSID3020122	Azinphos-methyl	C10H12N3O3PS2	317.0057706	COP(=S)(OC)SCN1N=NC2=C(C=CC=C2)C1=O

DTXSID0023901	Bentazone	C10H12N2O3S	240.0568634	CC(C)N1C(=O)C2=C(NS1(=O)=O)C=CC=C2
DTXSID7024586	Benzothiazole	C7H5NS	135.0142703	S1C=NC2=CC=CC=C12
DTXSID3029869	Bezafibrate	C19H20ClNO4	361.1080858	CC(C)(OC1=CC=C(CCNC(=O)C2=CC=C(Cl)C=C2)C=C1)C(O)=O
DTXSID4022020	Bromacil	C9H13BrN2O2	260.016041	CCC(C)N1C(=O)N=C(C)C(Br)C1=O
DTXSID0020232	Caffeine	C8H10N4O2	194.0803756	CN1C=NC2=C1C(=O)N(C)C(=O)N2C
DTXSID0022725	Candesartan	C24H20N6O3	440.1596885	CCOC1=NC2=CC=CC(C(O)=O)=C2N1CC1=CC=C(C=C1)C1=C(C=CC=C1)C1=NN=NN1
DTXSID4022731	Carbamazepine	C15H12N2O	236.094963	NC(=O)N1C2=CC=CC=C2C=CC2=C1C=CC=C2
DTXSID60891456	Carbamazepine epoxide	C15H12N2O2	252.0898776	NC(=O)N1C2=C(C=CC=C2)C2OC2C2=C1C=CC=C2
DTXSID4024729	Carbendazim	C9H9N3O2	191.0694765	COC(=O)NC1=NC2=CC=CC=C2N1
DTXSID4020458	Chlorpyrifos	C9H11Cl3NO3PS	348.9262845	CCOP(=S)(OCC)OC1=NC(Cl)=C(Cl)C=C1Cl
DTXSID8052853	Chlorotoluron	C10H13ClN2O	212.0716407	CN(C)C(=O)NC1=CC(Cl)=C(C)C=C1
DTXSID3034872	Chloridazon	C10H8ClN3O	221.0355896	ClC1C(=N)C=NN(C1=O)C1=CC=CC=C1
DTXSID7022833	Clenbuterol	C12H18Cl2N2O	276.0796186	CC(C)(C)NCC(O)C1=CC(Cl)=C(N)C(Cl)=C1
DTXSID2022836	Clindamycin	C18H33ClN2O5S	424.179871	CCCC1CC(N(C)C1)C(=O)NC(C(C)Cl)C1OC(SC)C(O)C(O)C1O
DTXSID5022857	Cortisone	C21H28O5	360.193674	CC12CC(=O)C3C(CCC4=CC(=O)CCC34C)C1CCC2(O)C(=O)CO
DTXSID5041809	Cyclamic acid	C6H13NO3S	179.0616145	OS(=O)(=O)NC1CCCCC1
DTXSID5020364	Cyclophosphamide	C7H15Cl2N2O2P	260.0248201	ClCCN(CCCl)P1(=O)NCCCO1
DTXSID2021995	DEET	C12H17NO	191.1310142	CCN(CC)C(=O)C1=CC=CC(C)=C1
DTXSID5037494	Deethylatrazine	C6H10ClN5	187.062473	CC(C)NC1=NC(Cl)=NC(N)=N1
DTXSID50212792	3(2H)-Pyridazinone, 5-amino-4-chloro-	C4H4ClN3O	145.0042895	ClC1C(=N)CN=NC1=O
DTXSID0037495	Deisopropylatrazine	C5H8ClN5	173.046823	CCNC1=NC(N)=NC(Cl)=N1
DTXSID0020440	Dichlorprop	C9H8Cl2O3	233.9850495	CC(OC1=C(Cl)C=C(Cl)C=C1)C(O)=O
DTXSID6022923	Diclofenac	C14H11Cl2NO2	295.016684	OC(=O)CC1=C(NC2=C(Cl)C=CC=C2Cl)C=CC=C1
DTXSID2034542	Dimethenamid-P	C12H18ClNO2S	275.0746777	COCC(C)N(C(=O)CCl)C1=C(C)SC=C1C
DTXSID7020479	Dimethoate	C5H12NO3PS2	228.9996226	CNC(=O)CSP(=S)(OC)OC
DTXSID7034545	Dimethomorph	C21H22ClNO4	387.1237359	COC1=C(OC)C=C(C=C1)C(=CC(=O)N1CCOCC1)C1=CC=C(Cl)C=C1
DTXSID0020446	Diuron	C9H10Cl2N2O	232.0170184	CN(C)C(=O)NC1=CC(Cl)=C(Cl)C=C1
DTXSID4022991	Erythromycin	C37H67NO13	733.4612412	CCC1OC(=O)C(C)C(OC2CC(C)(OC)C(O)C(C)O2)C(C)C(OC2OC(C)CC(C2O)N(C)C)C(C)(O)CC(C)C(=O)C(C)C(O)C1(C)O

DTXSID8034580	Ethofumesate	C13H18O5S	286.0874949	CCOC1OC2=C(C=C(OS(C)(=O)=O)C=C2)C1(C)C
DTXSID6021117	Phenazone	C11H12N2O	188.094963	CN1N(C(=O)C=C1C)C1=CC=CC=C1
DTXSID7023067	Fluoxetine	C17H18F3NO	309.1340487	CNCCC(OC1=CC=C(C=C1)C(F)(F)F)C1=CC=CC=C1
DTXSID6020648	Furosemide	C12H11ClN2O5S	330.0077203	NS(=O)(=O)C1=C(Cl)C=C(NCC2=CC=CO2)C(=C1)C(O)=O
DTXSID0020074	Gabapentin	C9H17NO2	171.1259288	NCC1(CC(O)=O)CCCCC1
DTXSID40215070	Gabapentin-lactam	C9H15NO	153.1153641	O=C1CC2(CN1)CCCCC2
DTXSID0020652	Gemfibrozil	C15H22O3	250.1568946	CC1=CC(OCCCC(C)(C)C(O)=O)=C(C)C=C1
DTXSID3043811	Guanylurea	C2H6N4O	102.0541608	NC(=N)NC(N)=O
DTXSID9027520	Hexa(methoxymethyl) melamine	C15H30N6O6	390.2226827	COCN(COC)C1=NC(=NC(=N1)N(COC)COC)N(COC)COC
DTXSID2020713	Hydrochlorothiazide	C7H8ClN3O4S2	296.9644758	NS(=O)(=O)C1=CC2=C(NCNS2(=O)=O)C=C1Cl
DTXSID7020714	Hydrocortisone	C21H30O5	362.2093241	CC12CC(O)C3C(CCC4=CC(=O)CCC34C)C1CCC2(O)C(=O)CO
DTXSID7020760	Ifosfamide	C7H15Cl2N2O2P	260.0248201	ClCCNP1(=O)OCCCN1CCCl
DTXSID0023169	Irbesartan	C25H28N6O	428.2324595	CCCCC1=NC2(CCCC2)C(=O)N1CC1=CC=C(C=C1)C1=CC=CC=C1C1=NN=NN1
DTXSID1042077	Isoproturon	C12H18N2O	206.1419132	CC(C)C1=CC=C(NC(=O)N(C)C)C=C1
DTXSID6020771	Ketoprofen	C16H14O3	254.0942943	CC(C(O)=O)C1=CC(=CC=C1)C(=O)C1=CC=CC=C1
DTXSID2023195	Lamotrigine	C9H7Cl2N5	255.0078506	NC1=NC(N)=C(N=N1)C1=CC=CC(Cl)=C1Cl
DTXSID3023215	Lincomycin	C18H34N2O6S	406.213758	CCCC1CC(N(C)C1)C(=O)NC(C(C)O)C1OC(SC)C(O)C(O)C1O
DTXSID2024163	Linuron	C9H10Cl2N2O2	248.011933	CON(C)C(=O)NC1=CC=C(Cl)C(Cl)=C1
DTXSID9024194	Mecoprop	C10H11ClO3	214.0396719	CC(OC1=C(C)C=C(Cl)C=C1)C(O)=O
DTXSID4058156	Metazachlor	C14H16ClN3O	277.0981898	CC1=CC=CC(C)=C1N(CN1C=CC=N1)C(=O)CCl
DTXSID40891454	Metazachlor ESA	C14H17N3O4S	323.0939772	CC1=CC=CC(C)=C1N(CN1C=CC=N1)C(=O)CS(O)(=O)=O
DTXSID00891455	metazachlor OXA	C14H15N3O3	273.1113414	CC1=CC=CC(C)=C1N(CN1C=CC=N1)C(=O)C(O)=O
DTXSID2023270	Metformin	C4H11N5	129.1014454	CN(C)C(=N)NC(N)=N
DTXSID6042157	Metobromuron	C9H11BrN2O2	258.000391	CON(C)C(=O)NC1=CC=C(Br)C=C1
DTXSID4022448	Metolachlor	C15H22ClNO2	283.1339067	CCC1=C(N(C(C)COC)C(=O)CCl)C(C)=CC=C1
DTXSID1037567	Metolachlor ESA	C15H23NO5S	329.129694	CCC1=CC=CC(C)=C1N(C(C)COC)C(=O)CS(O)(=O)=O
DTXSID6037568	Metolachlor OA	C15H21NO4	279.1470582	CCC1=CC=CC(C)=C1N(C(C)COC)C(=O)C(O)=O
DTXSID2023309	Metoprolol	C15H25NO3	267.1834437	COCCC1=CC=C(OCC(O)CNC(C)C)C=C1
DTXSID1042158	Metoxuron	C10H13ClN2O2	228.0665554	COC1=C(Cl)C=C(NC(=O)N(C)C)C=C1

DTXSID6024204	Metribuzin	C8H14N4OS	214.0888323	CSC1=NN=C(C(=O)N1N)C(C)(C)C
DTXSID2020892	Metronidazole	C6H9N3O3	171.0643912	CC1=NC=C(N1CCO)[N+]([O-])=O
DTXSID0020311	Monuron	C9H11ClN2O	198.0559907	CN(C)C(=O)NC1=CC=C(Cl)C=C1
DTXSID40232106	N-Acetylaminoantipyrine	C13H15N3O2	245.1164267	CC1N(C)N(C(=O)C1=NC(C)=O)C1=CC=CC=C1
DTXSID8049044	N-Acetyl sulfamethoxazole	C12H13N3O4S	295.0626771	CC(=O)NC1=CC=C(C=C1)S(=O)(=O)NC1=NOC(C)=C1
DTXSID4040686	Naproxen	C14H14O3	230.0942943	COC1=CC2=CC=C(C=C2C=C1)C(C)C(O)=O
DTXSID10168241	4-Formylaminoantipyrine	C12H13N3O2	231.1007767	CC1N(C)N(C(=O)C1=NC=O)C1=CC=CC=C1
DTXSID6034764	Nicosulfuron	C15H18N6O6S	410.1008535	COC1=CC(OC)=NC(NC(=O)NS(=O)(=O)C2=NC=CC=C2C(=O)N(C)C)=N1
DTXSID1020932	Nicotinic acid	C6H5NO2	123.0320284	OC(=O)C1=CC=CN=C1
DTXSID4035209	Oxypurinol	C5H4N4O2	152.0334254	O=C1NC2=NNC=C2C(=O)N1
DTXSID3022409	4,4'-Sulfonyldiphenol	C12H10O4S	250.02998	OC1=CC=C(C=C1)S(=O)(=O)C1=CC=C(O)C=C1
DTXSID3023425	Paroxetine	C19H20FNO3	329.1427217	FC1=CC=C(C=C1)C1CCNCC1COC1=CC=C2OCOC2=C1
DTXSID7023437	Pentoxifylline	C13H18N4O3	278.1378905	CN1C=NC2=C1C(=O)N(CCCCC(C)=O)C(=O)N2C
DTXSID7023437	Pentoxifylline	C13H18N4O3	278.1378905	CN1C=NC2=C1C(=O)N(CCCCC(C)=O)C(=O)N2C
DTXSID6021117	Phenazone	C11H12N2O	188.094963	CN1N(C(=O)C=C1C)C1=CC=CC=C1
DTXSID8023476	Pindolol	C14H20N2O2	248.1524779	CC(C)NCC(O)COC1=C2C=CNC2=CC=C1
DTXSID1032569	Pirimicarb	C11H18N4O2	238.1429758	CN(C)C(=O)OC1=C(C)C(C)=NC(=N1)N(C)C
DTXSID9021184	Prednisolone	C21H28O5	360.193674	CC12CC(O)C3C(CCC4=CC(=O)C=CC34C)C1CCC2(O)C(=O)CO
DTXSID6023525	Propranolol	C16H21NO2	259.1572289	CC(C)NCC(O)COC1=C2C=CC=CC2=CC=C1
DTXSID6023529	Propyphenazone	C14H18N2O	230.1419132	CC(C)C1=C(C)N(C)N(C1=O)C1=CC=CC=C1
DTXSID5021251	Saccharin	C7H5NO3S	182.9990142	O=C1NS(=O)(=O)C2=C1C=CC=C2
DTXSID5021255	Albuterol	C13H21NO3	239.1521435	CC(C)(C)NCC(O)C1=CC=C(O)C(CO)=C1
DTXSID4021268	Simazine	C7H12ClN5	201.0781231	CCNC1=NC(NCC)=NC(Cl)=N1
DTXSID70197572	Sitagliptin	C16H15F6N5O	407.1180791	NC(CC(=O)N1CCN2C(C1)=NN=C2C(F)(F)F)CC1=C(F)C=C(F)C(F)=C1
DTXSID0023589	Sotalol	C12H20N2O3S	272.1194637	CC(C)NCC(O)C1=CC=C(NS(C)(=O)=O)C=C1
DTXSID1040245	Sucralose	C12H19Cl3O8	396.0145507	OCC1OC(OC2(CCl)OC(CCl)C(O)C2O)C(O)C(O)C1Cl
DTXSID9045265	Sulfachloropyridazine	C10H9ClN4O2S	284.0134744	NC1=CC=C(C=C1)S(=O)(=O)NC1=CC=C(Cl)N=N1
DTXSID7044130	Sulfadiazine	C10H10N4O2S	250.0524468	NC1=CC=C(C=C1)S(=O)(=O)NC1=NC=CC=N1
DTXSID6021290	Sulfamethazine	C12H14N4O2S	278.0837469	CC1=CC(C)=NC(NS(=O)(=O)C2=CC=C(N)C=C2)=N1

DTXSID8026064	Sulfamethoxazole	C10H11N3O3S	253.0521124	CC1=CC(NS(=O)(=O)C2=CC=C(N)C=C2)=NO1
DTXSID8042424	Sulfaquinoxaline	C14H12N4O2S	300.0680968	NC1=CC=C(C=C1)S(=O)(=O)NC1=CN=C2C=CC=CC2=N1
DTXSID7021310	Terbutaline	C12H19NO3	225.1364935	CC(C)(C)NCC(O)C1=CC(O)=CC(O)=C1
DTXSID4027608	Terbutylazine	C9H16ClN5	229.1094232	CCNC1=NC(NC(C)(C)C)=NC(Cl)=N1
DTXSID7044396	2,5,8,11,14-Pentaoxapentadecane	C10H22O5	222.1467238	COCCOCCOCCOCCOC
DTXSID90858931	Tramadol	C16H25NO2	263.188529	COC1=CC=CC(=C1)C1(O)CCCCC1CN(C)C
DTXSID8026228	Triethyl phosphate	C6H15O4P	182.070796	CCOP(=O)(OCC)OCC
DTXSID2022121	Triphenylphosphine oxide	C18H15OP	278.0860521	O=P(C1=CC=CC=C1)(C1=CC=CC=C1)C1=CC=CC=C1
DTXSID3023712	Trimethoprim	C14H18N4O3	290.1378905	COC1=CC(CC2=CN=C(N)N=C2N)=CC(OC)=C1OC
DTXSID3021986	Tributyl phosphate	C12H27O4P	266.1646963	CCCCOP(=O)(OCCCC)OCCCC
DTXSID5021411	Tris(2-chloroethyl) phosphate	C6H12Cl3O4P	283.953879	ClCCOP(=O)(OCCCl)OCCCl
DTXSID5026259	Tris(2-chloroisopropyl)phosphate	C9H18Cl3O4P	326.0008292	CC(CCl)OP(=O)(OC(C)CCl)OC(C)CCl
DTXSID6023735	Valsartan	C24H29N5O3	435.2270398	CCCCC(=O)N(CC1=CC=C(C=C1)C1=C(C=CC=C1)C1=NNN=N1)C(C(C)C)C(O)=O
DTXSID20881090	Valsartan acid	C14H10N4O2	266.0803756	OC(=O)C1=CC=C(C=C1)C1=CC=CC=C1C1=NN=NN1
DTXSID6023737	Venlafaxine	C17H27NO2	277.2041791	COC1=CC=C(C=C1)C(CN(C)C)C1(O)CCCCC1

Figure S.M. 7 Spectra similarity plots of Parent compound (upper spectrum identified by CAS number_FeatureID) and Transformation Product (lower spectrum identified by FeatureID)

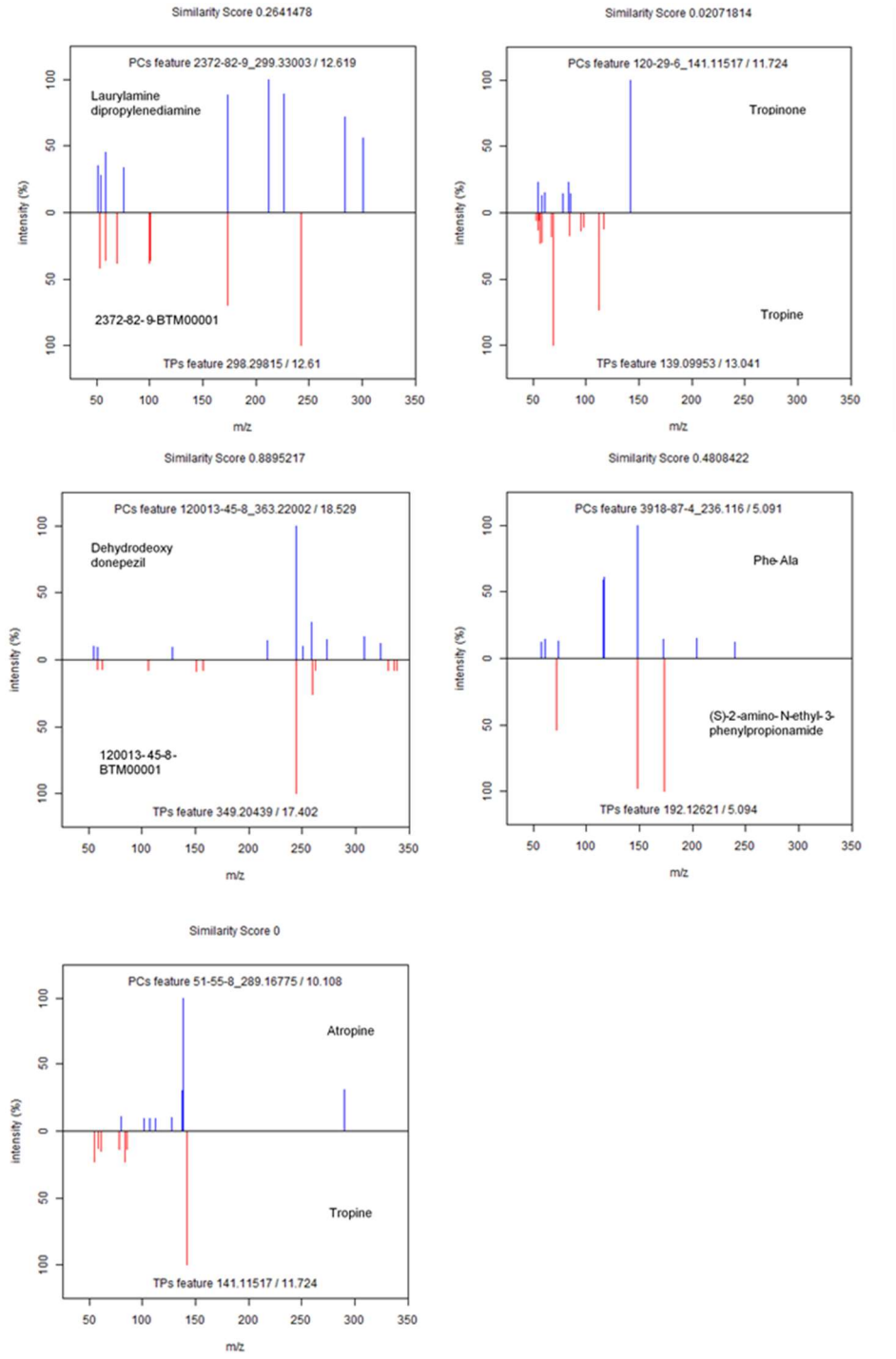

Figure S.M. 8 Concentration profiles of the detected TPs

Each plot is referred to one feature, reported in the title by the featureID (M.W./RT). The right side of the plots shows the internal standard equivalent concentration (IS-eq) in influent and effluent samples for the different locations. The left side of the plots shows the log2FC of the area between effluent and influent for the different locations: log2FC>0 indicates an increasing of the concentration during the treatments, instead log2FC<0 indicates a decrease of the concentration (removal).


169.11015 / 8.457
267.147 / 6.96
192.12621 / 5.094
141.11517 / 11.724
139.09953 / 7.441
662.19414 / 14.693
201.1729 / 10.52
187.15703 / 7.58
Effluent
Influent
WRK
WPCI_Kluizen
Loendereven
Kralingen
Heel
Bergambacht
Andijk
Location
IS-eq Conc. [ug/L]
log2FC

Figure S.M. 9 Control compound: Gabapentin-Lactam